UNIVERSITY OF TWENTE.

Faculty of Electrical Engineering, Mathematics & Computer Science

Stimulus Related Evoked Potentials

around the

Nociceptive Detection Threshold

B. van den Berg

M.Sc. Thesis
March 2018

Supervisor:
Dr. ir. J. R. Buitenweg
Committee:
Dr. ir. J. R. Buitenweg
Dr. ir. B. J. F. van Beijnum
Dr. ir. F. van der Heijden

Biomedical Signals and Systems Group
Faculty of Electrical Engineering,
Mathematics and Computer Science
University of Twente
P.O. Box 217
7500 AE Enschede
The Netherlands

Dedicated to human subjects in research.

Summary

In the Netherlands, 1 in 5 adults suffer from chronic pain. Besides consequences for individual patients and their relatives, chronic pain is a large burden for society due to absence at work and an increased consumption of medical resources. Chronic pain is the result of disturbed processes in the central nervous system. Early detection of these disturbances enables better treatments and less clinical efforts per patient. However, appropriate diagnostic methods are lacking.

New pain diagnostics can be developed by measuring the function of the central nervous system using EEG. With EEG, the neural processing of pain stimuli can be studied by estimation of the evoked potential using the averages of large sets of trials. However, experiments to gather the required data on human subjects cannot take too long and the number of stimuli is limited, which is problematic for the acquisition of sufficient trials. Often, stimulus selection methods are used for a more efficient probing of the stimulus parameter space. However, this results in different amounts of trials per stimulus property. Since the variance of the estimated evoked potential depends on the amount of acquired trials, analysis of those trials using conventional averaging is impeded. This could be overcome by using an analysis method which is robust for variations in the amount of acquired trials. Such a method is provided by a linear mixed model, which deals with those variations by using dependencies within the data.

It can be shown that for multi-stimulus EEG data the quality of an evoked potential estimate is improved by using a linear mixed model, which effectively deals with correlation between and within parameters in the data. Furthermore, linear mixed-effects regression enables us to study stimulus-related brain activity at the subject-level and group-level simultaneously, which brings us one step closer to the development of objective diagnostics based on brain activity.

Using a linear mixed model, it can be shown that conscious detection of nociceptive stimuli is of major influence on the amplitude of the evoked potential, while stimulus parameters only account for a minor part of the observed variations. This means that variation in stimulus parameters mainly influences the observed components of the evoked potential by modulating the detection probability of the stimulus.

Contents

List of acronyms

ACC	anterior cingulate cortex
ANOVA	analysis of variance
AP	optical beamforming network
BSS	biomedical signals and systems
D	stimulus detection
DP	stimulus detection probability
EEG	electroencephalogram or electroencephalography
EP	evoked potential
ERP	event-related potential
fMRI	functional magnetic resonance imaging
GLM	generalized linear model
GLMM	generalized linear mixed model
IASP	international association for the study of pain
IC	insular cortex
IES	intra-epidermal electrocutaneous stimulation
IPI	inter-pulse interval
LM	linear model
LMM	linear mixed model
LMER	linear mixed-effects regression
MEG	magnetoencephalography
MN	microneurography
MTT	multiple threshold tracking
N1	first negative EP component (Section 2.5.2)
N2	second negative EP component (Section 2.5.2)
NDT	nociceptive detection threshold
NOP	number of pulses
NS	nociception-specific
P2	seconf positive EP component (Section 2.5.2)
PET	positron emission tomography

PLV phase-locking value

SI primary somatosensory cortex

SII secondary somatosensory cortex

SNR signal-to-noise ratio

SP1 or P1 first pulse

SP2 or P2 second pulse

STT spino-thalamic tract

TRL number of trials/ number of received stimuli

VMpo ventromedial posterior nucleus of the thalamus

VPI ventroposterior inferior nucleus of the thalamus

VPL ventroposterior lateral nucleus of the thalamus

WDR wide dynamic range

1 Introduction

Pain is considered a major problem in modern day society, not only comprising a major physical and psychological burden for patients, but also a big economic and social burden for society. In Europe, it was found that over the range of one month 20.2% of all people suffer a form of pain [1]. Among those people is a big group that experiences chronic pain which was shown to have a prevalence of up to 30%, of which 40% receives inadequate treatment for the pain [2]. For a large part of those people, the pain is severely impairing and almost intolerable, which is shown by the numbers in Figure 1.1. These results emphasize the need for improved and new treatments for chronic pain. However, the development of those treatments requires a more profound understanding of the physiological as well as the psychological aspects of chronic pain.

Several types of chronic pain are linked to increased sensitivity of the central nervous system (e.g. post-surgical pain and complex regional pain syndrome [3, 4]). Therefore, it is important to study the plasticity of the nervous system with respect to pain in healthy subjects and patients. One major obstacle in doing so is the lack of an objective measure of the nociceptive system's response to nociceptive stimuli. Although in clinical practice a numerical rating scale is used to study the amount of pain perceived by a patient, the measured values do not give any insight in the alterations of the nociceptive system that are causing chronic pain. To enable a better diagnosis and treatment of chronic pain, an objective measure of the nociceptive system's behavior in healthy subjects and chronic pain patients is required.

1.1 Problem Statement

A method to determine properties of the nociceptive system is the measurement and analysis of cortical activity in response to nociceptive stimulation using electroencephalograpy (EEG) [5, 6]. Recently, researchers have found significant alterations of the time-locked EEG signal, also referred to as the evoked-potential (EP) [7–9] with respect to the parameters of nociceptive stimuli. However, interpretation of nociceptive stimulus-related brain activity has been fiercely debated [10, 11] due to

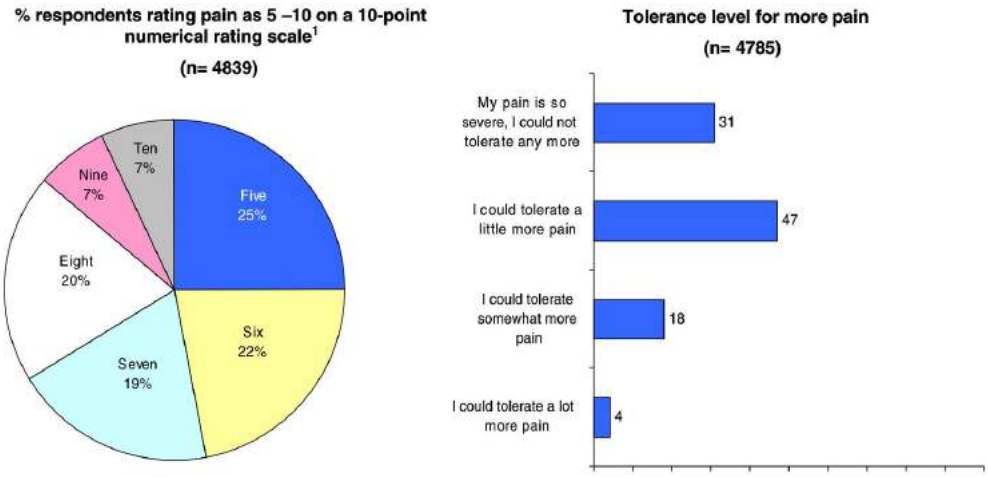

Figure 1.1: *The intensity of pain experience by chronic pain patients. Left: Intensity of pain expressed on a numerical rating scale. Right: Patient description of chronic pain. Adapted from Breivik et al. [2].*

the lack of a model for understanding the interactions in the peripheral and central nervous system which modulate the relation between the stimulus and the signal. To provide a basis for such a model, the phenomena related to alteration of the nociceptive stimulus should be observed.

Prior to this assignment, a method was developed to measure cortical activity with EEG during implementation of the multiple threshold tracking method [12]. However, due to the low signal-to-noise ratio (SNR) of the EEG signal, analysis is problematic. To measure relations between the stimulus, detection and neurophysiological activity, a more sophisticated method is required to process and interpret the data of EEG signals during multiple threshold tracking measurements.

1.2 Research Goal

The aim of this work is to combine the technique of multiple threshold tracking (Section 2.4.3) with techniques to record and analyze cortical activity to observe neurophysiological activation during nociceptive processing and detection. To do so, cortical signals will be recorded during multiple types of stimuli and analyzed with respect to the stimulus parameters to establish relations between the stimulus, detection and neurophysiological activity.

1.3 Strategy and Outline

The main focus of this work is to develop and test a statistical analysis method to process and interpret nociceptive EPs during multiple threshold tracking. First, a literature study on nociceptive processing, psychophysiology, evoked potentials and statistical analysis is summarized and discussed to specify relevant research questions (Chapter 2).

Subsequently, a method for analysis of EEG measurements during multiple threshold tracking is described and tested using a simulation of EEG data during multiple threshold tracking (Chapter 3). This method is used to analyze data from earlier exploratory research that combined multiple threshold tracking with EEG, and compared with conventional techniques for EEG analysis. The results from this comparison are presented in paper format, since this chapter was recently submitted for a conference (Chapter 4).

As a major component of this thesis, a new experiment was performed on 30 healthy participants, in which multiple threshold tracking and EEG analysis (using the method from earlier chapters) are combined to determine the influence of stimulus parameters on the EEG. An preliminary article about this study is presented in Chapter 5, which will be further refined and submitted after conclusion of this thesis. To conclude, results from this thesis are summarized and discussed to answer the research questions which are posed based on chapter 2 and formulate conclusions and recommendations for further research (Chapter 6).

Bibliography

[1] P. C. Langley, "The prevalence, correlates and treatment of pain in the European Union", *Current Medical Research and Opinion*, vol. 27, no. 2, pp. 463–480, 2011.

[2] H. Breivik, B. Collett, V. Ventafridda, R. Cohen, and D. Gallacher, "Survey of chronic pain in europe: Prevalence, impact on daily life, and treatment", *European Journal of Pain*, vol. 10, no. 4, pp. 287–333, 2006.

[3] C. J. Woolf, "Central sensitization: Implications for the diagnosis and treatment of pain", *Pain*, vol. 152, no. SUPPL.3, 2011.

[4] E. A. Shipton, "Complex regional pain syndrome - mechanisms, diagnosis, and management", *Current Anaesthesia and Critical Care*, vol. 20, no. 5-6, pp. 209–214, 2009.

[5] M. C. Lee, A. Mouraux, and G. D. Iannetti, "Characterizing the cortical activity through which pain emerges from nociception", *Journal of Neuroscience*, vol. 29, no. 24, pp. 7909–7916, 2009.

[6] R. J. Doll, "Psychophysical methods for improved observation of nociceptive processing", Thesis, 2016.

[7] S. Ohara, N. E. Crone, N. Weiss, R. D. Treede, and F. A. Lenz, "Amplitudes of laser evoked potential recorded from primary somatosensory, parasylvian and medial frontal cortex are graded with stimulus intensity", *Pain*, vol. 110, no. 1-2, pp. 318–328, 2004.

[8] C. Perchet, F. Godinho, S. Mazza, M. Frot, V. Legrain, M. Magnin, and L. Garcia-Larrea, "Evoked potentials to nociceptive stimuli delivered by CO2 or Nd:YAP lasers", *Clinical Neurophysiology*, vol. 119, no. 11, pp. 2615–2622, 2008.

[9] E. M. van der Heide, J. R. Buitenweg, E. Marani, and W. L. Rutten, "Single pulse and pulse train modulation of cutaneous electrical stimulation: A comparison of methods", *J Clin Neurophysiol*, vol. 26, no. 1, pp. 54–60, 2009.

[10] L. Hu and G. Iannetti, "Painful issues in pain prediction", *Trends in Neurosciences*, vol. 39, no. 4, pp. 212–220, 2016.

[11] G. D. Iannetti and A. Mouraux, "From the neuromatrix to the pain matrix (and back)", *Experimental Brain Research*, vol. 205, no. 1, pp. 1–12, 2010.

[12] M. U. Werner, H. N. Mjöbo, P. R. Nielsen, and A. Rudin, "Prediction of postoperative pain: A systematic review of predictive experimental pain studies", *Anesthesiology*, vol. 112, no. 6, pp. 1494–1502, 2010.

2 Background

In this chapter, the reader will be familiarized with important concepts in this thesis, such as pain, stimuli, psychophysics and evoked potentials. Additionally, the available experimental setup and statistical techniques for data analysis will be introduced. In the last section, these concepts will be combined to arrive at the subject of this research itself: measurement and analysis of evoked potentials during psychophysical threshold tracking.

2.1 Pain

Pain is defined by the International Association for the Study of Pain (IASP) as an unpleasant sensory and emotional experience associated with actual or potential tissue damage. In Europe, it was found that over the range of one month 20.2% of all people report a form of pain, of which 4.6% suffer severe pain. Additionally, about 8.9% of all persons have pain on a daily basis. Of the persons reporting pain, 41.4% receives prescribed pain medications. However, only 29.6% of this group of persons report to be satisfied with all prescribed medication [1], implying a demand for the development of more advanced pain reduction methods. This will require an advanced understanding of the mechanisms of pain.

Since the very beginning of medical science humanity has studied pain, succeeding to identify several key aspects of pain. The Greek philosopher Hippocrates, as one of the first experts in the field of pain research, was the first to describe the phenomenon of diffuse noxious inhibitory control, by observing that in patients with pain in two different body parts 'the stronger (pain) blunts the other' [3]. Since Hippocrates, many others have tried to explore the nature of pain, including famous philosophers such as Leonardo da Vinci and Descartes who respectively postulated involvement of the brain [4] and a nervous system [2] in the perception of pain based on their personal observations. The idea of Descartes that pain was directly transmitted to the brain by a hard-wired system and subsequently perceived, led to the notion of pain as an experience with a one-to-one relationship to painful stimuli [5].

However, it was not until last century that academics started to adopt a more empirical approach in pain research. Among some of the first researchers to doubt this one-to-one relationship, which is referred to as the specificity theory, were Melzack and Wall in their seminal work "Pain Mechanisms:

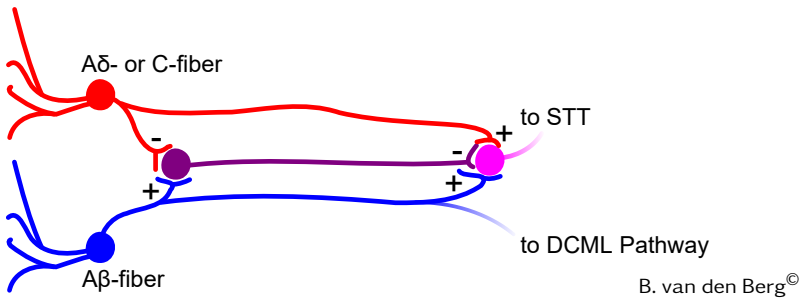

Figure 2.1: *Interaction between mechanoreceptive and nociceptive neurons was hypothesized by Melzack and Wall [2] to account for observed variations in nociception. Nociceptive information from the modulated neuron continues to the spinothalamic tract (STT) while tactile information from the Aβ-fiber is directly relayed to the dorsal colomn-medial lemniscus pathway (DCML). More information about the nociceptive pathways can be found in Section 2.2*

A New Theory" [2]. They proposed a new theory including dynamic modulation of pain, such as was observed in soldiers on the battlefield with severe injuries. In order to explain this modulation, the presence of inhibiting interneurons in the dorsal horn was hypothesized, which are activated based on earlier painful stimuli. This mechanism of inhibitory control is illustrated in Figure 2.1.

This theory, referred to as the gate-control theory, provided a more sophisticated explanation of the perception of pain. However, it has recently been observed that this theory does not fully account for changes in nociceptive perception. Instead, it has recently been hypothesized that pain is not only modulated in the spine, but also through the interaction of several cortical areas [6, 7]. Therefore, pain is nowadays considered to be an experience resulting from the complex interactions between i.a. tissue, peripheral nerves, central nerves, the thalamus and several cortical areas. The modern understanding of pain includes that pain does not only originate from tissue damage, but also from other reasons which are often unknown. Therefore, pain research is not only important for alleviating pain of patients with tissue damage, e.g. during surgery, but also for the treatment of chronic pain, which provides a substantial challenge for current medical science.

2.2 Nociceptive Pathways

Although the specificity theory was proven incorrect by empirical science, it did introduce an important concept in the perception of pain signals: pain travels through 'wires' in our body towards our brain. However, instead of a single wire, this network has been shown to include multiple 'wires' with many internal and external interactions, of which some have not been unraveled yet. In this chapter the most important part of this network, as far as it has been identified, is described.

2.2.1 Nociception in Peripheral Nerve Fibers

Nociception starts with a supra-threshold stimulus reaching nociceptive nerve fibers. These fibers are categorized as C-fibers and Aδ-fibers. C-fibers are polymodal nociceptors with a diameter of less than 2.0 µm and a conduction velocity of less than 2.0 $\mathrm{m\,s^{-1}}$ since they are not myelinated. Aδ-fibers are thinly myelinated fibers with a diameter of 2.0 µm to 5.0 µm and a much faster conduction velocity of 6.0 $\mathrm{m\,s^{-1}}$ to 30.0 $\mathrm{m\,s^{-1}}$. Although C-fibers are generally sensitive to all types of noxious stimuli, Aδ-fibers are more specifically sensitive to either chemical, mechanical, thermal or electrical stimuli, depending on their receptors. Nociceptors are normally either stimulated by chemical agents, liberated by tissue damage or thermally sensitive reactions, or by mechanical deformation of the membrane, which causes an influx of sodium ions triggering the action potential [8]. Electrical stimuli trigger a nociceptor more directly by causing a membrane potential which triggers the action potential when it raises above the threshold. Additionally, the threshold of a nociceptor to specific stimuli can be modulated by chemical substances. For example, a number of substances in the inflammatory soup lower the threshold of activation of most nociceptors causing hyperalgaesia, and spontaneous firing of nociceptors [9]. Besides nociceptive nerve endings, the skin contains many other types of receptors. Of those receptors, the mechanoreceptors are of particular interest since they are thought to interact with the nociceptive system. The majority of those receptors is innervated by Aβ-fibers, large myelinated fibers with a conduction velocity of 30.0 $\mathrm{m\,s^{-1}}$ to 70.0 $\mathrm{m\,s^{-1}}$.

2.2.2 Transduction of Nociceptive Stimuli in the Dorsal Horn

Most afferent sensory nerve fibers, including nociceptors, terminate in the so-called Rexed laminae in the dorsal horn, which are illustrated in Figure 2.2. Aδ-fibers mainly terminate in laminae I and V while C-fibers tend to terminate in laminae I and II. Partially coinciding with the endings of those afferents, are the endings of the Aβ-fibers, which terminate in laminae III to VI. The nociceptors terminating in lamina I are thought to connect to nociceptive specific (NS) neurons, which are mainly activated by Aδ-fibers. On the other hand, the nociceptors terminating in lamina V are thought to connect to wide dynamic range (WDR) neurons, which are activated by Aδ-fibers as well as Aβ-fibers. Therefore, these neurons also encode stimuli from mechanoreceptors [10]. Besides being activated by peripheral connections, the nociceptive neurons in the dorsal horn are also thought to be modulated by inhibitory control neurons, as was first postulated by Melzack and Wall [2]. Nowadays, these inhibitory neurons have been shown to be modulated by central top-down connections [8].

2.2.3 Central Nociceptive Pathways

Signals from nociceptors and mechanoreceptors are conducted in the spinal cord through several pathways. The first information of a stimulus to arrive in the brain is the information from mechanoreceptors, since branches of Aβ-fibers have a quick connection to the brain via the ipsilateral cuneate tract in the dorsal column, which terminates in the medulla. From there, the pathway continues contralateral until the ventroposterior lateral nucleus (VPL) in the thalamus. Transmission in this pathway reaches a velocity of around 60.0 $\mathrm{m\,s^{-1}}$.

The majority of the nociceptive neurons in the dorsal horn transmit their action potentials contralateral[1] through the spinothalamic tract (STT). This anterior part of the STT transmits potentials from the WDR neurons in lamina V with a coduction velocity of approximately 21 $\mathrm{m\,s^{-1}}$ [11], while the lateral part of this tract transmits potentials from the NS neurons in lamina I with a conduction velocity of approximately 10.0 $\mathrm{m\,s^{-1}}$ [12]. While the anterior part of the STT terminates in

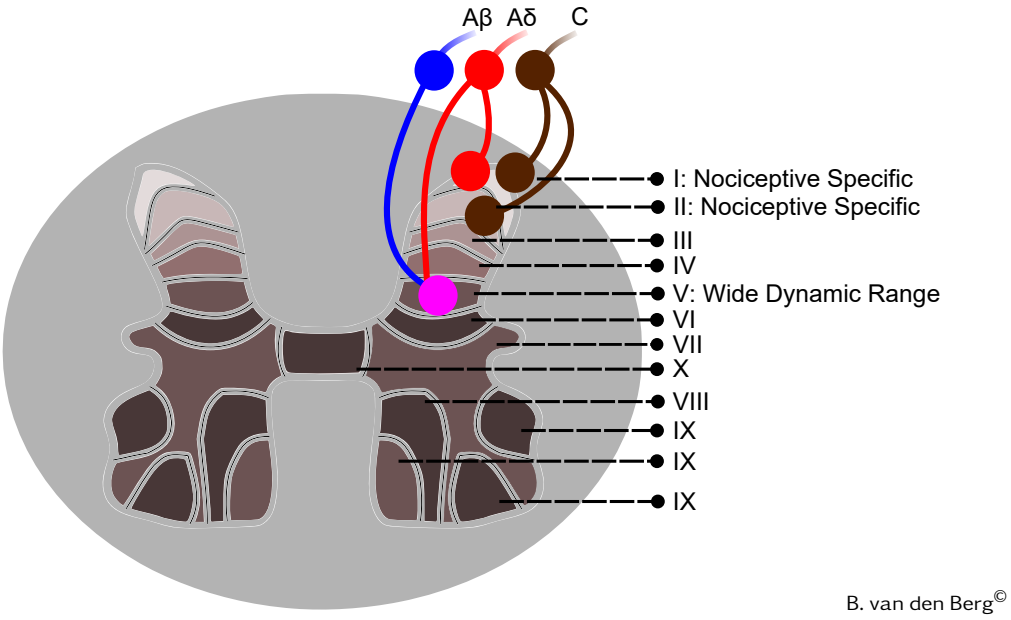

Figure 2.2: *Illustration of the Rexed laminae in the dorsal horn of the spinal cord.*

the VPL, the lateral part terminates in the ventromedial posterior (VMpo) and the ventroposterior inferior (VPI) nuclei in the thalamus. The majority of the C-fibers transmit their action potentials through the subreticular tract and trigeminal pathways, with a conduction velocity of approximately $2.2\,\mathrm{m\,s^{-1}}$ [12], eventually terminating decentralized in the SI, SII and a variety of other brain areas [10, 13].

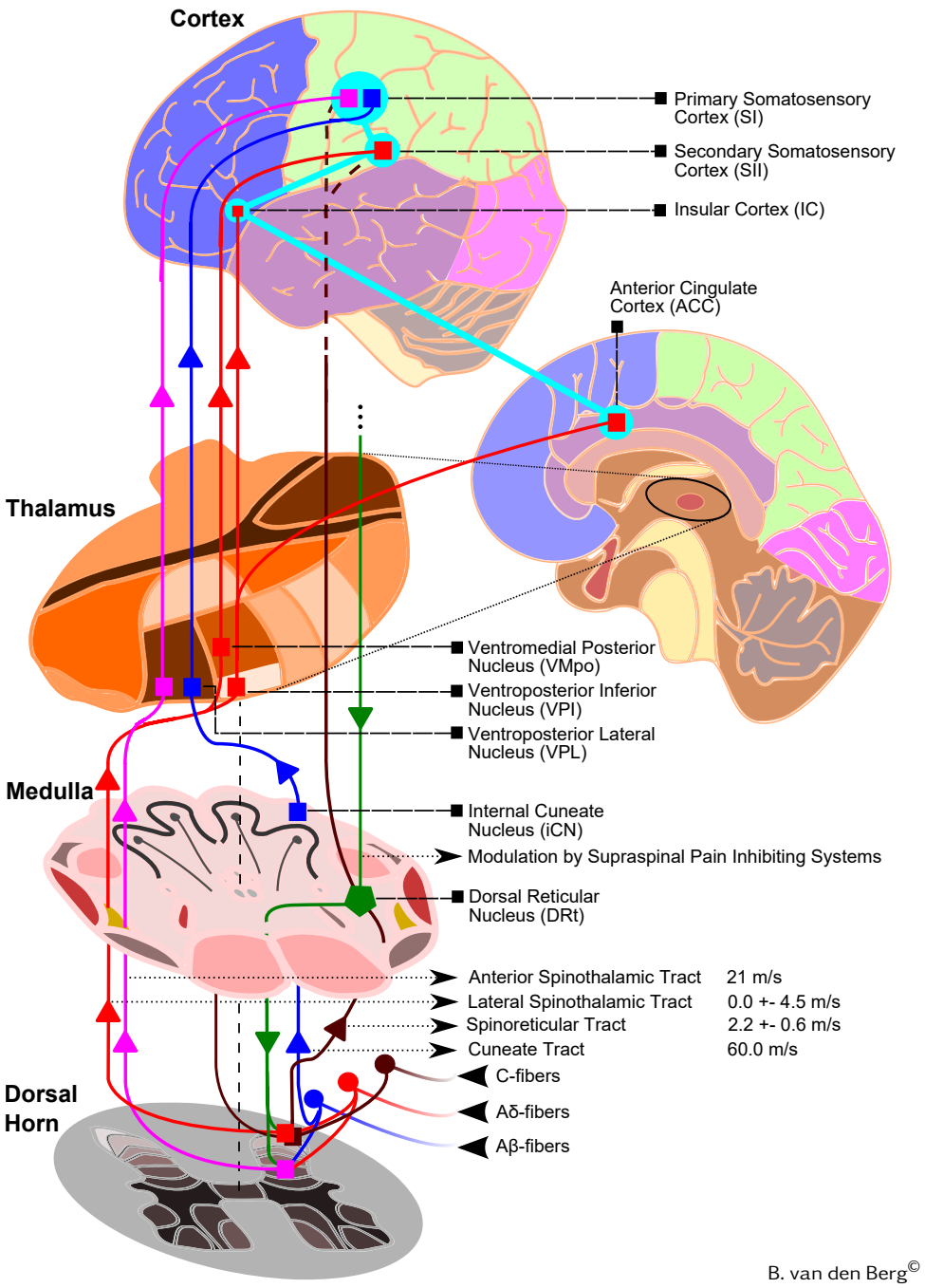

Figure 2.3: Illustration of several nociceptive pathways, as they are described in literature.

[1] Cortical activity related to nociception can therefore be observed in the contralateral part of the brain first, before the information is relayed to the other side of the cortex.

2.2.4 Nociception in the Cortex

Several brain areas have been shown to activate in response to nociceptive stimuli, including the primary somatosensory cortex (SI), secondary somatosensory cortex (SII), insular cortex (IC) and anterior cingulate cortex (ACC) [14–16]. The connections between those areas, as well as the several pathways of nociception are summarized in Figure 2.3.

One of the first and last areas to activate after a nociceptive stimulus is the SI [17]. The SI is somatotopically organized, which means that the location of a stimulus on the body is related to a specific location in the SI. Therefore, the SI is primarily related to the discrimination of stimulus location and the stimulus intensity. In addition to the SI, also the SII has been shown to represent stimulus intensity with a different somatotopic organization [18, 19]. The ACC and the IC receive afferents from the VMpo. In addition, the IC has been shown to have a forward connection to the ACC. Both areas belong to the limbic system and are thought to be involved in the emotional and cognitive aspects of pain [10, 14].

It is important to note that the same brain areas are also activated by other types of sensory stimuli. This means that, although it is possible to relate activation of those areas to nociceptive stimuli when the activity is phase-locked to the stimulus, it is not possible to relate a specific 'signature' of activation of those areas to pain in general [20]. Despite this overlap, there are subtle differences between the activation related to nociceptive stimuli and activation related to other modalities. For example, tactile information arriving from the cuneate tract has been shown to be projected from the VPL to Brodmann's area 3b and sequentially area 1 of the SI, while nociceptive specific information from the STT has been shown to be relayed directly from the thalamus to Brodmann's area 1 of the SI [21, 22]. However, so far it has not been possible to measure those differences with EEG due to it's spatial inaccuracy.

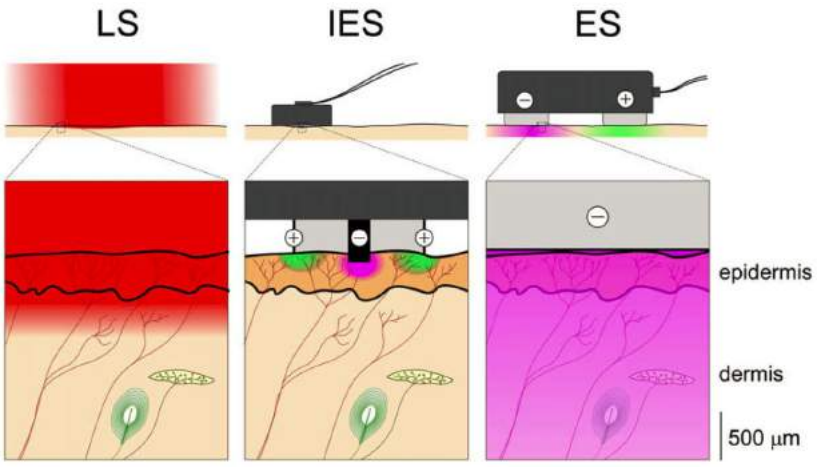

Figure 2.4: *The influence of laser stimulation (LS), intra-epidermal electrocutaneous stimulation (IES) and transcutaneous electrical stimulation (ES) on the skin. LS homogeneously stimulates superficial nociceptive afferents. IES acts as a point current source, and is suitable to exclusively stimulate the most superficial nociceptive afferents. ES creates an electric field that extends far beyond the skin, which therefore triggers other types of nervous afferents (e.g. mechanical). Adapted from Mouraux et al. [23].*

2.3 NOCICEPTIVE STIMULATION

A fundamental method to study the mechanisms of pain is through stimulation of nociceptive afferent nerve fibers in the skin. A wide variety of methods for nociceptive stimulation is available including mechanical (e.g. brushing and pinprick stimulation), thermal (e.g. cold pressor and heat stimulation), electrical (e.g. intra- and transcutaneous stimulation) and chemical (e.g. capsaicin and glutamate injection) methods [24]. Preferably, a method should be safe, reproducible and quantifiable. In addition, a method should specifically stimulate Aδ-fibers and C-fibers to study the nociceptive system without interferences from other systems [25]. Due to the quantifiabillity of subject responses, phasic electrical and laser stimuli are most commonly used and practical for analysis of nociceptive properties. Phasic laser stimulation is considered the best available tool to diagnose dysfunctions in the nociceptive system [26]. However, a great competitor of laser stimulation is intra-epidermal electrocutaneous stimulation (IES), which specifically activates nociceptors without damage to the skin. Advantages and disadvantages of both techniques are summarized in the next sections.

2.3.1 Laser Stimulation

Brief heat pulses generated by laser stimulators excite thermally sensitive free nerve endings in the superficial skin layers. A CO_2 or Thulium-YAG laser can be used to stimulate the most superficial skin layers within the epidermis, therefore exclusively activating nociceptive Aδ- and C-fiber afferents. However, the superficial penetration of laser light into the skin means that all energy will be absorbed by the skin, causing skin burns after application of multiple stimuli. Laser pulses with a shorter wavelength, such as pulses generated by Argon lasers, do not cause skin damage, but penetrate deeper into the skin causing aselective activation of afferents and possible vascular damage [27]. Despite those drawbacks, laser stimulation has been the golden-standard in nociceptive stimulation due to it's ease of use and quantifiable subject responses. A painful laser stimulus elicits a clear augmentation of the brain signal, providing insight into central nociceptive processing [28]. However, tissue damage and peripheral sensitization due to laser stimulation might affect the quality of those results [29].

2.3.2 Intra-epidermal Electrocutaneous Stimulation

During intra-epidermal electrocutaneous stimulation (IES), the localized current selectively activates superficial afferents. Stimulation around the detection threshold results in specific activation of Aδ- and C-fiber afferents without damage to the skin. Merits of IES are that (1) no expensive equipment is required for stimulation, (2) the stimulation can be applied to any part of the body and (3) a strictly time-locked response is generated since stimuli only generate a single action potential in peripheral nerve fibers. A drawback of IES is the limited amount of current that can be applied if one only wants to stimulate Aδ- and C-fiber afferents [25]. For example, a study by Mouraux et al. [23] showed that IES stimulation of 2.5 mA causes activation of Aβ-fibers. Therefore it is recommendable to only apply currents far below this value. However, the sensation of a stimulus as well as the brain response can be enhanced by applying multiple-stimuli consecutively, such as in a pulse train. In addition, the intensity of perception is enhanced by the IES electrode used in this study by using multiple needles in

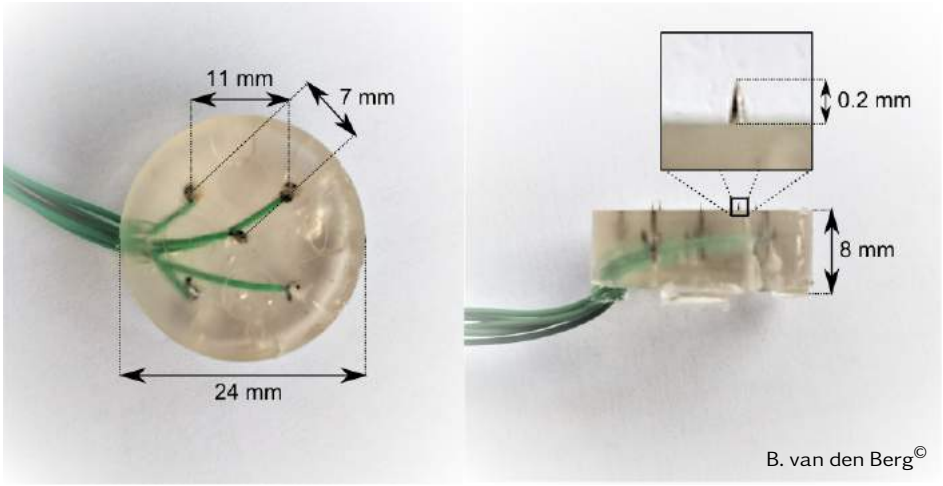

Figure 2.5: *Intra-epidermal needle electrode for nociceptive stimulation. The needles have a length of approximately 0.2 mm, enabling penetration of the stratum corneum and invasion of the most superficial layers in the epidermis. Due to it's ability to specifically stimulate nociceptive Aδ- and C-fiber afferents, this electrode is used in this thesis.*

one electrode. Figure 2.5 shows the used electrode, which was originally developed by Steenbergen et al. [30].

2.4 Psychophysical Measurements of Nociception

Psychophysics is a discipline dealing with the relationship between physical stimuli and their subjective correlates. Psychophysical methods can generally be applied to any sensory system for determining essential properties of the system, such as the sensation threshold [31]. Modern psychophysics involves measurement of those properties using adaptive paradigms which are often statistically optimized to converge to the true value. Using such a paradigm, the stimulus-response behavior of the nociceptive system can be measured. For example, Doll et al. [32] developed a method for continuously estimating the psychometric function of pain perception. In this section, important principles of psychophysics will be explained first, after which the method of Doll et al. will be outlined.

2.4.1 Stimuli and Perception

In psychophysics a mathematical approach is developed for relating the external physical world, stimuli, to the psychological domain, perception. In this context, perception can be defined as the ability to see, hear, or become aware of something through the senses. A stimulus can be defined as a physical object or event that evokes a specific functional reaction in an organ or tissue. Several paradigms have been developed to measure data about the relation between stimuli and perception. For example, in the method of constant stimuli the experimenter presents a set pre-determined stimuli which the subject has to compare to a reference stimulus to determine whether the stimulus is stronger or less strong than the reference. In the method of limits the experimenter varies the stimulus amplitude in ascending or descending steps while the subject reports if the stimulus is stronger or less strong than the reference [33]. Both methods present effective paradigms for measuring stimulus perception, but differ in efficiency. While the first paradigm uses pre-determined stimuli, the second paradigm is adaptive and can be expected to converge towards a step-dependent

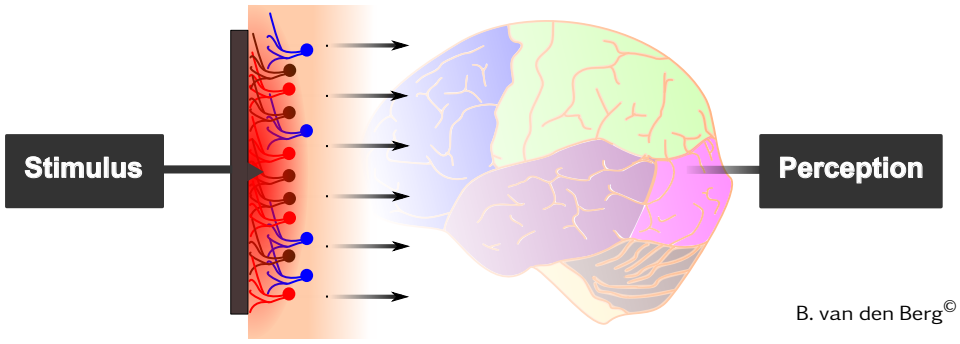

Figure 2.6: *Psychophysics investigates the direct relation between stimuli and perception.*

range around the true value. Therefore, the second method will require less repeated measures to accurately estimate the psychometric curve.

2.4.2 Psychometric Curve and Threshold Estimation

The psychometric curve is the probability density function representing the chance that the subject indicates that the stimulus is stronger than the reference. Based on the so-called high-threshold theory, this function is assumed to have the shape of a cumulative normal distribution. This theory states that a stimulus is perceived when accumulated sensory evidence exceeds a fixed internal criterion [31]. In this theory, noise of sensory evidence is assumed to be normally distributed, since the decision of a subject is determined by the sum of a large amount of neurons with each a random firing probability. However, in psychophysics the error distribution is shown to converge in its tails to a constant value instead of zero. This observation can be explained by the fact that, even when there is no stimulus present, the subject's mind can perceive a stimulus due to background activity, which causes a left-sided tail to the distribution. The right-sided tail can be explained by the fact that, even when there is a clear stimulus present, the subject's mind can fail to perceive this stimulus due to distractions or background activity. Both phenomena are respectively referred to as guessing and lapsing.

The cumulative normal distribution can be approximated by the logistic function, given by Equation 2.1, which is analytically more tractable. Therefore, the psychometric curve is generally described in psychophysical literature by Equation 2.2, in which $F(x;\theta,\sigma)$ denotes the logistic function with stimulus x, threshold θ and slope σ while γ and λ refer to the guessing and lapsing probability respectively.

$$F(x;\theta,\sigma) = \frac{1}{1+\exp^{-\sigma(x-\theta)}} \tag{2.1}$$

$$\psi(x;\theta) = \gamma + (1-\gamma-\lambda)F(x;\theta,\sigma) \tag{2.2}$$

The psychometric function can be estimated by maximizing the likelihood of the logistic curve. Such a procedure is described by Treutwein and Strausberger [35]. Their simulations have shown that this method provides a relatively unbiased estimate[1]of the threshold and slope of the psychometric

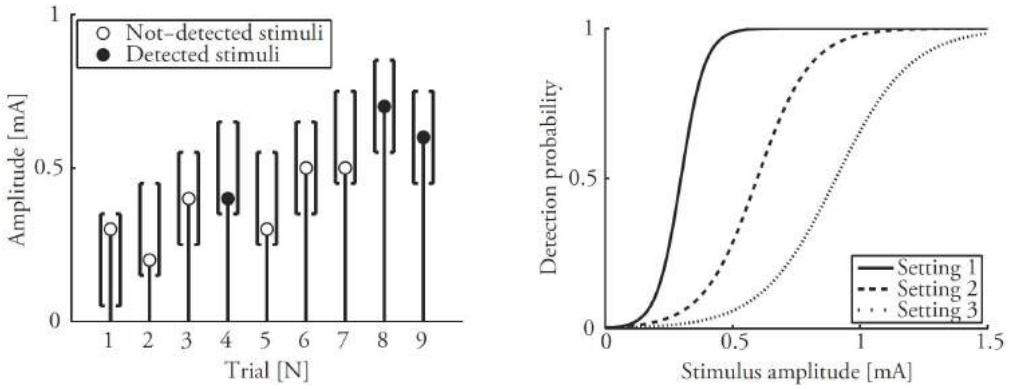

Figure 2.7: The method of threshold tracking from Doll et al. [32]. Left: The expected value of the randomized stimulus is increased/decreased during every step based on the subject's response. Right: By applying this paradigm for multiple stimulus types, either sequentially or simultaneously using multiple threshold tracking, the psychometric function can be estimated. Adapted from Doll et al. [34].

function for paradigms resembling the method of constants. However, for adaptive methods resembling the method of limits, this method has an accurate unbiased estimate for the threshold but an inaccurate negatively biased estimate for the slope. This occurs because the method of limits has been designed to measure the threshold and converges to points close to this threshold. When the method of limits approaches the threshold from below, there are mainly measurements around the threshold and a few below, resulting in a large variabillity of the slope estimation with a negative bias. The only methods to correct for this bias are by measuring over a wider range of values, which would decrease the accuracy of the threshold estimate, or by increasing the amount of repeated measures.

2.4.3 Multiple Threshold Tracking (MTT)

Based on the method of limits, Doll et al. [32] introduced a paradigm for tracking non-stationary psychophysical thresholds. However, in contrast with the method of limits, their method randomizes the stimulus for every step to prevent identification of the method by the subject, which might bias the results. This paradigm is shown in figure 2.7. To compute the psychometric function they use generalized linear regression to compute the model parameters in equation 2.3. In the work of Doll et al., stimulus amplitude, number of pulses and time with respect to the start of the trial are used as predictors in this model.

$$\ln\left(\frac{p(y_j)}{1-p(y_j)}\right) = \beta_0 + \sum_{k=1}^{p} \beta_k x_{jk} + \eta_j \tag{2.3}$$

For $j \in \{1, \ldots, m\}$ where:

- The binomial outcome variable for the j-th trial is given by: $y_j \in \{0, 1\}$
- The probability of an outcome is: $\{p(y_j) \in \mathbb{R} \mid 0 \leq p(y_j) \leq 1\}$

[1] Depending on the true values, for more information please refer to Treutwein and Strausberger [35].

- The intercept for the regression model is: $\beta_0 \in \mathbb{R}$
- The slope for the k-th predictor is: $\beta_k \in \mathbb{R}$
- The j-th measurement of the k-th predictor is: $x_{jk}(\tau) \in \mathbb{R}$
- The model residual is[1]: $\eta_j \overset{\text{iid}}{\sim} \mathcal{N}(0, \sigma_\eta^2)$

In simulations it was shown that applying linear regression to a limited time-window provides a relatively unbiased estimate of the slope and the threshold of the psychometric function. In further research, Doll et al. [34] have shown that this method also manages to simultaneously track multiple psychometric thresholds, e.g. with multiple types of stimuli. To do so, this method applies the threshold tracking paradigm to multiple types of stimuli, with random variations in stimulus order, as is shown in Figure 2.8. By doing so, this method has the benefit over other methods that it is possible to study different types of stimuli, such as stimuli with a different number of pulses. By varying the stimulus type randomly, observer and subject bias are decreased.

2.5 MEASUREMENT OF NOCICEPTIVE CORTICAL ACTIVITY

To study cortical activity related to nociceptive processing, an accurate measurement method for temporal and spatial variations in local potentials is required. Various techniques have been developed to observe such variations. In increasing order of temporal accuracy, these techniques include positron emission tomography (PET), functional magnetic resonance imaging (fMRI), magnetoencephalography (MEG), electroencephalography (EEG) and microneurography (MN). Although PET and fMRI provide a high spatial accuracy, they do not provide a high temporal accuracy, which is required for studying nociceptive evoked brain responses, which are thought to occur in much less than a second. While MEG is temporally accurate and provides a higher spatial resolution than EEG, it is mainly sensitive to tangential current sources in the sulci. A spatially and temporally accurate technique is MN. However, this technique is tedious and very invasive since it requires the insertion of needle electrodes at exact pre-determined locations inside the brain. Therefore EEG

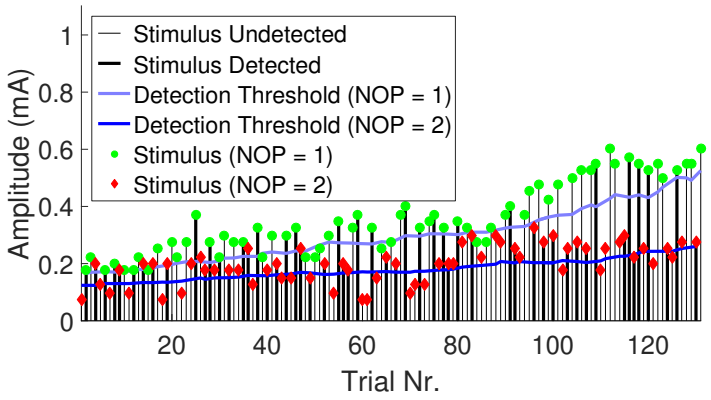

Figure 2.8: *The MTT measurement method applies multiple types of stimuli in a randomized sequence. By measuring the subject's responses a psychophysical threshold can be determined by generalized linear regression. For more information, please refer to Doll et al. [34].*

[1] The abbreviation 'iid' in the equation stands for: Independent and Identically Distributed.

provides a good trade-off between temporal and spatial accuracy besides being relatively low-cost and easy to use.

2.5.1 Electroencephalography

Electroencephalography was first measured on human subjects by Hans Berger in 1924. Using EEG, he observed that brain rhythms are dependent on a person's state of consciousness. In the first half of last century, EEG has mainly been used to study spontaneous brain activity, such as EEG during REM sleep and the EEG during an epileptic seizure [36]. Later on, EEG was also used frequently to study phase-locked brain activity related to events, the so-called evoked potentials (EP) or event-related potentials (ERP).

The EEG technique is mainly sensitive to radially oriented current sources in the brain, but can also measure tangential activity due to conduction effects, therefore measuring activity from the cortical gyri as well as the sulci. However, it is important to realize that the main part of the measured signal is generated by large masses of synchronously firing neurons on the surface of the cortical gyri. A large part of the measured activity consists of so-called 'spontaneous' activity: activity which cannot be related to an event. In EEG research, the signal of interest is often related to an event, which is a stimulus, activity or thought. In general, those signals are measured with a signal-to-noise ratio (SNR) far below one and require statistical techniques to extract significant information, which will be treated in Section 2.7.

2.5.2 Evoked Potential

One way to characterize EEG activation with respect to nociceptive stimuli is the evoked potential (EP). The EP is the transient response of the cortex to a stimulus and is measured by phase-locked activity in the EEG after stimulus administration [37].

In literature, components in the EP are generally described based on the polarity of the maximum amplitude, which is positive (P) or negative (N), and the order in which these components occur (1,2,3, etc.). However, in the description of experimental results, these peaks are generally described by their polarity and the time (in ms) at which the component reaches the maximum value (e.g. 420 ms), since those components are only matched with the components found in literature in the discussion section.

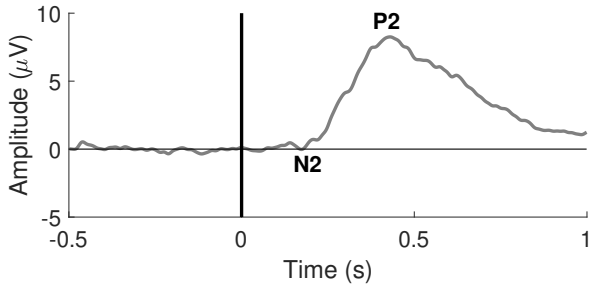

Figure 2.9: *Evoked potential at the CPz-M1M2 derivation (with a band-pass filter of* 0.1 Hz *to* 40.0 Hz*) in response to a nociceptive stimulus, averaged over 12 subjects.*

Important components of nociceptive EPs in literature include the N1, N2 and P2. An example of an EP including a possible N2 and P2 is shown in Figure 2.9. Those components are thought to represent processing of sensory stimuli in the brain. The N1 and N2 are early negative components, best measured at the lateral side of the head (e.g. T7-FPz), which are thought to originate from activity in the somatosensory cortices. Since the N1 peak is the first activation feature in the EEG to emerge after stimulation, it is thought to reflect early sensory processing, while the N2 component has been shown to modulate stimulus perception with respect to attention. Another major component is the P2, which can be measured at central locations of the scalp (e.g. Cz-A1A2) and originates from the ACC [38, 39]. The P2 is thought to be related to arousal and attention [40–42]. The N1 as well as the N2 and P2 peaks are not considered to be specific to nociceptive stimuli, but rather related to stimulus salience of both sensory and nociceptive stimuli [7, 43]. Therefore, they are rather a modulated representation of the signals from nociceptive afferents entering the brain.

2.6 MTT-EP SETUP

In earlier work, the MTT-EP setup has been developed with the objective to measure nociceptive evoked potentials during psychophysical response measurements [44]. To do so, instrumentation and protocols of the MTT setup have been linked to instrumentation of an EEG setup for measuring EPs. The MTT setup, available at the BSS group of the University of Twente, uses the procedure described by Doll et al. [34] to perform multiple threshold tracking[1]. For stimulation, the setup uses a NociTrack Ambustim stimulator, which generates square current pulses for cathodal intra-epidermal stimulation

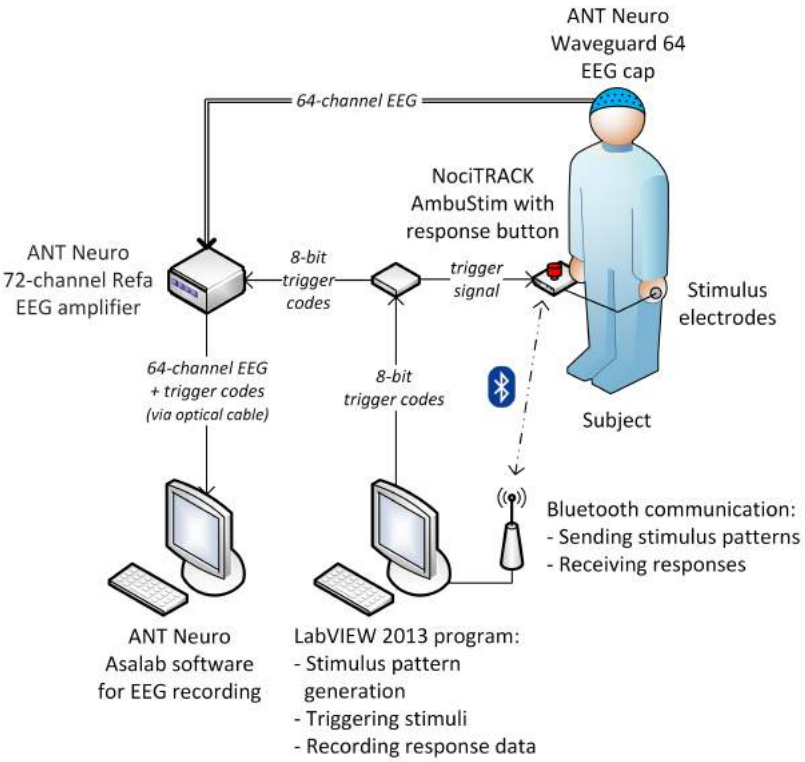

Figure 2.10: *The MTT-EP setup. Adapted from Schooneman [44].*

with electrode described in section 2.3. The setup for EEG measurement contains a 64-channel ANT Waveguard electrode cap with a 72-channel TMSi Refa amplifier[2] and a 128-channel ANT Waveguard electrode cap with a 136-channel TMSi Refa amplifier[3]. The stimulator is controlled via Bluetooth with a LabView application on a desktop computer, sending the stimulus sequences according to the MTT procedure and receiving the subject's response, which is measured using the stimulator's response button. The EEG signals are recorded using ANT ASA software and preprocessed using the Fieldtrip toolbox [45] in Matlab.

Both setups are linked together by a trigger cable, which connects the desktop computer running the LabView application with the EEG amplifier and the stimulator. Therefore, the stimulator and amplifier receive the trigger signal simultaneously. The 255-bit trigger signal includes all information about the stimulus settings, which is used for accurate event-related epoch extraction from the EEG signal during preprocessing and registration of the settings related to every epoch. The combination of both setups is depicted schematically in figure 2.10.

2.7 Analysis of Evoked Potentials

EEG data obtained during a multi-stimulus experiment on multiple subjects is a high-dimensional dataset with a considerable amount of background activity and therefore challenging dataset to analyze. Due to the low signal-to-noise ratio (SNR), the measured signal has a high trial-to-trial variability despite application of band-pass filtering and removal of EOG components. This is partly due to the nature of EEG background activity, which often has a $1/f$-scaled power spectrum [46], containing significant power in the same frequencies as the EP. Several methods are available to deal with this variability.

2.7.1 Timelocked Averaging

The most common method to estimate the EP is averaging of the phase-locked signal over a big set of trials of the same category, which works under the assumption that the noise is centered around zero and ergodic. A better understanding of the method can be obtained by looking at a set of trials of which the stimulus parameters are the same. First, the measured signal (y_j) during a trial (j) can for every specific point in time with respect to the stimulus be split into the evoked potential $(\beta_0(\tau))$, which is assumed to be trial-invariant, and a residual (η_j) such as in Equation 2.4.

$$y_j(\tau) = \beta_0(\tau) + \eta_j(\tau) \tag{2.4}$$

[1] For more information, please refer to section 2.4.
[2] Used with the exploratory measurements of M. Schooneman, which are analyzed in Chapter 4.
[3] Used with the experiment described in Chapter 5.

If we measure the signal during m EEG trials, we can minimize the residual using least mean squares estimation which leads to Equation 2.5. This is equal to taking the average over m trials.

$$\frac{1}{m}\sum_{j=1}^{m} y_j(\tau) = \hat{\beta}_0(\tau) \tag{2.5}$$

As is shown in Equation 2.6, this reduces the variance of the noise (σ^2) by a factor m, when it is assumed that the variance among trials is caused by stationary noise. Therefore, averaging m trials also leads to an increase in the SNR of a factor m.

$$Var\left(\frac{1}{m}\sum_{j=1}^{m} y_j(\tau)\right) = \frac{1}{m^2}\sum_{j=1}^{m} Var(y_j(\tau)) = \frac{1}{m^2} m\sigma^2 = \frac{1}{m}\sigma^2 \tag{2.6}$$

Since the SNR is usually very low in EEG measurements, about 0.3 to 0.01 in measurements of nociceptive EPs, this method requires a big amount of trials to obtain a reliable estimate for the true values of $\beta_0(\tau)$. The number of measurements especially increases when the EP has to be determined for multiple combinations of fixed effects. Additionally, averaging implicitly assumes an unbiased random distribution of the EP values over multiple trials. However, this is not valid if any trial has an influence on future trials, such as is the case with habituation effects.

Despite these drawbacks, this method is commonly used in research. In current nociception research, this method appears to be the golden standard and is frequently used [38, 43, 47].

2.7.2 Linear Regression

A more efficient method of dealing with EPs is by using linear regression. Linear regression computes the optimal linear model by minimizing the residual in Equation 2.7, which is equivalent to fitting an p-dimensional plane to p predictors using a set of m trials.

$$y_j(\tau) = \beta_0(\tau) + \sum_{k=1}^{p} \beta_k(\tau) x_{jk} + \eta_j(\tau) \tag{2.7}$$

For $j \in \{1, ..., m\}$ where:

- The outcome variable for the j-th measurement at time τ is given by: $y_j(\tau) \in \mathbb{R}$
- The fixed intercept for the regression model is at time τ: $\beta_0(\tau) \in \mathbb{R}$
- The fixed slope for the k-th predictor at time τ is: $\beta_k(\tau) \in \mathbb{R}$
- The j-th measurement of the k-th fixed predictor at time τ is: $x_{jk}(\tau) \in \mathbb{R}$
- The model residual at time τ is[1]: $\eta_j(\tau) \overset{\text{iid}}{\sim} \mathcal{N}(0, \sigma_\eta(\tau)^2)$

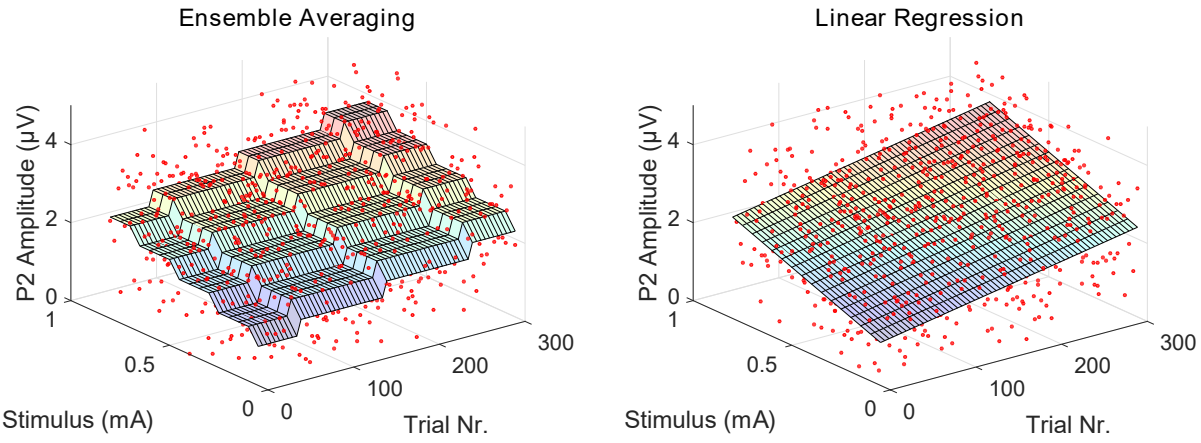

Figure 2.11: *Linear regression fits an p-dimensional plane to p predictors, whereas averaging fits a constant value per subset of variables, which is also referred to as ensemble or pooled averaging.*

Equation 2.4 can be considered an extremely simple linear model. However, the model in Equation 2.4 just accounts for a single factor or a single combination of factors, since the presence of unmodeled significant factors will result in confounding and therefore in incorrect results. Equation 2.7 takes linear combinations of multiple factors into account, which could include both categorical effects by dummy coding[2] and factors with a continuous scale. While in classical EEG research Equation 2.4 is solved separately for every combination of factor levels, Equation 2.7 estimates the EPs for every combination at once using all trials available by assuming that the effects are linear, resulting in a significantly lower SNR of the computed EP.

Although the assumption of linearity of brain activity with respect to stimuli might seem arbitrary, the general linear model[1] is already very popular in fMRI research [48]. In addition, the assumption of linearity often turns out to result in a useful model of brain activity in the EEG [49]. The correctness of this assumption can be studied using the residual, which will be demonstrated in Section 3.4.1.

Linear modeling of EEG signals has attracted substantial attention in the last decade. For example, marginal linear models have been proven useful to study psycholinguistic brain processes. Hauk et al. [50] have used multiple linear regression to study visual word recognition and to test the significance of various word properties during recognition. In another article [51], the same researchers specifically emphasize the value of multiple linear regression in combination with source localization. More recently, the method of analyzing EPs using multiple linear regression has been generalized into a framework allowing for analysis of EPs using linear regression, overlap correction [49] and non-linear regression [52]. Despite the succesfull application of this method and its efficiency in treating data, this method has barely been applied to EEG signals in nociception research. As one of the few, Schulz et al. [53] have used a linear model to fit EEG activity of every electrode at every frequency to the pain perceived by the subjects, to determine areas and frequencies of interest in pain perception. Other articles on linear modeling in nociception research are written by Vossen et al. [54], who propose to analyze EPs using linear mixed models, which will be treated in the next section.

[1] The abbreviation 'iid' in the equation stands for: Independent and Identically Distributed.

[2] Assigning a categorical factor with 0 or 1 for every category.

2.7.3 Linear Mixed Models

Since linear models provide a method for modeling all linearly correlated factors in one model, they provide efficient means of studying data within a single subject. Additionally, when a linear model is applied to data from multiple subjects, the linear model provides an estimation of the average factors and their associated response over all subjects. However, a linear model does not account for variation among subjects, e.g. differences in brain activity of the subject due to age, gender, genes or unknown subject-specific factors. In addition, they do not quantify the contribution of separate random factors, such as the subject, to the model residual. When it is more appropriate to take random effects into account, a linear mixed-effects model can be used to explain the data. This model can generally be written as Equation 2.8, when there are n subjects, m trials per subject and p predictors.

$$y_{ij}(\tau) = \beta_0(\tau) + \sum_{k=1}^{p} \beta_k(\tau) x_{ijk} + v_{i0}(\tau) + \sum_{k=1}^{p} v_{ik}(\tau) z_{ijk} + \eta_{ij}(\tau) \tag{2.8}$$

For $i \in \{1, ..., n\}$ and $j \in \{1, ..., m_i\}$ where:

- The outcome variable for the j-th measurement of the i-th subject at time τ is given by: $y_{ij}(\tau) \in \mathbb{R}$
- The fixed intercept for the regression model is at time τ: $\beta_0(\tau) \in \mathbb{R}$
- The fixed slope for the k-th predictor at time τ is: $\beta_k(\tau) \in \mathbb{R}$
- The j-th measurement of the k-th fixed predictor for the i-th subject at time τ is: $x_{ijk}(\tau) \in \mathbb{R}$
- The random intercept for the i-th subject at time τ is[1]: $v_{i0}(\tau) \overset{\text{iid}}{\sim} \mathcal{N}(0, \sigma_0(\tau)^2)$
- The random slope for the k-th predictor of the i-th subject at time τ is[1]: $v_{ik}(\tau) \overset{\text{iid}}{\sim} \mathcal{N}(0, \sigma_k(\tau)^2)$
- The j-th measurement of the k-th random predictor for the i-th subject at time τ is: $z_{ijk} \in \mathbb{R}$
- The model residual at time τ is[1]: $\eta_{ij}(\tau) \overset{\text{iid}}{\sim} \mathcal{N}(0, \sigma_\eta(\tau)^2)$

In addition to fitting an n-dimensional plane, this equation can account for the dependence of data within random factors, e.g. by including a random intercept and random slope that is dependent on the subject. This is done by assuming that the random factors can be parametrized by a multivariate normal distribution, resulting in a more robust within-subject estimate of the fixed-effects. Depending on the method of fitting the model, additional constraints are applied on the covariance matrix of the multivariate distribution to reduce the number of parameters, which can increase the significance of computed parameters.

Linear mixed-effect models are a widely applied statistical method for analyzing data with a hierachical component. However, they are not often used in the analysis of EEG signals, possibly due to the the important role ANOVA historically played in neuroscientific research. In the last decade,

[1] The abbreviation 'iid' in the equation stands for: Independent and Identically Distributed.

the technique has been adopted in several neurolinguistic applications and in the analysis of EPs. In nociception research, Vossen et al. [54] proposed the first linear mixed model of nociceptive EPs to model group-specific habituation effects. They argue that linear-mixed modeling allows for a large number of repeated measures without using many subjects, that it deals more efficiently with missing data than the ANOVA, that it is flexible in modeling covariates and correlation structures and that it can incorporate random factors. This being said, it is easy to conclude that linear mixed modeling provides an efficient method to deal with EP data.

2.7.4 Non-linear Mixed Models

Even though the assumption of linearity is approximately valid in many cases, in some cases it might be desirable to derive a non-linear model, such as when the residual does not appear to be normally distributed. Especially in phenomena related to perception a logistic curve might be more likely than a linear curve. This curve can succesfully be approximated by a predictor with a logistic basis function, which is simply done by transforming the independent variable using this function. Complex non-linear functions can be approximated using a combination of multiple non-linear basis functions. In this case, the regression can be computed by simply extending the set of predictors with their non-linear transformations. For example, this method can be applied to the linear mixed model in Equation 2.9.

$$y_{ij}(\tau) = \beta_0(\tau) + \beta_1(\tau)x_{ij1} + v_{i0}(\tau) + v_{i1}(\tau)z_{ij1} + \eta_{ij}(\tau) \tag{2.9}$$

If a quadratic effect from predictor x_{ij1} is expected, this equation can be rewritten to Equation 2.10 to account for the related non-linear variation.

$$y_{ij}(\tau) = \beta_0(\tau) + \beta_{1,1}(\tau)x_{ij1} + \beta_{1,2}(\tau)x_{ij1}^2 + v_{i0}(\tau) + v_{i1,1}(\tau)z_{ij1} + v_{i1,2}(\tau)z_{ij1}^2 + \eta_{ij}(\tau) \tag{2.10}$$

If the shape of a non-linear function is unknown, this function might still be approximated by a set of non-linear basis functions, e.g. the cubic B-spline basis functions, by creating a transformed predictor for every basis function in the set. The regression will automatically determine the optimal combination of those basis functions in this case.

Non-linear modeling of EPs has been implemented in several publications. For example, Tremblay et al. demonstrated a framework for non-linear mixed EP analysis with applications in psycholinguistics [55]. In addition, non-linear modeling of EPs has been applied for succesful analysis of the effect of stimulus response times in a forced go/no-go task, by separating the EP related to the stimulus from the EP related to the response [52]. In nociception research, Vossen et al. [54] were the first to introduce non-linear modeling in the analysis of EPs, which was applied within the framework of the linear-mixed model presented in their article. By incorporating an inverse, an exponential and a quadratic basis function for the effect of trials, they demonstrated a significant non-linear habituation effect. Additionally, in a later publication, this model was used for the comparison of subjects with chronic pain to healthy subjects, in which subjects with chronic pain were shown to exhibit significantly less habituation effects [56].

2.8 DISCUSSION

Chronic pain is a big burden to society, causing continuous discomfort to the patients and a considerable negative economic impact by decreasing an individuals ability to live and to work [1]. Even though significant efforts have been made throughout history to study and describe the nociceptive system, our current knowledge does not provide satisfactory explanations for chronic pain yet, complicating diagnosis and treatment. Despite the wealth of information provided by thousands of neuroimaging studies on pain, most studies do not attempt to find a suitable clinical measure [57]. Although chronic pain is generally related to clearly described clinical phenomena, such as central sensitization [58] and several abnormalities in brain activity [59], the occurence in patients is difficult to predict and to assess due to a lack of objective and specific diagnostic methods.

Detection and perception of nociceptive stimuli can be measured using psychophysical methods, which measure the stimulus-response behavior of the subject. Using such methods, the sensation and pain threshold can be used to track the development of chronic pain [60, 61]. However, major drawbacks of those measurements are that they depend on the subjective perception of the stimuli and that they are not specific to central or peripheral properties of the nociceptive system. A method to observe multiple time-dependent psychophysical functions simultaneously was developed by Doll et al. [34]. By tracking the sensation threshold for multiple types of stimuli simultaneously, properties of peripheral (e.g. Aδ-fiber recruitment) and central (e.g. synaptic summation) processing of nociceptive stimuli can be measured. However, this method does depend on the subjective interpretation of the sensation related to the nociceptive system and does not include a direct measure of neurophysiological activity related to nociception.

Objective information about the nociceptive system can be obtained by measuring the neurophysiological activity related to nociception. Due to a high temporal resolution, EEG signals are suitable to study the cortical activity related to nociception [62]. By measuring the EEG signal of a specific part of the cortex, stimulus-related activity can be interpreted based on the neuroanatomical connections and functional descriptions of this part. More specifically, early components of the EP at lateral EEG derivations are thought to originate from the activation of somatosensory cortices and related to early sensory processing of stimuli and top-down modulation by attention. On the other hand, late positive components at central EEG derivations originate from activation of the ACC and are thought to be related to stimulus perception, arousal and attention [38]. Input to the SI originates from the cuneate tract and the anterior spinothalamic tract, while input to the SII originates from the subthalamic tract [14–16]. By combining this anatomical information with assumptions about the function of the nociceptive

Primary Objective

Describe the quality and content of electrical brain responses of pain free subjects to electrocutaneous stimuli during multiple threshold tracking by analyzing the variance of averaged responses and by exploration of the use of a linear mixed model to explain the variability in these responses.

Questions

Can a linear mixed model be used to improve analysis of the evoked potential during multiple threshold tracking?

- To which extend can a LMM be used to describe the data?
- To which extend can a LMM improve the quality of the measurements?
- Are the LMM coefficients significant in exploratory data?

system, components of the EP can be proscribed to the behavior of specific parts of the nociceptive system, which can be used to formulate a parametric model of nociception.

To measure significant variations of the EP with respect to nociceptive stimuli, advanced signal processing and statistical analysis techniques are required to attenuate background activity and amplify the signal to an observable level. Reduction of background activity and analysis of EP components is normally done by averaging the EEG signal over multiple trials. However, since the stimulus amplitude during multiple threshold tracking is around the detection threshold, the SNR of related EPs is problematic. Due to the considerable amount of noise and a large amount of stimulus parameters, including stimulus amplitude, inter-pulse interval, stimulus detection and trial number, averaging does not provide sufficient noise reduction for the analysis of these electrocutaneous nociceptive EPs. However, a linear mixed model can be used to combine information of all trials to effectively enhance the SNR, compute model parameters and test for significant modulations by stimulus properties [49, 52, 54].

Secondary Objective

Analyze if and how brain responses are associated with the properties of applied stimuli, the amount of previously received stimuli and the response of the subject concerning the stimulus.

Questions

How is neurophysiological activity related to stimulus parameters during multiple threshold tracking?

- Can evoked potentials be used in combination with multiple threshold tracking to observe relations between stimulus properties and the neurophysiological response?
- Which stimulus parameters are significantly related to the neurophysiological response during multiple threshold tracking ?
- To which extend is neurophysiological activity dependent on stimulus parameters?

The **aim** of this work is to combine the technique of multiple threshold tracking with EEG recording and analysis to observe neurophysiological activity during nociceptive processing. Succesfully dealing with noise and background activity is essential for obtaining interpretable data. Therefore, the **primary objective** of this work is to describe the quality and content of electrical brain responses of pain free subjects to electrocutaneous stimuli during multiple threshold tracking by analyzing the variance of averaged responses and by exploration of the use of a LMM to explain the variation in these responses. To study if these brain responses could provide a useful objective measure to assess peripheral and central functions of the nociceptive system, the **secondary objective** of this study is to analyze if and how brain responses are associated with the properties of applied stimuli (e.g. stimulus amplitude, number of pulses and inter-pulse interval), the stimulus application time (e.g. the number of received stimuli) and the response of the subject concerning the stimulus (e.g. stimulus detection).

Bibliography

[1] P. C. Langley, "The prevalence, correlates and treatment of pain in the European Union", *Current Medical Research and Opinion*, vol. 27, no. 2, pp. 463–480, 2011.

[2] R. Melzack and P. D. Wall, "Pain mechanisms: A new theory", *Science*, vol. 150, no. 3699, pp. 971–979, 1965.

[3] Hippocrates, *Hippocratic Writings*. Penguin Classics, 1984.

[4] L. Tosunlar and S. Richards, "History of chronic pain", 2003.

[5] D. Santoro, G. Bellinghieri, and V. Savica, "Development of the concept of pain in history", *Journal of Nephrology*, vol. 24, no. SUPPL. 17, S133–S136, 2011.

[6] K. Inui, T. Tsuji, and R. Kakigi, "Temporal analysis of cortical mechanisms for pain relief by tactile stimuli in humans", *Cerebral Cortex*, vol. 16, no. 3, pp. 355–365, 2006.

[7] G. D. Iannetti and A. Mouraux, "From the neuromatrix to the pain matrix (and back)", *Experimental Brain Research*, vol. 205, no. 1, pp. 1–12, 2010.

[8] C. E. Steeds, "The anatomy and physiology of pain", *Surgery (Oxford)*, vol. 34, no. 2, pp. 55–59, 2016.

[9] M. J. Hudspith, "Anatomy, physiology and pharmacology of pain", *Anaesthesia and Intensive Care Medicine*, vol. 17, no. 9, pp. 425–430, 2016.

[10] K. Usunoff, A. Popratiloff, O. Schmitt, and A. Wree, "Functional neuroanatomy of pain.", *Advances in anatomy, embryology, and cell biology.*, vol. 184, pp. 1–115, 2006.

[11] G. Cruccu, G. Iannetti, R. Agostino, A. Romaniello, A. Truini, and M. Manfredi, "Conduction velocity of the human spinothalamic tract as assessed by laser evoked potentials", *NeuroReport*, vol. 11, no. 13, pp. 3029–3032, 2000.

[12] Y. Qiu, K. Inui, X. Wang, T. D. Tran, and R. Kakigi, "Conduction velocity of the spinothalamic tract in humans as assessed by CO2 laser stimulation of C-fibers", *Neuroscience Letters*, vol. 311, no. 3, pp. 181–184, 2001.

[13] E. M. Van der Heide, "Neurophysiological observation of the nociceptive system using electrocutaneous stimulation", Thesis, 2009.

[14] D. Bouhassira, L. Villanueva, Z. Bing, and D. le Bars, "Involvement of the subnucleus reticularis dorsalis in diffuse noxious inhibitory controls in the rat", *Brain Research*, vol. 595, no. 2, pp. 353–357, 1992.

[15] R. Peyron, B. Laurent, and L. García-Larrea, "Functional imaging of brain responses to pain. a review and meta-analysis (2000)", *Neurophysiologie Clinique*, vol. 30, no. 5, pp. 263–288, 2000.

[16] R.-D. Treede, D. Kenshalo, R. Gracely, and A. Jones, "The cortical representation of pain", *Pain*, vol. 79, no. 2-3, pp. 105–111, 1999.

[17] L. Hu, E. Valentini, Z. G. Zhang, M. Liang, and G. D. Iannetti, "The primary somatosensory cortex contributes to the latest part of the cortical response elicited by nociceptive somatosensory stimuli in humans", *NeuroImage*, vol. 84, pp. 383–393, 2014.

[18] L. Timmermann, M. Ploner, K. Haucke, F. Schmitz, R. Baltissen, and A. Schnitzler, "Differential coding of pain intensity in the human primary and secondary somatosensory cortex", *Journal of Neurophysiology*, vol. 86, no. 3, pp. 1499–1503, 2001.

[19] K. Torquati, V. Pizzella, S. Della Penna, R. Franciotti, C. Babiloni, P. Rossini, and G. Romani, "Comparison between SI and SII responses as a function of stimulus intensity", *NeuroReport*, vol. 13, no. 6, pp. 813–819, 2002.

[20] L. Hu and G. Iannetti, "Painful issues in pain prediction", *Trends in Neurosciences*, vol. 39, no. 4, pp. 212–220, 2016.

[21] K. Inui, X. Wang, Y. Qiu, B. Nguyen, S. Ojima, Y. Tamura, H. Nakata, T. Wasaka, T. Tran, and R. Kakigi, "Pain processing within the primary somatosensory cortex in humans", *European Journal of Neuroscience*, vol. 18, no. 10, pp. 2859–2866, 2003.

[22] M. Ploner, F. Schmitz, H.-J. Freund, and A. Schnitzler, "Differential organization of touch and pain in human primary somatosensory cortex", *Journal of Neurophysiology*, vol. 83, no. 3, pp. 1770–1776, 2000.

[23] A. Mouraux, G. D. Iannetti, and L. Plaghki, "Low intensity intra-epidermal electrical stimulation can activate A-delta nociceptors selectively", *Pain*, vol. 150, no. 1, pp. 199–207, 2010.

[24] L. Arendt-Nielsen and H. Hoeck, "Optimizing the early phase development of new analgesics by human pain biomarkers", *Expert Review of Neurotherapeutics*, vol. 11, no. 11, pp. 1631–1651, 2011.

[25] K. Inui and R. Kakigi, "Pain perception in humans: Use of intraepidermal electrical stimulation", *Journal of Neurology, Neurosurgery and Psychiatry*, vol. 83, no. 5, pp. 551–556, 2012.

[26] G. Cruccu, P. Anand, N. Attal, L. Garcia-Larrea, M. Haanpää, E. Jørum, J. Serra, and T. Jensen, "EFNS guidelines on neuropathic pain assessment", *European Journal of Neurology*, vol. 11, no. 3, pp. 153–162, 2004.

[27] K. Inui, T. Tran, M. Hoshiyama, and R. Kakigi, "Preferential stimulation of A-delta fibers by intra-epidermal needle electrode in humans", *Pain*, vol. 96, no. 3, pp. 247–252, 2002.

[28] G. Iannetti, M. Leandri, A. Truini, L. Zambreanu, G. Cruccu, and I. Tracey, "A-delta nociceptor response to laser stimuli: Selective effect of stimulus duration on skin temperature, brain potentials and pain perception", *Clinical Neurophysiology*, vol. 115, no. 11, pp. 2629–2637, 2004.

[29] J.-P. Lefaucheur, R. Ahdab, S. Ayache, I. Lefaucheur-Ménard, D. Rouie, D. Tebbal, D. Neves, and D. C. de Andrade, "Pain-related evoked potentials: A comparative study between electrical stimulation using a concentric planar electrode and laser stimulation using a CO2 laser", *Neurophysiologie Clinique/Clinical Neurophysiology*, vol. 42, no. 4, pp. 199–206, 2012.

[30] P. Steenbergen, J. R. Buitenweg, J. Trojan, E. M. van der Heide, T. van den Heuvel, H. Flor, and P. H. Veltink, "A system for inducing concurrent tactile and nociceptive sensations at the same site using electrocutaneous stimulation", *Behavior Research Methods*, vol. 44, no. 4, pp. 924–933, 2012.

[31] F. Kingdom and N. Prins, *Psychophysics*. Academic Press, 2010.

[32] R. Doll, P. Veltink, and J. Buitenweg, "Observation of time-dependent psychophysical functions and accounting for threshold drifts", *Attention, Perception, and Psychophysics*, vol. 77, no. 4, pp. 1440–1447, 2015.

[33] B. Treutwein, "Adaptive psychophysical procedures", *Vision Research*, vol. 35, no. 17, pp. 2503–2522, 1995.

[34] R. J. Doll, "Psychophysical methods for improved observation of nociceptive processing", Thesis, 2016.

[35] B. Treutwein and H. Strasburger, "Fitting the psychometric function", *Perception and Psychophysics*, vol. 61, no. 1, pp. 87–106, 1999.

[36] J. Stone and J. Hughes, "Early history of electroencephalography and establishment of the american clinical neurophysiology society", *Journal of Clinical Neurophysiology*, vol. 30, no. 1, pp. 28–44, 2013.

[37] O. David, J. Kilner, and K. Friston, "Mechanisms of evoked and induced responses in MEG/EEG", *NeuroImage*, vol. 31, no. 4, pp. 1580–1591, 2006.

[38] L. Garcia-Larrea, M. Frot, and M. Valeriani, "Brain generators of laser-evoked potentials: From dipoles to functional significance", *Neurophysiologie Clinique*, vol. 33, no. 6, pp. 279–292, 2003.

[39] M. C. Lee, A. Mouraux, and G. D. Iannetti, "Characterizing the cortical activity through which pain emerges from nociception", *Journal of Neuroscience*, vol. 29, no. 24, pp. 7909–7916, 2009.

[40] V. Legrain, J. M. Guérit, R. Bruyer, and L. Plaghki, "Attentional modulation of the nociceptive processing into the human brain: Selective spatial attention, probability of stimulus occurrence, and target detection effects on laser evoked potentials", *Pain*, vol. 99, no. 1-2, pp. 21–39, 2002.

[41] M. I. Posner, "Orienting of attention", *The Quarterly journal of experimental psychology*, vol. 32, no. 1, pp. 3–25, 1980.

[42] R. Parasuraman, "The psychobiology of sustained attention", *Sustained Attention in Human Performance*, pp. 61–101, 1984.

[43] Z. G. Zhang, L. Hu, Y. S. Hung, A. Mouraux, and G. D. Iannetti, "Gamma-band oscillations in the primary somatosensory cortex: A direct and obligatory correlate of subjective pain intensity", *Journal of Neuroscience*, vol. 32, no. 22, pp. 7429–7438, 2012.

[44] M. Schooneman, "Measurement of evoked potentials during multiple threshold tracking of nociceptive electrocutaneous stimuli", Thesis, 2015.

[45] R. Oostenveld, P. Fries, E. Maris, and J.-M. Schoffelen, "Fieldtrip: Open source software for advanced analysis of MEG, EEG, and invasive electrophysiological data", *Computational Intelligence and Neuroscience*, vol. 2011, 2011.

[46] W. S. Pritchard, "The brain in fractal time: 1/f-like power spectrum scaling of the human electroencephalogram", *International Journal of Neuroscience*, vol. 66, no. 1-2, pp. 119–129, 1992.

[47] E. M. van der Heide, J. R. Buitenweg, E. Marani, and W. L. Rutten, "Single pulse and pulse train modulation of cutaneous electrical stimulation: A comparison of methods", *J Clin Neurophysiol*, vol. 26, no. 1, pp. 54–60, 2009.

[48] J.-B. Poline and M. Brett, "The general linear model and fmri: Does love last forever?", *NeuroImage*, vol. 62, no. 2, pp. 871–880, 2012, cited By 36.

[49] N. J. Smith and M. Kutas, "Regression-based estimation of ERP waveforms: I. the rERP framework", *Psychophysiology*, vol. 52, no. 2, pp. 157–168, 2015.

[50] O. Hauk, M. H. Davis, M. Ford, F. Pulvermüller, and W. D. Marslen-Wilson, "The time course of visual word recognition as revealed by linear regression analysis of ERP data", *NeuroImage*, vol. 30, no. 4, pp. 1383–1400, 2006.

[51] O. Hauk, F. Pulvermüller, M. Ford, W. D. Marslen-Wilson, and M. H. Davis, "Can I have a quick word? Early electrophysiological manifestations of psycholinguistic processes revealed by event-related regression analysis of the EEG", *Biological Psychology*, vol. 80, no. 1, pp. 64–74, 2009.

[52] N. J. Smith and M. Kutas, "Regression-based estimation of ERP waveforms: Ii. nonlinear effects, overlap correction, and practical considerations", *Psychophysiology*, vol. 52, no. 2, pp. 169–181, 2015.

[53] E. Schulz, E. May, M. Postorino, L. Tiemann, M. Nickel, V. Witkovsky, P. Schmidt, J. Gross, and M. Ploner, "Prefrontal gamma oscillations encode tonic pain in humans", *Cerebral Cortex*, vol. 25, no. 11, pp. 4407–4414, 2015.

[54] H. Vossen, G. van Breukelen, H. Hermens, J. van Os, and R. Lousberg, "More potential in statistical analyses of event-related potentials: A mixed regression approach", *International Journal of Methods in Psychiatric Research*, vol. 20, no. 3, e56–e68, 2011.

[55] A. Tremblay and A. Newman, "Modeling nonlinear relationships in ERP data using mixed-effects regression with R examples", *Psychophysiology*, vol. 52, no. 1, pp. 124–139, 2015.

[56] C. Vossen, H. Vossen, E. Joosten, J. Van Os, and R. Lousberg, "Does habituation differ in chronic low back pain subjects compared to pain-free controls? A cross-sectional pain rating ERP study reanalyzed with the ERFIA multilevel method", *Medicine (United States)*, vol. 94, no. 19, 2015.

[57] T. Wager, in, ser. The Brain Adapting with Pain. 2015, ch. Using Neuroimaging to Understand Pain: Pattern Recognition and the Path from Brain Mapping to Mechanisms.

[58] C. J. Woolf, "Central sensitization: Implications for the diagnosis and treatment of pain", *Pain*, vol. 152, no. SUPPL.3, 2011.

[59] K. Walton and R. Llinas, in, ser. Frontiers in Neuroscience. Nov. 2009, ch. Central Pain as a Thalamocortical Dysrhythmia.

[60] A. Wright, P. Moss, K. Sloan, R. J. Beaver, J. B. Pedersen, G. Vehof, H. Borge, L. Maestroni, and P. Cheong, "Abnormal quantitative sensory testing is associated with persistent pain one year after tka", *Clinical Orthopaedics and Related Research*, vol. 473, no. 1, pp. 246–254, Jan. 2015.

[61] V. Wylde, S. Palmer, I. Learmonth, and P. Dieppe, "The association between pre-operative pain sensitisation and chronic pain after knee replacement: An exploratory study", *Osteoarthritis and Cartilage*, vol. 21, no. 9, pp. 1253–1256, 2013.

[62] R. Treede and U. Baumgartner, in, ser. The Brain Adapting with Pain. 2015, ch. Monitoring Brain Electrical and Magnetic Activity for Assessing Pain: Advantages and Limitations.

3 Linear Mixed Models

In the background chapter, it was proposed that a linear mixed-model might be used to include information from all EEG trials to reduce background activity in the computed EP. Moreover, this model can be used to compute the influence of stimulus parameters on the amplitude of the EP. However, there is an infinite amount of models that might explain the measured EP, and there are numerous methods to compute the parameters of each of those models. Therefore, a framework is necessary in which a sensible model can be derived, computed and interpreted. This chapter provides such a framework by describing how a linear mixed model can be computed, tested and validated. Furthermore, important strengths and weaknesses of the method are demonstrated using simulated data.

3.1 When to Use a Linear Mixed Model?

Linear mixed models are suitable to use when the outcome variables can be expected to be normally distributed, but may not be independent or have a constant variance [1].

- When a study contains clustered data, such as patients in multiple hostpitals, or stimuli that are applied on multiple occasions in multiple blocks, a linear mixed-effect model can be used to account for the dependence of data within one patient and within one hospital.
- When a study contains longitudinal or repeated-measures data for multiple subjects, a linear mixed-effect model can be used to account for the dependence of the repeated-measures data within one subject, which will be used in this thesis to analyze evoked potentials.

The MTT-EP experiments in this thesis can be considered repeated-measured data which is clustered within the subject, which is the unit of analysis in our studies. Therefore LMMs are useful to describe the structure in the MTT-EP experimental data.

3.2 Model Solving

In this section, we briefly summarize how a linear mixeds model is formulated and solved mathematically[1]. Some steps leading towards the solution will be skipped, since a full mathematical treatment of the problem would be out of the scope of this thesis. For complete information about the mathematical theory behind LMMs, please refer to 'Linear and Generalized Linear Mixed Models and Their Applications' [2].

3.2.1 Mathematical Formulation

By using a linear mixed model, we assume a linear and a random structure in the data which enable us to use all data in a single regression. More specifically, we assume that the outcome variable

[1] The information about linear mixed models presented in the Background (Section 2.7.3) is presumed as prior knowledge.

is linearly dependent on a set of deterministic variables (x_{ijk}) and stochastic variables (z_{ijk}), and furthermore contains a normally distributed residual (η_{ij}). For clarity, we leave out the dependence of model variables on the time with respect to the stimulus (τ) and start out with the formulation of a linear mixed model that was introduced in the background (Section 2.7.3), shown in Equation 3.1.

$$y_{ij} = \beta_0 + \sum_{k=1}^{p} \beta_k x_{ijk} + v_{i0} + \sum_{k=1}^{p} v_{ik} z_{ijk} + \eta_{ij} \tag{3.1}$$

For $i \in \{1, ..., n\}$ and $j \in \{1, ..., m_i\}$ where:

1. The outcome variable for the j-th measurement of the i-th subject is given by: $y_{ij} \in \mathbb{R}$
2. The fixed intercept for the regression model is: $\beta_0 \in \mathbb{R}$
3. The fixed slope for the k-th predictor is: $\beta_k \in \mathbb{R}$
4. The j-th measurement of the k-th fixed predictor for the i-th subject is: $x_{ijk} \in \mathbb{R}$
5. The random intercept for the i-th subject is[1]: $v_{i0} \overset{\text{iid}}{\sim} \mathcal{N}(0, \sigma_0^2)$
6. The random slope for the k-th predictor of the i-th subject is[1]: $v_{ik} \overset{\text{iid}}{\sim} \mathcal{N}(0, \sigma_k^2)$
7. The j-th measurement of the k-th random predictor for the i-th subject is: $z_{ijk} \in \mathbb{R}$
8. The model residual is[1]: $\eta_{ij} \overset{\text{iid}}{\sim} \mathcal{N}(0, \sigma_\eta^2)$

3.2.2 Mathematical Solution

To solve the model in Equation 3.1, we first reformulate it to matrix notation (Equation 3.2).

$$\mathbf{y_i} = \mathbf{X_i}\beta + \mathbf{Z_i}\mathbf{v_i} + \eta_\mathbf{i} \tag{3.2}$$

For $i \in \{1, ..., n\}$ where:

1. The i-th subject's response vector is: $\mathbf{y_i} = (y_{i1}, ..., y_{im_i})^T$
2. The fixed effects design matrix, with $\mathbf{x_{ik}} = (x_{i1k}, ..., x_{im_ik})^T$, is: $\mathbf{X_i} = [\mathbf{1}, \mathbf{x_{i1}}, ..., \mathbf{x_{ip}}]$
3. The fixed effects vector is: $\beta = (\beta_0, \beta_1, ..., \beta p)^T$
4. The random effects design matrix, with $\mathbf{z_{ik}} = (z_{i1k}, ..., z_{im_ik})^T$, is: $\mathbf{Z_i} = [\mathbf{1}, \mathbf{z_{i1}}, ..., \mathbf{z_{iq}}]$
5. The random effects vector is: $\mathbf{v_i} = (v_{i0}, v_{i1}, ..., v_{iq})^T$
6. The residual vector is: $\eta_\mathbf{i} = (\eta_{i1}, \eta_{i2}, ..., \eta_{im_i})^T$

[1] The abbreviation 'iid' in the equation stands for: Independent and Identically Distributed.

Based on the assumptions in last section, we can derive that the outcome variable must also be normally distributed with $\mathbf{y_i} \sim \mathcal{N}(\mathbf{X_i}\beta, \Sigma_\mathbf{i})$ in which the covariance matrix for the i-th subject's data is equal to $\Sigma_\mathbf{i} = \mathbf{Z_i}\Sigma\mathbf{Z_i^T} + \sigma^2\mathbf{I_n}$.

After a vast amount of linear algebra, we can derive that the log-likelihood of the model in Equation 3.2 is given by Equation 3.3.

$$\ln(L(\Sigma, \sigma^2|\mathbf{y_1}, ..., \mathbf{yn})) = -\frac{n_{TRL}}{2}\ln(2\pi) - \frac{1}{2}\ln(|\Sigma_*|) - \frac{1}{2}(\mathbf{y_i} - \mathbf{X_i}\hat{\beta})^T\Sigma_\mathbf{i}^{-1}(\mathbf{y_i} - \mathbf{X_i}\hat{\beta}) \tag{3.3}$$

Where:

1. The generalized least squares estimate of the fixed effects is: $\hat{\beta} = (\sum_{i=1}^{n}\mathbf{X_i^T}\Sigma_\mathbf{i}^{-1}\mathbf{X_i})^{-1}\sum_{i=1}^{n}\mathbf{X_i^T}\Sigma_\mathbf{i}^{-1}\mathbf{y_i}$
2. The total number of measures is: $n_{TRL} = \sum_{i=1}^{n} m_i$
3. The matrix of random predictors with respect to all subjects is: $\begin{bmatrix} \mathbf{Z_1} & \mathbf{0} & \dots & \mathbf{0} \\ \mathbf{0} & \mathbf{Z}_2 & \dots & \mathbf{0} \\ \vdots & \vdots & \ddots & \vdots \\ \mathbf{0} & \mathbf{0} & \dots & \mathbf{Z_n} \end{bmatrix}$
4. The covariance matrix with respect to all subjects is: $\Sigma_* = \mathbf{Z}\Sigma_\mathbf{b}\mathbf{Z^T} + \sigma^2\mathbf{I}$

Equation 3.3 can be used to solve for the unknown Σ, σ^2 and β in Equation 3.2 by maximizing the likelihood using an optimization algorithm. This method of model estimation is also referred to as Maximum Likelihood (ML) estimation. However, this formulation of the log-likelihood does not compensate for the loss of degrees of freedom, resulting from estimation of fixed effects, in the estimation of the model variances [3]. A variant of the log-likelihood formulation, the restricted log-likelihood, is given by Equation 3.4. Estimation of the model using this formulation is also referred to as Restricted Maximum Likelihood (REML) estimation, and results generally in a better model fit for unbalanced data and a better estimation of the variances [4].

$$\ln(L(\Sigma, \sigma^2|\mathbf{y_1}, ..., \mathbf{yn}, \mathbf{X_1}, ..., \mathbf{X_n})) = -\frac{\widetilde{n}_{TRL}}{2}\ln(2\pi) - \frac{1}{2}\ln(|\Sigma_*|) - \frac{1}{2}\ln(|\mathbf{X^T}\Sigma_*^{-1}\mathbf{X}|) - \frac{1}{2}(\mathbf{y} - \mathbf{X}\hat{\beta})^T\Sigma^{-1}(\mathbf{y} - \mathbf{X}\hat{\beta}) \tag{3.4}$$

Where:

1. The generalized least squares estimate of the fixed effects is: $\hat{\beta} = \mathbf{X^T}\Sigma_*^{-1}\mathbf{X})^{-1}\mathbf{X^T}\Sigma_*^{-1}\mathbf{y}$
2. The corrected number of measures is: $\widetilde{n}_{TRL} = n_{TRL} - p - 1$
3. The vector resulting from the concatenation of all subject predictors is: $\mathbf{X} = [\mathbf{X_1}, ..., \mathbf{X_n^T}]$

3.3 Model Testing

Computing the linear mixed model using REML estimation results in the best linear unbiased estimator for the fixed effects, $\hat{\beta}$. Test statistics based on REML estimates perform better than those based on

ML estimates [4]. Four methods for testing of LMM coefficients are: 1) a Wald test, 2) a likelihood ratio test, 3) a parametric bootstrap test or 4) Markov Chain Monte Carlo testing.

Although testing of the coefficients using a parametric bootstrap test or using Markov Chain Monte Carlo testing offer the strongest statistical tests, they have a high computational complexity and are therefore unpractical to use for the analysis of evoked potentials, which requires the computation and testing of several thousands of linear-mixed models. Furthermore, EEG data would have to be transferred to a different software platform, since Matlab does not include implementations of those analyses for LME type models. Therefore, these testing methods are considered out of the scope of this thesis.

Two remaining valid options for statistical testing of the model coefficients are the Wald Test and the Likelihood Ratio Test. In general the Likelihood Ratio Test is considered a stronger statistical test of linear models. However, since the REML log-likelihood function is corrected for the amount of degrees-of-freedom in the model, it cannot be used for comparisons between models with a different amount of fixed effects. Therefore, it is not straightforward to test a model derived using REML using a likelihood ratio test. Manor and Zucker have shown that for a small number of subjects a model computed using REML has a lower type I error rate for both the Likelihood Ratio Test and the Wald Test, but that in this case the type I error rate for the Wald Test is lower [4]. Therefore, the Wald test is used throughout this thesis for statistical testing of model coefficients.

3.4 Model Validation

Even though a model shows constant and significant coefficients, this model might be invalid if the underlying assumptions of such a model are invalid. In this section, we will discover how a linear mixed model might lead to an incorrect description of the data, and how we can discover such an error.

3.4.1 Anscombe's Quartet

In 1973, the English statistician Francis Anscombe demonstrated the importance of visual inspection of model validity by graphing the data before statistical analysis [5]. In a battle against the mainstream vision that a valid model can be derived purely on exact equations, he provided four examples of datasets which would be interpreted incorrectly without visual inspection (Anscombe's quartet), which is shown in Figure 3.1. Although distinctly different, linear regression of each set in the quartet leads to the same values. We can study each of those examples to identify why data might be interpreted incorrectly and how we can prevent false assumptions.

Set 1 resembles data as we normally assume in linear regression: the dependent variable varies linearly with the independent variable and has additive normally distributed noise. This leads to a correct model fit which follows the central axis of the pointcloud.

Set 2 involves a non-linear deterministic data. Even though linear regression leads to the same values in this case, the linear model clearly does not correctly model the variation of the dependent variable with respect to the independent variable.

Set 3 involves linear deterministic data with a set of outliers. Due to the outliers, linear regression leads to an incorrect intercept and slope of the estimated curve.

Set 4 involves normally distributed data with respect to two values of the independent variable (8 and 19). However, only 100 samples are available for the value of 19 while 1000 samples are available for the value of 8.

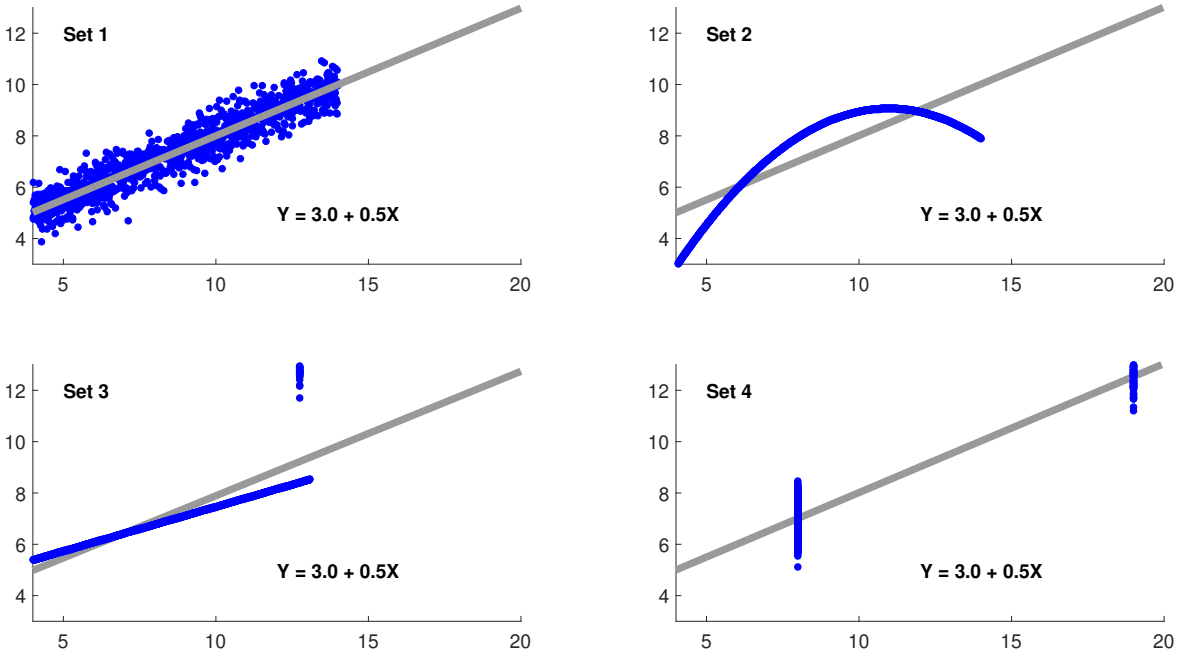

Figure 3.1: Four sets of data which were generated using the functions of the dataset used by Francois Anscombe to demonstrate the importance of graphing the data [5]. Each set results in an similar linear regression, even though each set is clearly different.

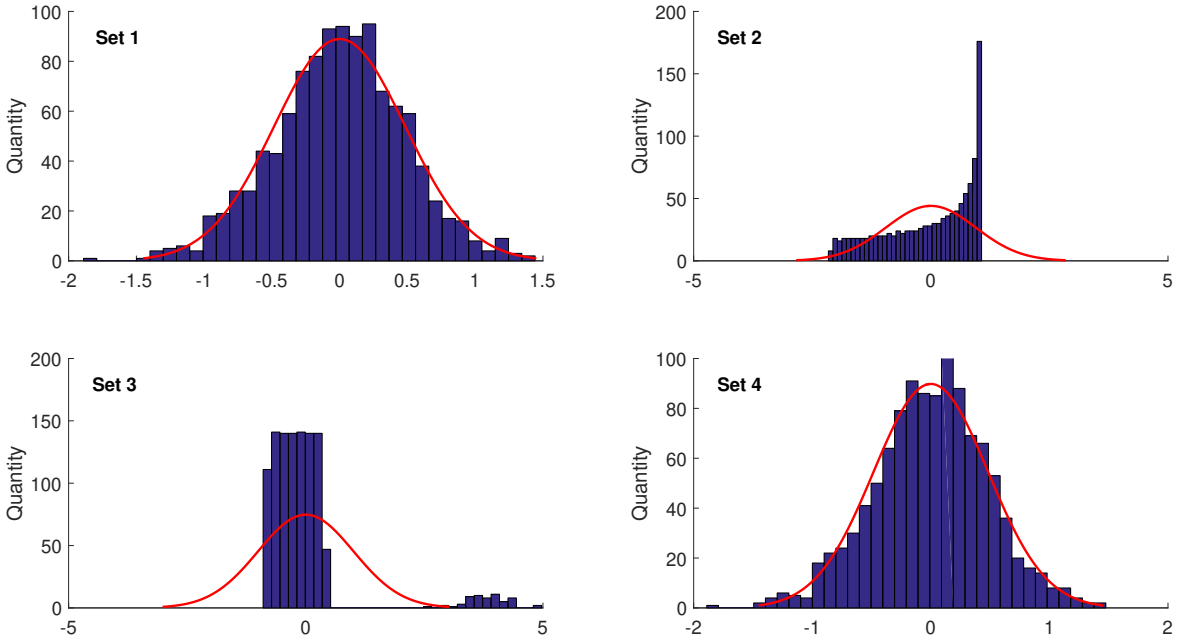

Figure 3.2: Residual histograms of each linear regression in Figure 3.1. Incorrectly assuming that the variations are linear results in a histogram which is not normally distributed.

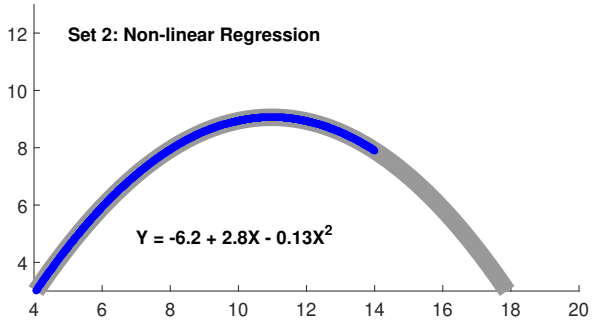

Figure 3.3: *Nonlinear regression of Set 2. In this case, the regression correctly models the data.*

The huge difference between the datasets in the quartet emphasizes the need to validate the model fit. This can be done by checking if the residual of the regression is normally distributed, which can be done using a boxplot, QQ-plot, residual-fit plot or a histogram. Figure 3.2 shows histograms of the data in Anscombe's quartet with respect to a normal distribution. Clearly, the residuals of Set 2 and Set 3 are not normally distributed. Therefore, checking the residuals for normality helps to identify relevant non-linearity and outliers in the data. In this way, identified outliers can be removed or the linear regression can be adapted to accommodate for non-linearities. For example, in the case of Set 2, we can achieve a good model fit by adding a quadratic term to the regressor, which is shown in Figure 3.3.

Set 4 highlights another problem of linear regression: when only two values of the independent variable are available (e.g. in this research NOP = 1 and NOP = 2), the estimated slope is equally dependent on the set of samples for each of those values, irrespective of the amount of samples that available for those values. For example, if one would measure 10 EP amplitudes for NOP = 1 and 1 EP amplitude for NOP = 2, the slope would be fully dependent on the single measurement made for NOP = 2. There is no analytical method to circumvent this problem. However, a smart experimental design can prevent this problem by making sure that sufficient data is measured for each of the two values of the independent variable in this case.

3.4.2 Mixed Effects

In an experimental dataset, relations might exist between subsets of the data which violate the assumptions of independence and normality. For example, the measured value might depend on the observer, on the subject, on both or on the combination of both. As outlined earlier, the intercept or the coefficient of model parameters are expected to vary randomly with respect to such a condition, you can account for those random variations by adding random effects to the model.

Figure 3.4 shows how a dataset obtained from 2 subjects, with each a random intercept and slope, might look like. It is also shown in Figure 3.4, that in this case the LM will simply approximate the average effect size with respect to the two subjects. The assumption of normality of the residual is violated. Therefore, model testing will no longer render correct results, and the model will not return an accurate fit. However, as is shown in Figure 3.5, it is easy to identify such a modeling error in the histogram of the residual, since this error will cause non-normality of the residual.

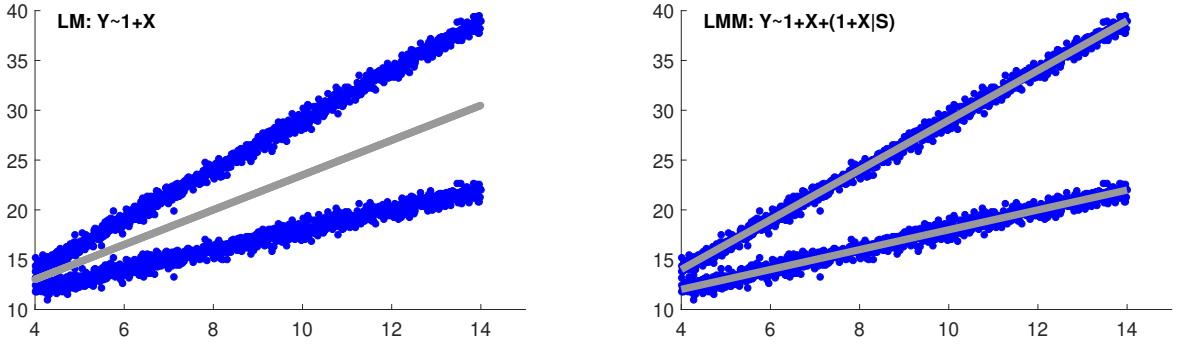

Figure 3.4: Regression of a set with a random intercept and random slope for two subjects, using a LM (left) and a LMM (right).

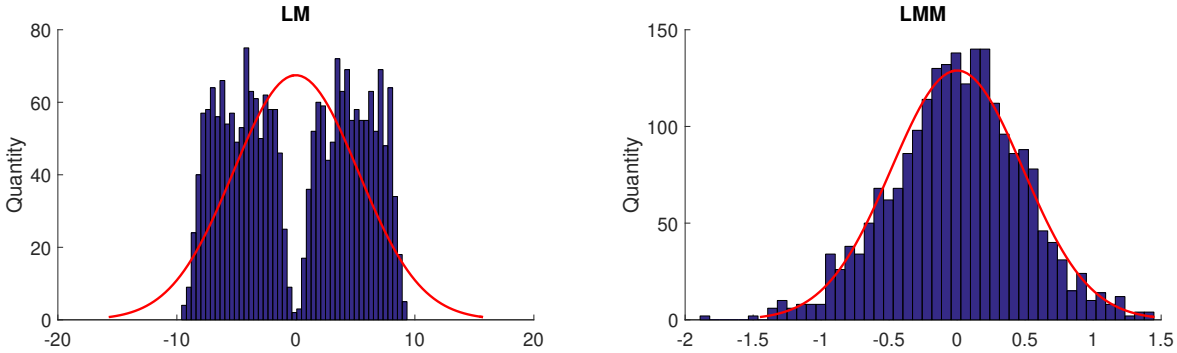

Figure 3.5: Residual histograms of each regression in Figure 3.4. Incorrectly excluding random effects results in a histogram which is not normally distributed.

3.5 Models of Evoked Potentials

In the last sections, it was shown that we can successfully compute, test and validate simple linear mixed-effects models. The next step is to use linear mixed models to compute EPs and analyze model coefficients. With conventional averaging, the EP is estimated by the mean EP amplitude at a specific time-point with respect to the stimulus. Instead of estimating every EP time-point by averaging, we might do the same using a linear mixed model. This model can be written as Equation 3.5[1] in which τ denotes the time with respect to application of the stimulus.

$$y_{ij}(\tau) = \beta_0(\tau) + \sum_{k=1}^{p} \beta_k(\tau) x_{ijk} + v_{i0}(\tau) + \sum_{k=1}^{p} v_{ik}(\tau) z_{ijk} + \eta_{ij}(\tau) \qquad 3.5$$

Subsequently, we can compute the EP by defining the parameters[2] to be included in Equation 3.5 and computing a LMM for every point in time[3].

We will demonstrate and test the method using a set of simulated EEG trials. A simulated trial is generated with one Gaussian waveform, similar to the P2 component in the nociceptive EP. The

[1] As was introduced in the Background section about LMMs. For more information about the annotation, please refer to Section 2.7.3 of the Background.

[2] For more information about the definition of the parameters in the model for this thesis, please refer to Section 3.6.

[3] The same method might be used for analysis of time-frequency spectra. In this case, one LMM might be computed for every time/frequency combination in the data.

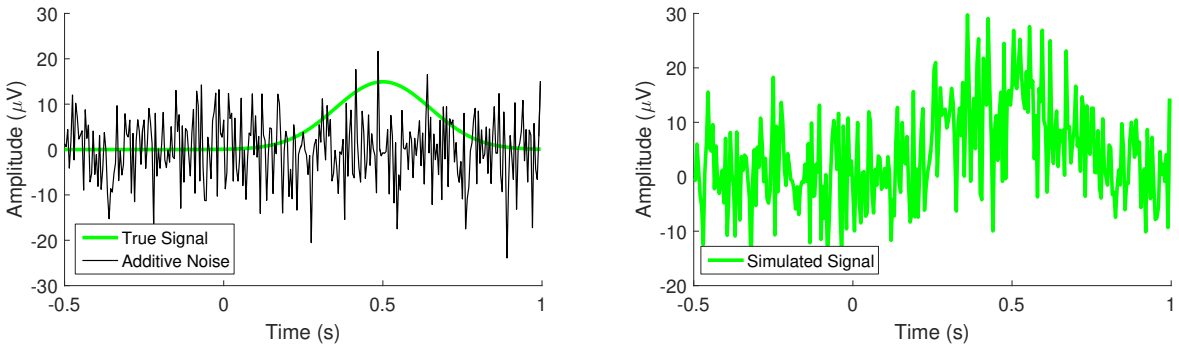

Figure 3.6: *A simulation of one trial. The figure on the left shows the true signal (green), which is determined by modulating a Gaussian waveform by a known model, using parameters from a previous MTT-EP experiment as input for the model. Subsequently, noise is added to the true signal, which is also shown on the left (black). This results in the simulation of a single trial (right).*

amplitude of the Gaussian waveform is modulated by experimental parameters with a simulated effect size, and random Gaussian white noise is added to the signal. For every effect in every subject a random intercept and random slope between -5 μV/unit and +5 μV/unit is added. We simulate an entire set of trials by using the dataset from previous MTT-EP experiments from 10 subjects. In other words, each trial is modulated by the set of stimulus parameters from the corresponding trial of the MTT-EP experiment. An example of a simulated trial is shown in Figure 3.6.

3.5.1 Model Computation

Model computation and analysis is performed in Matlab (The Mathworks Inc., version 2015b). Model coefficients are estimated for every point in time by optimization of the restricted maximum likelihood, using the 'lmefit()' function. To verify model validity, the model residuals are assessed for normality along the entire EP interval using a continuous boxplot, kurtosis and skewness of the residual, which will be demonstrated in Section 3.5.4. Significance of the model coefficients is tested against the null-hypothesis using a Wald t-test. To reduce the chance of false significance due to retesting, the requirement is imposed that a coefficient should be significant ($p < 0.05$) for at least 4 subsequent time points.

3.5.2 Identification of Model Coefficients

We start out by simulation of two EPs with a subject-dependent linear modulation of the amplitude of the Gaussian waveform. Since we want to simulate the EP as accurately as possible, we use and effect size and background activity similar to the one identified in the exploratory data from M. Schooneman[1]: the effect size of stimulus detection (8 μV/detection) and the standard deviation of the background activity around the P2 (7.2 μV). The peak latency of the Gaussian waveform is set to 500 ms and every simulated effect is by default given the effect size of 8 μV/unit. We simulate and analyze two models:

1. The EP amplitude is a function of the intercept and one effect (in this case, the amplitude): $y_i(\tau) = (8 + v_{Int.})G(t) + (8 + v_{AMP})x_{AMP}$

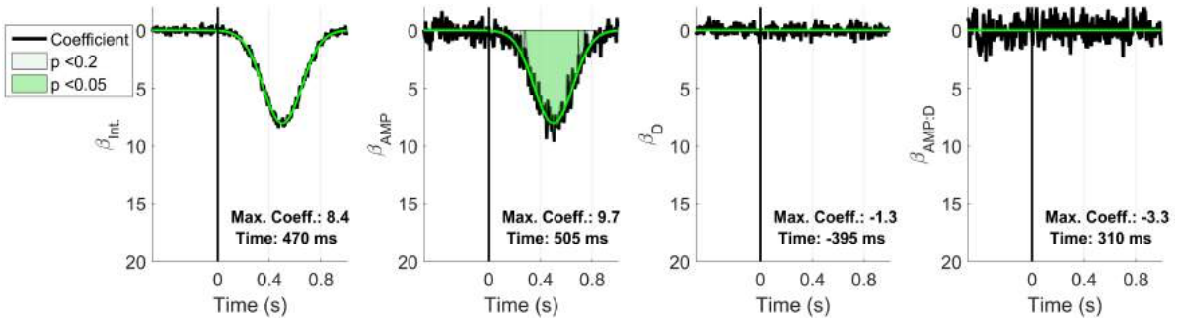

Figure 3.7: The coefficients (black) computed on simulated data in which the EP amplitude is a function of the intercept and one effect. The simulated coefficients are displayed in green for comparison.

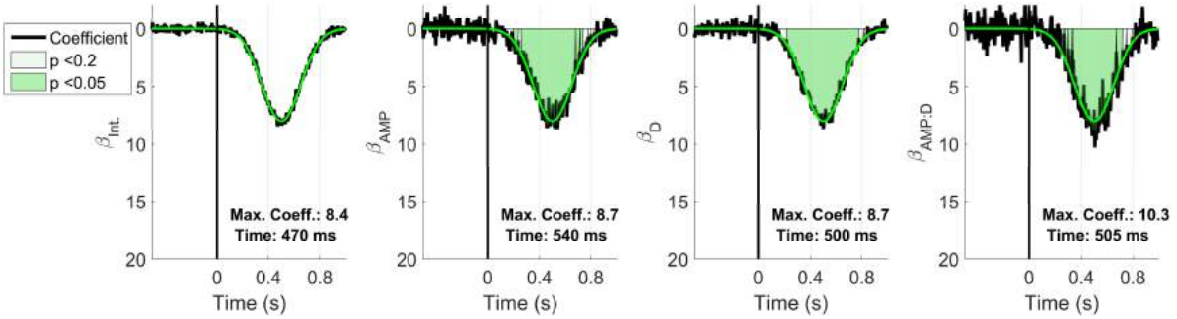

Figure 3.8: The coefficients (black) computed on simulated data in which the EP amplitude is a function of the intercept and interaction of two effects. The simulated coefficients are displayed in green for comparison.

2. The EP amplitude is a function of the intercept and the interaction of two effects:
   $y_i(\tau) = (8 + v_{Int.})G(t) + (8 + v_{AMP})x_{AMP} + (8 + v_D)x_D + (8 + v_{AMP:D})x_{AMP}x_D$

In which $G(t)$ is a Gaussian waveform with unit amplitude. We analyze both sets of simulated data using the model[2]:

$$EP \sim 1 + AMP * D + (1 + AMP * D|Subject)$$

Results

Computed coefficients are shown in Figures 3.7 and 3.8. The simulated effect coefficients (green) are compared to the computed effect coefficients (black). The computed effect coefficients are correctly centered around the simulated effect coefficients. The noise induces visible variations around the simulated coefficients, but is sufficiently reduced to achieve effect significance during the simulated EP component. Effect coefficients that were simulated as 0 are also correctly shown to have no influence on the EP.

[1] Both values were obtained by a preliminary analysis of experimental data using a LMM

[2] For clarity, the model is described in Wilkinson notation. Wilkinson notation is an efficient way to describe a statistical model, and is frequently used in software such as Matlab (used for this thesis) and R. For more information about Wilkinson notation, please refer to the original article [6].

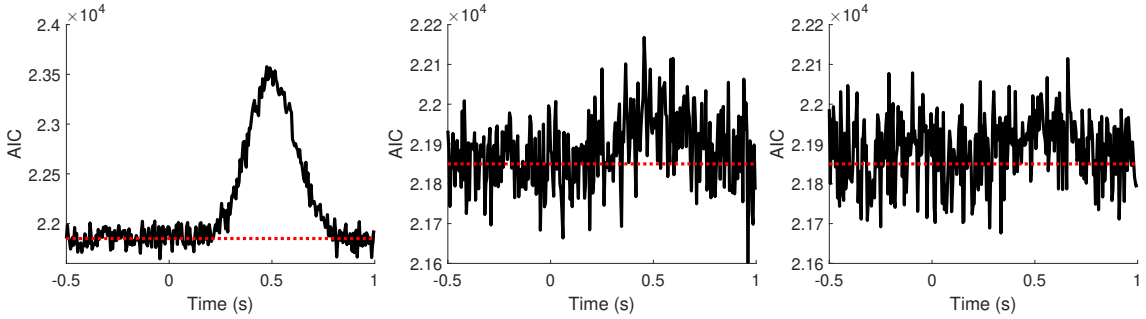

Figure 3.9: *The AIC value over time for model 1 (left), 2 (middle) and 3 (right).*

3.5.3 Identification of Missing Effects and Interactions

The influence of stimulus parameters on the evoked potential might be described by several different statistical models. In the process of model selection, you might add and remove model parameters and interactions between model parameters to test which model is correct. However, inspection of the model coefficients is not sufficient for model selection. Generally, when adding a parameter to the model the likelihood of the model will increase. However, an increased likelihood is not always due to an increase in the quality of the model, as the additional parameters might also lead to overfitting. An elegant entropic information criterion was derived by the Japanese mathematician Hirotogu Akaike [7] to determine which model is most likely to be the true model based on the entropy of the information. We can use this criterion for model comparison and selection, if we first compute the available models based on ML estimation. Subsequently, we can proceed with computation of the coefficients of the optimal model using REML estimation.

To show the application of AIC estimation for analysis of the EP, we use the dataset generated by the second model in last section, where the EP was a function of the intercept and the interaction of two effects. We analyze the data using three models:

1. $EP \sim 1 + AMP + (1 + AMP|Subject)$
2. $EP \sim 1 + AMP + D + (1 + AMP + D|Subject)$
3. $EP \sim 1 + AMP * D + (1 + AMP * D|Subject)$

Each model is computed using ML optimization.

Results

Figure 3.9 shows the AIC value over time for each of the computed models. For the first model, the AIC shows a large peak which corresponds with the simulated Gaussian waveform that is modulated by the effects. This means that, when the signal is modulated by the coefficients, the quality of the model decreases, indicating that the model might not correctly describe the data at those points in time. The maximum value of the AIC subsequently decreases for the second and the third model, showing that the third model is most likely to be the true model.

3.5.4 Identification of Non-Linearities

Next, we study if we can identify a non-linearity in the model, and how we migh improve on the model after identifying one. In Section 3.4.1 it was shown that a non-linear effect might be identified by studying the histogram of the residual. However, since we now generate a model for every time-point, we cannot identify non-linearity based on the histogram, since it would be impractical to study an histogram for every time-point and every model. Instead, we use three measures of normalite to analyze the normality of the residual over the entire EP interval:a continuous boxplot, skewness and kurtosis.

When the residual has a normal distribution, it will have a skewness of approximately 0 and a kurtosis of approximately 3. Therefore, we can use deviations of both properties to identify non-normality, and therefore a possible non-linearity. Additionally, we use the Akaike Information Criterion as a measure of the relative quality of the statistical model [8].

We simulate and analyze one model with a low amount of background activity (1.0 μV std) and a high amount of background activity (7.2 μV std):

1. The EP amplitude is a function of the intercept and the interaction between two effects of which one (in this case, the amplitude) is quadratic:
   $y_i(\tau) = (8 + v_{Int.})G(t) + (8 + v_{AMP})x_{AMP}^2 + (8 + v_D)x_D + (8 + v_{AMP:D})x_{AMP}^2 x_D$

We first use an incorrect, linear, model to analyze the data:

$$EP \sim 1 + AMP * D + (1 + AMP * D|Subject)$$

Subsequently, we use the correct model to analyze the data:

$$EP \sim 1 + AMP^2 * D + (1 + AMP^2 * D|Subject)$$

Results

Figure 3.10 shows the continuous boxplot, skewness and kurtosis of the linear model residual when there is a low amount of background activity. Around 500 ms, the limits of the continuous boxplot are larger, indicating that the amount of unexplained variance increases around this point in time. Furthermore, there is a clear increase in kurtosis of the model at 500 ms, indicating that at this point in time the model residual is not normally distributed, and therefore not correctly modelling the effects. Figure 3.11 shows the continuous boxplot, skewness and kurtosis of the linear model residual when there is a high amount of background activity. There is no longer a clear increase in kurtosis, due to the high amount of background activity, which increases the error in the estimation of kurtosis. This shows that non-linearity can only be identified if it's effect is sufficiently strong with respect to the background activity. In case of a suspicion of non-linearity, one might try to model several non-linear versions of the model based on plausible underlying mechanisms of the measured variations, and observe the value of the AIC. The value of the AIC tends to be the lowest for the model with the highest relative quality. In Figure 3.12, it can be seen that for the correct model, the AIC is indeed lower than in Figure 3.11.

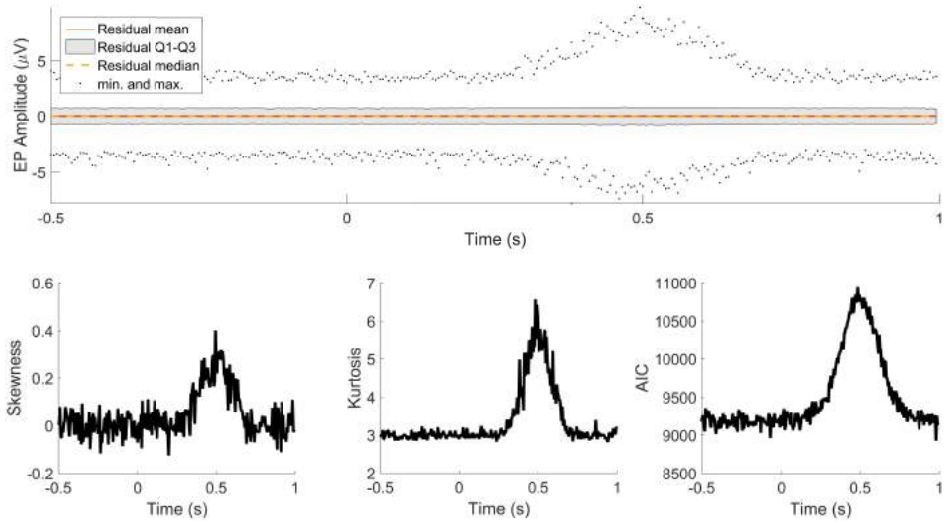

Figure 3.10: Continuous boxplot, skewness and kurtosis of the residual when a linear model is fitted to a simulated EP waveform including a non-linear effect. Since there is a low amount of noise in the simulated data, the incorrectness of the model during the Gaussian waveform is readily identifiable.

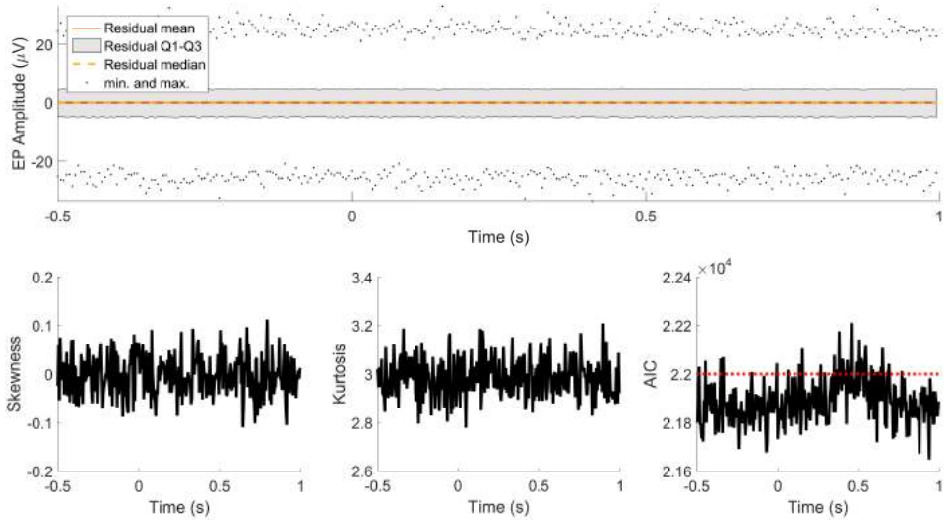

Figure 3.11: Continuous boxplot, skewness and kurtosis of the residual when a linear model is fitted to a simulated EP waveform including a non-linear effect. Since there is a low high of noise in the simulated data, the incorrectness of the model during the Gaussian waveform is almost invisible.

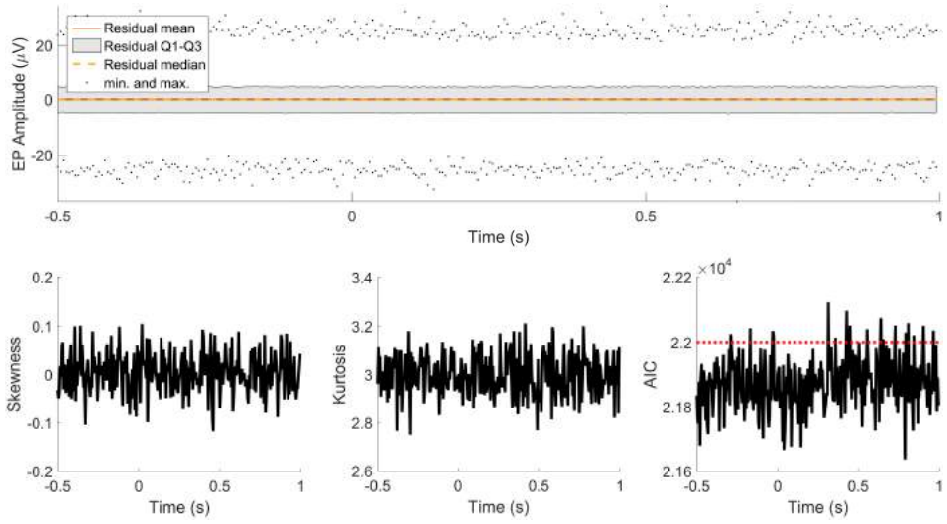

Figure 3.12: Continuous boxplot, skewness and kurtosis of the residual when a correct non-linear model is fitted to a simulated EP waveform including a non-linear effect. The fact that this model provides a better explanation for the simulated data than the previous linear model is reflected by a lower AIC.

3.6 Model Formulation

A statistical model should sufficiently describe variations within the data, by including all parameters within an experiment that might influence the data. However, including too many parameters might lead to overfitting of the model. Therefore, for the inference of a statistical model for brain activity with respect to stimulus parameters, it is most sensible to include only the parameters that might lead to a variation of the signal through known physiological mechanisms to prevent overfitting and unrealistic model parameters.

There is not much known about the exact interactions in the nociceptive system that lead to the processing of a stimulus. From earlier studies, we know that the average brain response can be increased or decreased with respect to stimulus parameters [9–12], but we do not know which system interactions lead to this increase or decrease. The most accurate information about the steps of stimulus processing within the brain comes from microneurography studies. Those studies suggest that acitivity in the primary somatosensory cortex is closely related to the stimulus pattern itself, whereas activity in the SII and areas further downstream is more closely related to the fact that a stimulus occured but not to the pattern [13, 14]. Therefore, the activity in those downstream areas is more likely to be related to conscious stimulus detection and assessment itself.

Based on this information we can formulate a general model of stimulus processing in the brain (Figure 3.13):

1. A stimulus evokes stimulus-related activity in the cortex.
2. Stimulus-related activity in the cortex determines the probability that a stimulus is detected.
3. If a stimulus is detected, various downstream areas are activated.

This means that the time-locked EEG signal is a combination of stimulus related activity and detection related activity. Furthermore, neural activity might change over the amount of received stimuli due to plasticity of the system. Therefore, for a stimulus consisting of two pulses, we can decompose the

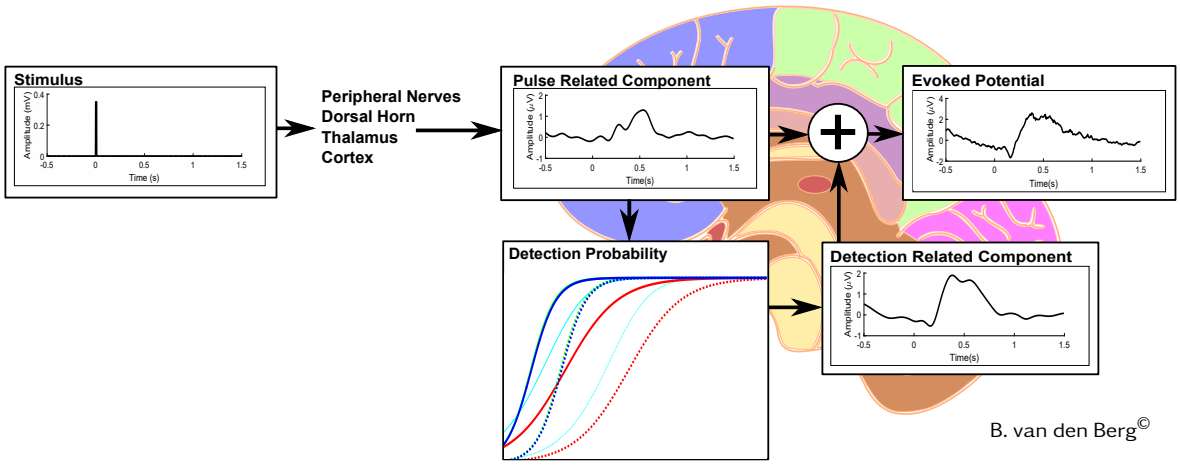

Figure 3.13: A stimulus evokes stimulus-related and detection-related activity in the cortex. A mixture of both types of activity is measured by EEG.

EEG signal of the j-th trial of the i-th subject at the time τ with respect to the stimulus according to Equation 3.6.

$$y_{EP,ij}(\tau) = \underbrace{\beta_{Int.}(\tau)}_{\text{average EP}} + \underbrace{\beta_{P1}(\tau)x_{P1,ij} + \beta_{P2}(\tau)x_{P2,ij}}_{\text{activity due to first and second pulse}} + \underbrace{\beta_D(\tau)x_{D,ij}}_{\text{activity due to detection}} + \underbrace{\beta_{TRL}(\tau)x_{TRL,ij}}_{\text{habituation}} + \underbrace{u_{Int.,i}(\tau) + u_{P1,i}(\tau)x_{P1,ij} + u_{P2,i}(\tau)x_{P2,ij} + u_{D,i}(\tau)x_{D,ij} + u_{TRL,i}(\tau)x_{TRL,ij}}_{\text{random intercept and slope per subject}} + \underbrace{\eta_{ij}}_{\text{background activity}} \quad 3.6$$

Where:

1. EP refers to the evoked potential.
2. $P1$ refers to the amplitude of the first pulse of a stimulus.
3. $P2$ refers to the amplitude of the second pulse of a stimulus.
4. D refers to stimulus detection.
5. TRL refers to the amount of received stimuli.

In Wilkinson notation, this model can be written as Equation 3.7 for every point in time with respect to the stimulus.

$$EP \sim 1 + P1 + P2 + D + TRL + (1 + P1 + P2 + D + TRL|Subject) \quad 3.7$$

3.7 DISCUSSION

In this chapter, basic principles of linear mixed-regression were outlined and demonstrated using simulated data. Using Anscombe's quartet, we saw that it is essential to check the residual of the model fit in order to identify if the assumptions of normality and independence are sufficiently satisfied. We extended the technique of linear mixed-regression by using the technique to applying linear mixed-regression to every point in time. Doing so, the variation of model coefficients can be studied and tested in the time-domain. In addition, we saw that analysis of the model residual and the model AIC can also be extended to the time domain by plotting the AIC, and the kurtosis and skewness of the residual distribution with respect to time, in combination with a continuous boxplot. If the AIC value is augmented during a component of the EP, it is likely that the model is either missing an important parameter to account for this component, or contains a non-linear effect during this component. If the kurtosis and skewness of the residual distribution increase simultaneously with the AIC, this increase in AIC is likely contributed to a non-linearity in the data. Therefore, we can investigate the validity of the LMM by investigating the variation of the residual over time. A weak point of the analysis of the EP using linear-mixed regression was identified in Figure 3.11: if the background activity has a high power with respect to the modelling error due to a non-linearity or a missing parameter, one might not be able to identify this error anymore. To decrease the chance on modeling errors, it is important to extensively test and compare physically plausible models to select the model which is most likely to correctly model the data.

Bibliography

[1] B. T. West, K. B. Welch, and A. T. Galecki, *Linear mixed models: a practical guide using statistical software*. CRC Press, 2014.

[2] J. Jiang, *Linear and Generalized Linear Mixed Models and Their Applications*. Springer, 2007.

[3] D. A. Harville, "Maximum likelihood approaches to variance component estimation and to related problems", *Journal of the American Statistical Association*, vol. 72, no. 358, pp. 320–338, 1977.

[4] O. Manor and D. M. Zucker, "Small sample inference for the fixed effects in the mixed linear model", *Computational Statistics and Data Analysis*, vol. 46, no. 4, pp. 801–817, 2004.

[5] F. J. Anscombe, "Graphs in statistical analysis", *The American Statistician*, vol. 27, no. 1, pp. 17–21, 1973.

[6] G. N. Wilkinson and C. E. Rogers, "Symbolic description of factorial models for analysis of variance.", *Appl Stat*, vol. 22, pp. 392–399, Jan. 1973.

[7] H. Akaike, "Information theory and an extension of the maximum likelihood principle", in *Selected Papers of Hirotugu Akaike*, E. Parzen, K. Tanabe, and G. Kitagawa, Eds. New York, NY: Springer New York, 1998, pp. 199–213.

[8] H. Bozdogan, "Model selection and Akaike's information criterion (AIC): The general theory and its analytical extensions", *Psychometrika*, vol. 52, no. 3, pp. 345–370, Sep. 1987.

[9] E. M. van der Heide, J. R. Buitenweg, E. Marani, and W. L. Rutten, "Single pulse and pulse train modulation of cutaneous electrical stimulation: A comparison of methods", *J Clin Neurophysiol*, vol. 26, no. 1, pp. 54–60, 2009.

[10] Z. G. Zhang, L. Hu, Y. S. Hung, A. Mouraux, and G. D. Iannetti, "Gamma-band oscillations in the primary somatosensory cortex: A direct and obligatory correlate of subjective pain intensity", *Journal of Neuroscience*, vol. 32, no. 22, pp. 7429–7438, 2012.

[11] A. Mouraux, E. Marot, and V. Legrain, "Short trains of intra-epidermal electrical stimulation to elicit reliable behavioral and electrophysiological responses to the selective activation of nociceptors in humans", *Neuroscience Letters*, vol. 561, pp. 69–73, 2014.

[12] S. Ohara, N. E. Crone, N. Weiss, R. D. Treede, and F. A. Lenz, "Amplitudes of laser evoked potential recorded from primary somatosensory, parasylvian and medial frontal cortex are graded with stimulus intensity", *Pain*, vol. 110, no. 1-2, pp. 318–328, 2004.

[13] E. Salinas, A. Hernández, A. Zainos, and R. Romo, "Periodicity and firing rate as candidate neural codes for the frequency of vibrotactile stimuli", *Journal of Neuroscience*, vol. 20, no. 14, pp. 5503–5515, 2000.

[14] Y. Vázquez, E. Salinas, and R. Romo, "Transformation of the neural code for tactile detection from thalamus to cortex", *Proceedings of the National Academy of Sciences*, vol. 110, no. 28, E2635–E2644, 2013.

4 Analysis of Nociceptive Evoked Potentials during Multi-Stimulus Experiments using Linear Mixed Models

Conference paper (submitted)

Experimental data in this chapter was acquired in exploratory research by M. Schooneman and R.J. Doll.

Analysis of Nociceptive Evoked Potentials during Multi-Stimulus Experiments using Linear Mixed Models

B. van den Berg[1] and J. R. Buitenweg[1]

***Abstract*— Neural processing of sensory stimuli can be studied using EEG by estimation of the evoked potential using the averages of large sets of trials. However, it is not always possible to include all stimulus parameters in a conventional analysis, since this would lead to an insufficient amount of trials to obtain the evoked potential by averaging. Linear mixed models use dependencies within the data to combine information from all data for the estimation of the evoked potential. In this work, it is shown that in multi-stimulus EEG data the quality of an evoked potential estimate can be improved by using a linear mixed model. Furthermore, the linear mixed model effectively deals with correlation between parameters in the data and reveals the influence of individual stimulus parameters.**

I. INTRODUCTION

To study neural processing of sensory stimuli using EEG, the evoked potential (EP) must be estimated using sufficient amounts of trials. To identify important parameters of stimulus processing, it is required to apply stimuli with multiple properties. However, experiments to gather the required data on human subjects cannot take too long and the amount of stimuli is limited, which is problematic for the acquisition of sufficient trials. Often, stimulus selection methods are used for a more efficient probing of the stimulus parameter space. However, this results in different amounts of trials per stimulus property. Since the variance of the estimated EP depends on the amount of acquired trials, analysis of those trials using conventional averaging is impeded. This could be overcome by using an analysis method which is robust for variations in the amount of acquired trials. Such a method is provided by a linear mixed model (LMM), which deals with those variations by using dependencies within the data. This means that a lower amount of trials is required to accurately estimate the effect of stimulus parameters with respect to averaging.

Recently, we have used EPs to study neural processing of single and double pulse nociceptive electrical stimuli around the detection threshold, which is defined as the stimulus amplitude at which 50% of the stimuli are detected. For optimal estimation of the probability that a stimulus is detected roughly equal amounts of detected and undetected stimulus-response pairs have to be acquired. To keep stimulus amplitudes around the detection threshold, we developed a method for simultaneous tracking of nociceptive detection thresholds (NDTs) for multiple types of stimuli [1]. A single detection threshold is tracked by an adaptive randomized stimulus sequence which automatically varies the stimulus amplitude with respect to the amount of detected and undetected stimuli. Detection thresholds for multiple stimulus types are tracked by randomly interchanging the stimulus types (*single-pulse* and *double-pulse*) during stimulation, which is shown in Figure 1. Because NDTs change over time due to habituation of the nociceptive system, a wide variety of stimulus amplitudes is used throughout the experiment. Because of this variety, the data does not include equal amounts of trials per stimulus amplitude. This leads to a poor estimation of the signal by averaging, which is shown in Figure 2. To extract and analyze the brain activity during detected and undetected stimuli, a more efficient method than averaging is required.

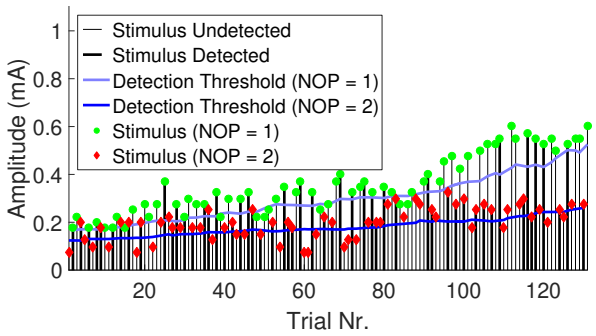

Fig. 1. Simultaneous tracking of NDTs for multiple stimulus types by randomized stimulation around the nociceptive detection threshold [1]. In this case, stimuli with a single pulse (NOP = 1) and a double pulse with 10 ms inter-pulse interval (NOP = 2) were used.

A tool which successfully accounts for the effects of multiple stimulus parameters simultaneously is the linear model (LM). Regression using a LM has the benefit over averaging that it allows for a large number of repeated measures without using many subjects, deals more efficiently with missing data and is flexible in modeling covariates and correlation structures. Although LMs are a popular statistical tool in fMRI research, they have been used by few researchers for EEG analysis, of which some interesting examples include [2] and [3].

Recently Vossen et al. [4] used linear mixed models (LMMs) in EEG analysis to account for between-subject variations and habituation. A major difference with LMs is that LMMs attempt to model the distribution of random effects in the data, enabling subject-level and group-level intercepts and slopes. This provides a convenient way of

[1]B. van den Berg and J. R. Buitenweg are with the Biomedical Signals and Systems group at the MIRA Institute for Biomedical Technology and Technical Medicine, University of Twente, 7500 AE Enschede, The Netherlands.

Correspondence: b.vandenberg@utwente.nl

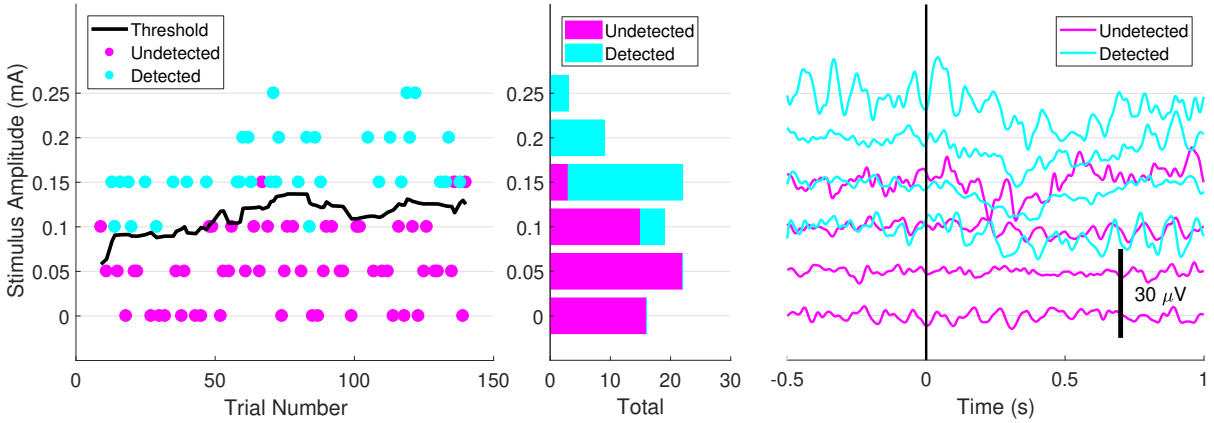

Fig. 2. Summary of data acquired from one of the subjects. The figure on the left shows the amplitudes of all detected and undetected double-pulse stimuli with respect to the NDT. The histogram in the middle shows that at most 25 times the same stimulus was used. This leads to a poor estimation of the EP by averaging, which is shown in the figure on the right.

modeling the dependence of EEG data within one subject or one group. Considering their efficiency in dealing with high-dimensional data, trial-to-trial variability and between-subject variations, they provide an ideal tool for analysis of multivariate EEG data. In addition, they provide means to measure the influence of within-subject and between-subject variations simultaneously, which is useful in clinical studies.

In this work, it is demonstrated that a LMM enables the analysis of variations within EEG data with respect to stimulus intensity and stimulus properties, such as the variation of the EEG signals obtained during NDT tracking experiments. It will be shown that a LMM effectively reduces the amount of background activity, and can be used to measure and test relations between stimulus parameters, psychophysical responses and nociceptive EPs.

II. METHOD

A. Experiment

Single and double-pulse stimuli are applied to twelve healthy subjects (5 male, 7 female) via intra-epidermal electrocutaneous stimulation. Nociceptive detection thresholds are tracked by randomized application of stimuli around the detection threshold [1]. A vector of 5 stimulus amplitudes with a step size of 0.025 mA is initialized, of which one amplitude is chosen randomly for the next stimulus of that type. During the experiment, all amplitudes in this vector are increased or decreased depending on the previous response of the subject. In total 171 ± 24 trials were recorded for every stimulus type from each subject, with a variable amplitude. Figure 1 shows an example of the paradigm.

B. EEG Data Recording and Pre-processing

EEG data was recorded continuously with a sampling rate of 1024 Hz at 64 Ag-AgCl electrodes placed on the scalp according to the international 10-20 system using a TMSi REFA amplifier. In this work, data from the Cz channel is analyzed. Signals are pre-processed using FieldTrip [5], a Matlab toolbox for scientific EEG and MEG analysis. Contamination of the EEG by eye-blinks or movements is corrected using an independent component analysis algorithm [6]. Trials for EP analysis are extracted from the EEG using a window ranging from 0.5 s before until 1.0 s after the stimulus, bandpass filtered from 0.1 to 40 Hz and baseline corrected using the interval ranging from -0.5 s to 0 s relative to stimulus onset. EP data is downsampled to 200 Hz to increase computational speed.

C. Model Formulation

The statistical model should ideally include all relevant experimental parameters. However, the total amount of model parameters should be restricted to prevent overfitting. In this case, the detection of a stimulus (SD) can be expected to be of major influence on the EP. Furthermore, another part of the activity might be directly related to the intensity of the pulse. Both pulses (P1 and P2) can cause an independent increase of brain activity. Brain activity can decrease over time with respect to the number of received stimuli (TRL) due to habituation. Additionally, effect sizes might be dependent on the subject and the measurement session. In this case, there was only one measurement session per subject. The LMM that is used to describe those modulations and random effects is shown in equation 1.

$$\begin{aligned} y = {} & \beta_{Int.} + \beta_{P1}x_{P1} + \beta_{P2}x_{P2} + \beta_{SD}x_{SD} + \beta_{TRL}x_{TRL} \\ & + u_{P1,i}x_{P1} + u_{P2,i}x_{P2} + u_{SD,i}x_{SD} + u_{TRL}x_{TRL} \\ & + u_{Int.,i} + \epsilon \end{aligned} \tag{1}$$

D. Analysis and Statistical Testing

The model variables are centered and scaled based on their mean and standard deviation. Next, model coefficients are estimated for every point in time by optimization of the restricted maximum likelihood using Matlab (The MathWorks Inc., version 2015b). To verify model validity, the model residuals are assessed for normality along the entire EP interval. Significance of the model coefficients is tested against the null-hypothesis using a Wald t-test. To reduce the chance of false significance due to retesting, the requirement

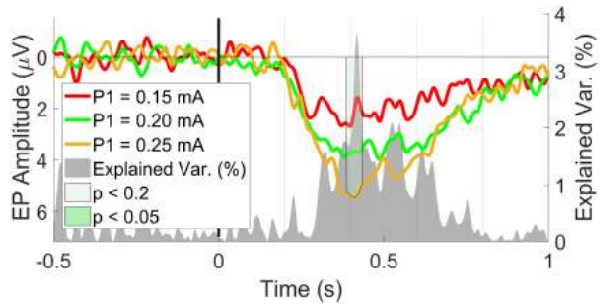

Fig. 3. Grand averages of the EEG signal at Cz, pooled with respect to amplitude values with more than 300 trials. Significance is computed using cluster-based permutation testing [7].

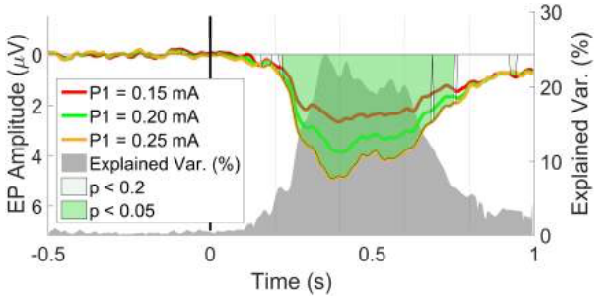

Fig. 4. Average model fit for amplitude values with more than 300 trials at Cz, and the percentage of explained variance of the average model fit. Significance was computed by a Wald t-test of the model coefficient.

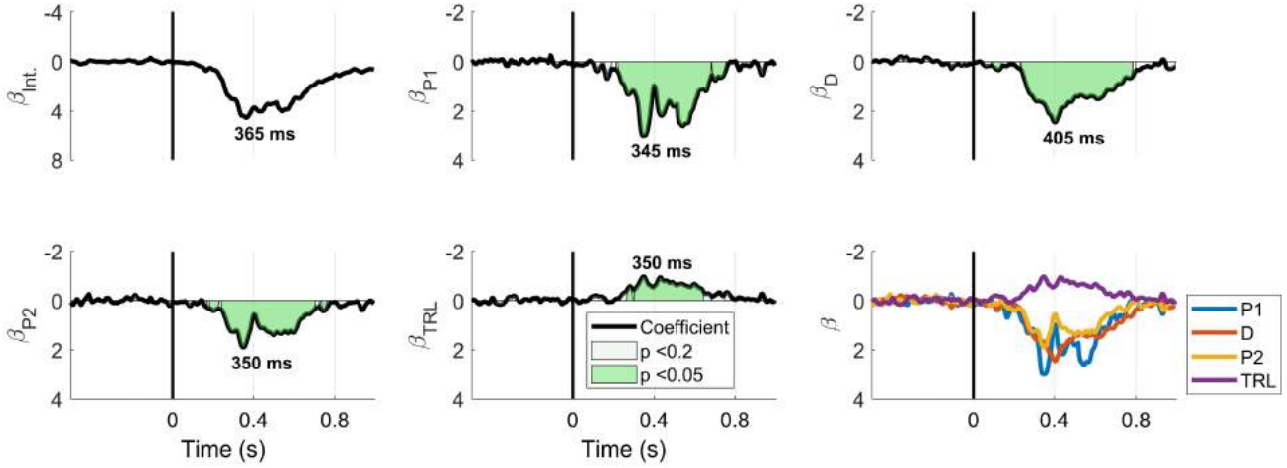

Fig. 5. The model coefficients and their significance based on a Wald t-test at Cz. All coefficients are significant during post-stimulus interval. The influence of the first pulse and second pulse is computed by the coefficients β_{P1} and β_{P2}. The influence of stimulus detection and the number of received stimuli is computed by the coefficients β_D and β_{TRL}.

is imposed that a coefficient should be significant ($p < 0.05$) for at least 4 subsequent time points. Furthermore, the residual is checked for normality along the entire interval.

III. RESULTS

A. Reduction of Background Activity

Figure 2 shows that averaging data for every amplitude and stimulus type per subject results in estimated EPs where post-stimulus activity is difficult to distinguish from pre-stimulus activity due to the high amount of background activity. One way to obtain information about how the EP varies with respect to the stimulus amplitude is by pooling the data with respect to the amplitude and average over considerably larger sets of trials. Figure 3 shows EP waveforms computed by averaging over trials pooled for the three stimulus amplitudes with the largest number of trials. Although the estimate EPs show a clear variation with respect to stimulus amplitude, the pre-stimulus period shows that our estimate still contains a considerable amount of background activity. Figure 4 shows the average fit of an LMM model on the same data. In this figure, the pre-stimulus period shows clearly less background activity.

For both figures, the percentage of explained variance was computed by dividing the variance of the model fit by the total variance on each point in time. In the case of averaging, the average was considered the model fit. A comparison between the amount of explained variance in Figure 3 and Figure 4 shows that the data from all trials using a LMM increases the amount of explained variance. A comparison of the significance returned by cluster-based permutation testing [7] of the contrast (left) and the significance of the model coefficient (right), shows that the significance of the model coefficient a higher and more sustained significance of the effect of stimulus amplitude.

B. Influence of Stimulus Parameters

Model coefficients are shown in Figure 5. All coefficients show a significant modulation of the EP. The coefficients can be used to predict the variation of the EP with respect to the variation of a single parameter. In Figure 6 the variation of EP with respect to the pulse amplitudes and stimulus detection is predicted using the model. The Figures 3 and 4 both show a strong modulation by the stimulus amplitude. However, the prediction of the linear mixed model in Figure 6 mostly varies with respect to stimulus detection.

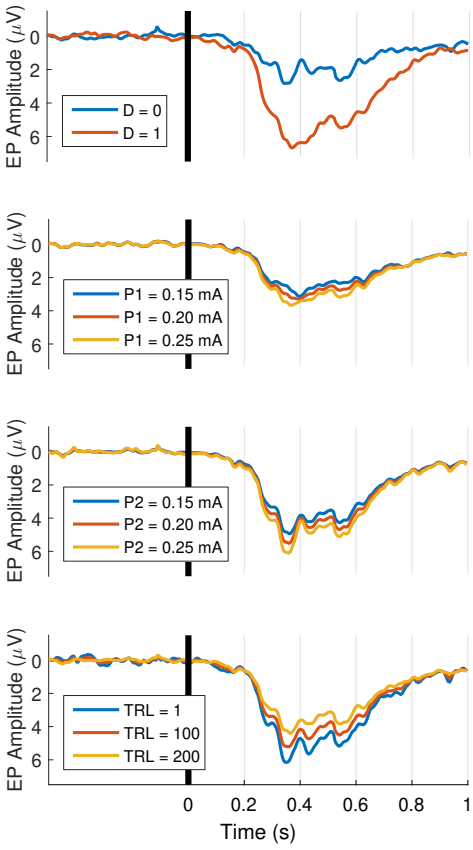

Fig. 6. The effect of variation of stimulus detection (D) the pulse amplitude (P1 and P2) and the amount of received stimuli (TRL) with respect to the model intercept at Cz.

IV. Discussion

A. Reduction of Background Activity

Figure 5 shows that evoked potentials that are estimated using a linear mixed model include less background activity and therefore provide a more accurate estimate of the stimulus-related electrophysiological activity. Furthermore, using a LMM increases the percentage of explained variance with respect to averaging by using a larger amount of trials. This was successfully demonstrated in Figures 3 and 4, where an increase of the explained variance from 3.6% to 24.4% can be observed around 0.4 s. The significance returned by a Wald t-test of the model coefficient returned a higher and more sustained significance of the effect of stimulus amplitude than cluster-based permutation testing. This demonstrates that for a multi-stimulus experiment a Wald t-test of the model coefficient is a more efficient statistical test than cluster-based permutation testing of the contrast.

B. Influence of Stimulus Parameters

The model shows significant modulation of the EP by all factors. As can be expected based on neurophysiology, the coefficient of the first pulse modulates an earlier part of the EP than the coefficient of the second pulse and the coefficient of stimulus detection. A major part of the EP waveform is significantly modulated by the amount of received stimuli: due to habituation the EP will be lower with respect to stimuli of the same amplitude at the end of the experiment. While conventional averaging would not have enabled analysis of the influence of stimulus amplitude and the amount of received stimuli, the LMM successfully accounts for those effects.

Since stimulus detection is correlated with the pulse amplitude (i.e. a higher pulse amplitude results in an increased detection probability), the variation in the average EP in Figures 3 and 4 is likely confounded by stimulus detection. The model prediction in Figure 6 shows that the observed variation of the EP is mainly caused by stimulus detection, while changes in pulse amplitudes only result in minor changes of the EP. Conventional averaging might not have revealed these relations between stimulus parameters and the EP, since inclusion of all potential confounders in the analysis would not be possible due to a lack of trials.

V. Acknowledgment

The authors would like to thank M. Schooneman and R.J. Doll for acquiring the experimental data used in this study.

References

[1] R. Doll, J. Buitenweg, H. Meijer, and P. Veltink, "Tracking of nociceptive thresholds using adaptive psychophysical methods," *Behavior Research Methods*, vol. 46, no. 1, pp. 55–66, 2014.

[2] O. Hauk, F. Pulvermüller, M. Ford, W. D. Marslen-Wilson, and M. H. Davis, "Can I have a quick word? early electrophysiological manifestations of psycholinguistic processes revealed by event-related regression analysis of the EEG," *Biological Psychology*, vol. 80, no. 1, pp. 64–74, 2009.

[3] N. J. Smith and M. Kutas, "Regression-based estimation of ERP waveforms: I. the rERP framework," *Psychophysiology*, vol. 52, no. 2, pp. 157–168, 2015.

[4] H. Vossen, G. van Breukelen, H. Hermens, J. van Os, and R. Lousberg, "More potential in statistical analyses of event-related potentials: A mixed regression approach," *International Journal of Methods in Psychiatric Research*, vol. 20, no. 3, e56–e68, 2011.

[5] R. Oostenveld, P. Fries, E. Maris, and J.-M. Schoffelen, "Fieldtrip: Open source software for advanced analysis of MEG, EEG, and invasive electrophysiological data," *Computational Intelligence and Neuroscience*, vol. 2011, 2011.

[6] A. Delorme and S. Makeig, "EEGLAB: An open source toolbox for analysis of single-trial EEG dynamics including independent component analysis," *Journal of Neuroscience Methods*, vol. 134, no. 1, pp. 9–21, 2004.

[7] E. Maris and R. Oostenveld, "Nonparametric statistical testing of EEG- and MEG-data," *Journal of Neuroscience Methods*, vol. 164, no. 1, pp. 177–190, 2007.

5 Modulation of Central and Lateral Nociceptive Evoked Potentials by Stimulus Parameters

Journal article (to be submitted)

Experimental data was acquired in an experiment that was performed in relation to this thesis. Approval of the Medical Ethics Committee Twente was obtained for this experiment. For more information about the experimental procedure, please refer to Appendix B.

Modulation of Central and Lateral Nociceptive Evoked Potentials by Stimulus Parameters

B. van den Berg[1] and J. R. Buitenweg[1] *(more authors might be included in final version)*

***Abstract*— Studies of the electroencephalogram (EEG) have demonstrated variations of the nociceptive evoked potential with respect to parameters of nociceptive stimuli above the detection threshold. However, it is unknown how the evoked potential is modulated by detected and undetected stimuli close to the detection threshold. Variations of the evoked potential with respect to those stimuli might be directly caused by variations in sub-cortical neural activity, or by the cognitive processes involved with conscious detection of the stimulus. In this work, we assess how brain responses are modulated by the combination of stimulus parameters and stimulus detection to discover how the nociceptive evoked potential is modulated by stimuli around the detection threshold. It is shown that the detection of stimuli causes significant central and contralateral changes of the evoked potential and that detection is the main reason for modulation of the N1, N2 and P2 by stimuli around the detection threshold, while stimulus parameters are only of minor influence.**

I. INTRODUCTION

Nociceptive processing of a stimulus into a consciously detected sensation depends on the amount of peripheral activation and central properties of the nociceptive system. The amount of peripheral activation can be specifically modulated by variations in stimulus amplitude, while variation the the number of pulses and inter-pulse interval of a stimulus are thought to modulate central neural activity [1]. Stimulus-related neural activity arrives via several pathways in the brain, where a network of sensory areas determines whether a stimulus is detected or not. Studies of the electroencephalogram have demonstrated variations of the evoked potential with respect to parameters of the nociceptive stimulus [2–4]. However, it is unknown if those variations are caused by direct modulation of neural activity by the stimulus properties, or by brain activity involved with conscious detection of a stimulus. In the second case, variations of the evoked potential would simply reflect changes in the probability that a stimulus is detected.

Variations of the detection probability with respect to stimulus properties are described by the psychometric curve. Tracking changes in the psychometric curve and the closely related nociceptive detection threshold (NDT) can facilitate the investigation of underlying mechanisms of nociceptive processing [5]. Recently, a method was developed for simultaneous tracking of NDTs with respect to multiple types of intra-epidermal electrocutaneous stimuli. This method, which is referred to as multiple threshold tracking (MTT), was shown to be sensitive to modulations of the detection threshold by stimulus parameters [1], perturbations of nociceptive processing by application of contra-lateral thermal stimuli, and capsaicin induced sensitization [6, 7].

The decision whether a stimulus is detected or not is determined by processing in the brain. Research on tactile detection in macaques has shown that neurons in the primary (SI) and secondary (SII) somatosensory cortex are active whether a stimulus detected or not [8]. However, neural activity in the SI of macaques closely follows the stimulus pattern, whereas downstream areas in tactile processing such as the SII show extremely weak phase-locking to the stimulus pattern [9]. For nociceptive stimuli, stimulus processing occurs simultaneously in the SI and SII [10], whereas downstream areas related to stimulus perception include the prefrontal, anterior cingulate and insular cortex [11]. An objective measure of nociception related activity in the cortex is the electroencephalographic (EEG) signal. The EEG signal measures a summation of activity from multiple cortical areas, and can therefore be expected to contain a combination of stimulus-related and perception-related activity. Transient variations of the EEG which are phase-locked to stimuli are reflected by the evoked potential (EP). For nociceptive stimuli, lateral EP components have been shown to be largely related to neural activity in the SI and SII while central EEG components are related to activity in the anterior cingulate cortex (ACC) and insular cortex (IC) [12].

A tool to study modulation of the EP by stimulus parameters is general linear regression. General linear models are a popular statistical tool in neuroscience due to their relative simplicity and suitability for analysis of neuroscientific experimental paradigms. Despite their popularity for fMRI analysis they are rarely used for analysis of EEG signals, where classical methods such as signal averaging are more popular. Linear modeling of the EP has only started to attract substantial attention in the last decade [13–16]. Vossen et al. [17] demonstrated how a linear mixed model might be used to show group-level habituation effects in nociceptive EPs. They argue that linear-mixed modeling (1) allows for a large number of repeated measures without using many subjects, (2) deals more efficiently with missing data than the ANOVA, (3) is flexible in modelling covariates and correlation structures and (4) can incorporate random factors. Considering their efficiency in dealing with high-dimensional data and trial-to-trial variability, linear mixed-effect models provide an efficient method for analysis of the EP during

[1]B. van den Berg and J. R. Buitenweg are with the Biomedical Signals and Systems group at the MIRA Institute for Biomedical Technology and Technical Medicine, University of Twente, 7500 AE Enschede, The Netherlands.

Correspondence: b.vandenberg@utwente.nl

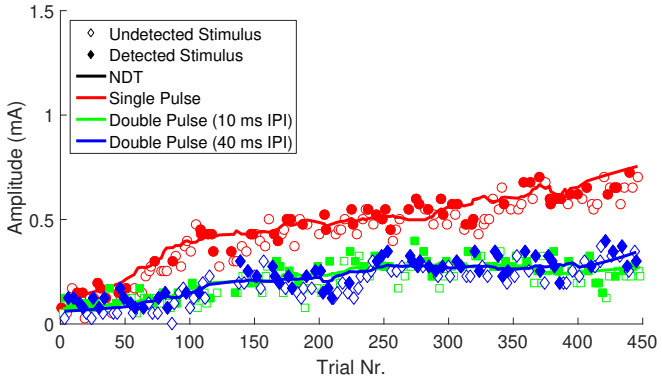

Fig. 1. The MTT paradigm track NDTs for multiple stimulus types simultaneously and continuously by randomized stimulation around the NDT [7]. The sequence of stimuli is varied randomly. All stimulus types are applied in equal amounts.

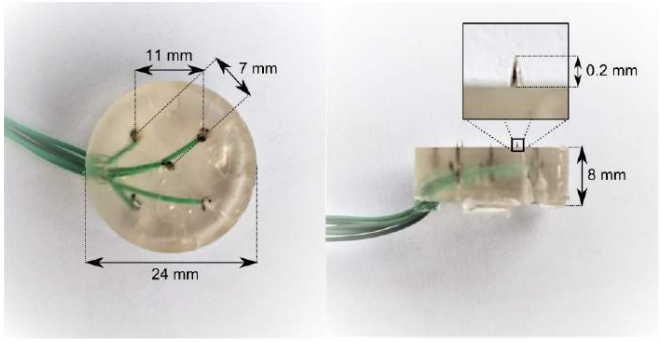

Fig. 2. Intra-epidermal stimulation electrode. Low intensity intra-epidermal stimulation has been shown to specifically activate Aδ nociceptors [].

tracking of NDTs, enabling simultaneous psychophysical and electrophysiological analysis of nociceptive processing. Moreover, they can be used to account for the ambiguous variation of signal components with respect to both stimulus processing and stimulus detection.

By measuring the probability of stimulus detection and stimulus-related brain activity simultaneously, we can characterize the relation between stimuli, neurophysiological activity and conscious stimulus detection. We study how conscious stimulus detection changes the evoked brain potential. Subsequently, we use the technique of linear mixed-regression to determine whether those changes are mostly influenced by conscious stimulus detection itself, or directly modulated by the stimulus parameters.

II. METHOD

A. Multiple Threshold Tracking

Nociceptive detection thresholds were tracked simultaneously for 3 stimulus types on 30 subjects, with a total of 150 stimuli per stimulus type per subject. The Medical Ethics Committee Twente approved all experimental procedures. All subjects provided written informed consent and were rewarded for participation in the experiment.

Subjects are instructed to press and hold a button, and release the button as soon as they feel a sensation that they ascribe to the application of a stimulus. A stimulus is identified as not detected if the subject does not release the response button within 1 second after the stimulus is given. While the button is pressed, the stimulator applies stimuli to the subject with randomized amplitudes around the detection threshold. Subjects are instructed to re-press and hold the button again after approximately second. This procedure repeats until the end of the experiment.

The detection threshold for a specific stimulus setting is initially determined by applying a step-wise increase in stimulus amplitude, until the subject reports stimulus detection. Subsequently, a vector of 5 stimulus amplitudes with a stepsize of 0.025 mA is initialized, of which one amplitude is chosen randomly for the next stimulus of that type. When the stimulus is detected, all amplitudes in the vector of this setting are decreased by the stepsize, while all vector amplitudes are increased by the stepsize when the stimulus is not detected. Figure 1 shows how MTT follows the NDTs for multiple stimulus types simultaneously by using this paradigm.

B. Stimuli

Intra-epidermal electrocutaneous stimuli are applied using a custom made needle electrode (Figure 2) [18]. Needles protrude only 0.2 mm through the *stratum corneum* of the skin. Such a superficial intrusion in the epidermis permits specific activation of Aδ-fibers [19]. Each stimulus consists of one or two cathodic square-wave electrical current pulses with a pulse width of 0.21 ms applied by a AmbuStim single-channel stimulator. The double pulse stimuli have an inter-pulse interval of 10 or 40 ms. Stimuli are selected according to a threshold tracking algorithm [7, 20]. The threshold for each combination of the number of pulses and the inter-pulse interval is tracked simultaneously by measuring the subject's response (*detected* or *not detected*) to a randomized set of stimulus amplitudes, resulting in 3 simultaneously tracked nociceptive detection thresholds. All types of stimuli are selected the same number of times but in a random order.

C. Nociceptive Detection Threshold

The NDT is determined post-hoc for every stimulus by a generalized linear mixed model (GLMM) using the data from all subjects (Equation 1). Individual and group-level NDTs are determined by computation of the GLMM on a moving window of 30 stimulus-response pairs. The GLMM models the subject's response as a logistic curve which is modulated by the stimulus and habituation. The stimulus is described in terms of the amplitude of the first pulse ($SP1$), the amplitude of a second pulse with an inter-pulse interval of 10 ms ($SP2_{10}$) and the amplitude of a second pulse with the inter-pulse interval of 40 ms ($SP2_{40}$). Habituation is modeled with respect to the amount of received stimuli (TRL). Random effects are used to account for dependence of the model coefficients within the subjects. Significance of model coefficients is determined by testing the GLMM coefficients against the null-hypothesis using a t-test.

$$D \sim 1 + SP1 + SP2_{10} + SP2_{40} + TRL + (1 + SP1 + SP2_{10} + SP2_{40} + TRL|Subject) \quad (1)$$

D. EEG Data Recording and Pre-processing

The scalp EEG was recorded continuously with a sampling rate of 1024 Hz at 64 Ag-AgCl electrodes placed on the scalp according to the international 10-20 system using a TMSi REFA amplifier. During the experiment, the subject sits in a comfortable chair and has to focus on a spot on the wall. The subjects are asked to blink as few times as possible during the times they press the response button and hence receive stimuli. Subjects with impedances of higher than 5 kΩ on the channels included in this analysis (CPz, T7, T8, FPz, M1 and M2) were excluded from this analysis. A total of 25 subjects (16 males and 9 females, age 23 ± 3.6, 1 left-handed) was used for analysis.

EEG data is pre-processed using FieldTrip [21], a Matlab toolbox for EEG and MEG signal processing. Contamination of the EEG by eye-blinks or movements is corrected using an independent component analysis algorithm [22], with which components with a clear EOG component and a frontal scalp distribution are removed. Trials for EP analysis are extracted from the EEG using a window ranging from 0.5s before until 1.0s after the stimulus, bandpass filtered from 0.01 to 40Hz and baseline corrected using the interval ranging from -0.5s to 0s relative to stimulus onset.

Components of the EP are identified using a butterfly plot of the grand average over all stimuli, shown in Figure 3. Peaks of the butterfly plot that are associated to seperate EP components are identified at 165ms, 205ms and 420ms. To analyze changes of those EP components, the electrode derivations (referenced to either the average, M1M2 or FPz) with the highest absolute potential at 165ms, 205ms and 420ms are chosen for signal analysis. At 165ms and 205ms, this is the Tc-Fpz (contralateral, T7-FPz or T8-FPz) derivation and at 420ms this is the CPz-A1A2 derivation. For comparison, also the Ti-FPz derivation (ipsilateral, T7-FPz or T8-FPz) is shown in the results. Grand average EPs are computed by averaging trials for detected and for undetected stimuli over those components.

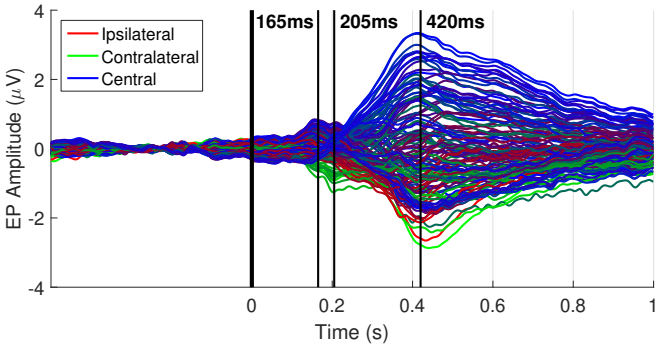

Fig. 3. A butterfly plot of the grand average EP over all stimuli. Peaks of the butterfly plot that are associated to seperate EP components are identified at 165ms, 205ms and 420ms.

E. Analysis and Statistical Testing

Changes of the grand average EP at Tc-Fpz, Ti-Fpz and CPz-A1A2 with respect to stimulus detection are tested for significance using cluster-based non-parametric permutation testing [23].

Subsequently, we study the variation of the EP with respect to stimulus parameters. First, we test if the EP is rather modulated by stimulus detection, stimulus parameters or by a combination of both by testing 5 linear mixed models on the maxima of the N2 and the P2, with the hypotheses that the evoked potential is linearly related to:

1) Stimulus detection:

$$EP \sim 1 + D + TRL + (1 + D + TRL|Subject)$$

2) The probabillity of stimulus detection:

$$EP \sim 1 + DP + TRL + (1 + DP + TRL|Subject)$$

3) Stimulus parameters:

$$EP \sim 1 + SP1 + SP2_{10} + SP2_{40} + TRL + (1 + SP1 + SP2_{10} + SP2_{40} + TRL|Subject)$$

4) Stimulus parameters and detection:

$$EP \sim 1 + D + SP1 + SP2_{10} + SP2_{40} + TRL + (1 + D + SP1 + SP2_{10} + SP2_{40} + TRL|Subject)$$

5) Stimulus parameters and probability of detection:

$$EP \sim 1 + DP + SP1 + SP2_{10} + SP2_{40} + TRL + (1 + DP + SP1 + SP2_{10} + SP2_{40} + TRL|Subject)$$

For each model stimulus detection (D) is determined by the subject's response (*detected* or *not detected*) in the respective trial. The detection probability (DP) is computed based on the subject's individual psychometric curve over a window of 30 stimuli of each type, computed by fitting an LMM using Equation 1. The stimulus is described in terms of the amplitude of the first pulse ($SP1$), the amplitude of the second pulse with an inter-pulse interval of 10 ms ($SP2_{10}$) and the amplitude of the second pulse with an inter-pulse interval of 40 ms ($SP2_{40}$). Habituation is modeled with respect to the amount of received stimuli (TRL).

Each model is computed at Tc-Fpz and CPz-A1A2 with respect to the maximum EP value of the N205 and P420 by optimization of the maximum likelihood. Subsequently, we pick the best general model of the data based on the Akaike Information Criterion (AIC) [24] for further analysis of the principal behavior of the evoked potential component with respect to stimulus properties. Furthermore, we check if adding any interactions between model components might result in a lower AIC.

The most likely model is used for analysis of the entire EP interval (-0.5 to 1.0 ms) of Tc-Fpz and CPz-A1A2. Model computation and analysis is performed in Matlab

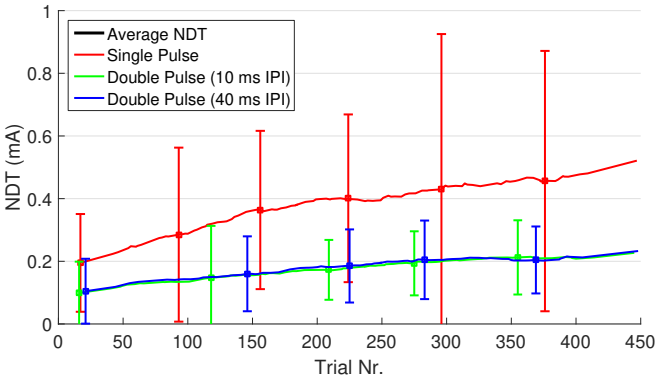

Fig. 4. Nociceptive detection thresholds with respect to stimulus type and the amount of received stimuli, which is reflected by the trial number. Error bars indicate the standard deviation of the NDTs between subjects.

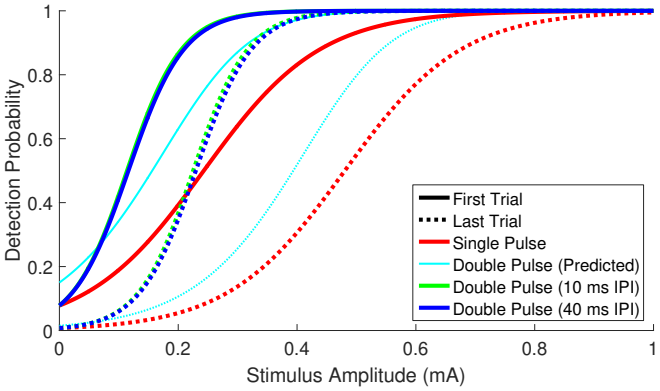

Fig. 5. Psychometric curves for every stimulus type at the start of the experiment (solid line) and at the end of the experiment (dotted line).

(The MathWorks Inc., version 2015b). Model variables are centered and scaled to speed up the estimation progress.

Model coefficients are estimated for every point in time by optimization of the restricted maximum likelihood. To verify model validity, the model residuals are assessed for normality along the entire EP interval using a continuous boxplot, skewness and kurtosis of the residual. Significance of the model coefficients is tested against the null-hypothesis using a Wald t-test. To reduce the chance of false significance due to retesting, the requirement is imposed that a coefficient should be significant ($p < 0.05$) for at least 4 subsequent time points.

III. RESULTS

A. Detection Threshold

The average NDTs that were determined by analysis of the stimulus-response pairs are shown in Figure 4. For all stimulus types, the NDT increases over time, indicating that the average psychometric curve shifts to higher stimulus intensities during the experiment. The standard deviation of the subject-specific NDTs, displayed by the vertical error bars, is much smaller for subject NDTs of double pulse stimuli than for the subject NDTs with respect to single pulse stimuli. Additionally, NDTs of double pulse stimuli show a smaller increase in time than the NDTs measured for single pulse stimuli.

Psychometric curves determined using the GLMM in Equation 1 are shown in Figure 5. Corresponding with the observed NDTs, there is a major shift of the psychometric curve with respect to time. Additionally, the amount of pulses causes a major change in the offset and the slope of the psychometric curve, which is much bigger than the predicted variation based on probability summation. However, a change in the inter-pulse interval does not change the offset or slope of the curve.

Table I shows the computed GLMM coefficients and their p-values. The first and the second pulse are both significantly modulating the psychometric curve (p<0.001). Furthermore, the psychometric curve significantly shifts over time, modulated by the amount of received stimuli (p<0.001). However, the coefficient related to the second pulse remains roughly equal with respect of the inter-pulse interval.

B. Grand Average EPs

Grand average scalp topographies of the EP with respect to detected and undetected stimuli are shown in Figure 6. At 165 ms and 205 ms, the topography shows a clear negative contralateral component with its maximum in the temporal area at Tc and a smaller ipsilateral component at Ti. At 420 ms a strong central component dominates scalp EEG activity with its maximum at CPz-A1A2.

The grand average EP with respect to detected and undetected stimuli at CPz-A1A2, Tc-Fpz and Ti-Fpz is shown in Figure 7. At CPz-A1A2, detected stimuli elicit a clear positive component with a maximum at approximately 420 ms after stimulus onset, which will be referred to as the P420. Stimuli that were not detected show a late positive component without a clear waveform. There is a significant difference between detected and undetected stimuli during the P420 at Cz-A1A2.

At Tc-Fpz detected and undetected stimuli elicited an early negative component with peaks at 165 ms and 205 ms, which will be referred to as the N165 and N205 respectively, followed by a small positive component which is considered to be related to the activity measured by the P420. At Ti-

Parameter	**Coefficient**	t**-statistic**	p**-value**
Intercept	-2.41	-10.96	<0.001
First Pulse	10.26	6.05	<0.001
Second Pulse (10 ms)	11.82	8.14	<0.001
Second Pulse (40 ms)	11.37	8.02	<0.001
Nr. of Received Stimuli	-0.0056	-6.12	<0.001

TABLE I

GLMM COEFFICIENTS AND P-VALUES WITH RESPECT TO STIMULUS PARAMETERS. THE FIRST AND THE SECOND PULSE ARE BOTH SIGNIFICANTLY MODULATING THE PSYCHOMETRIC CURVE (P<0.001). FURTHERMORE, THE PSYCHOMETRIC CURVE SIGNIFICANTLY SHIFTS OVER TIME, MODULATED BY THE AMOUNT OF RECEIVED STIMULI (P<0.001).

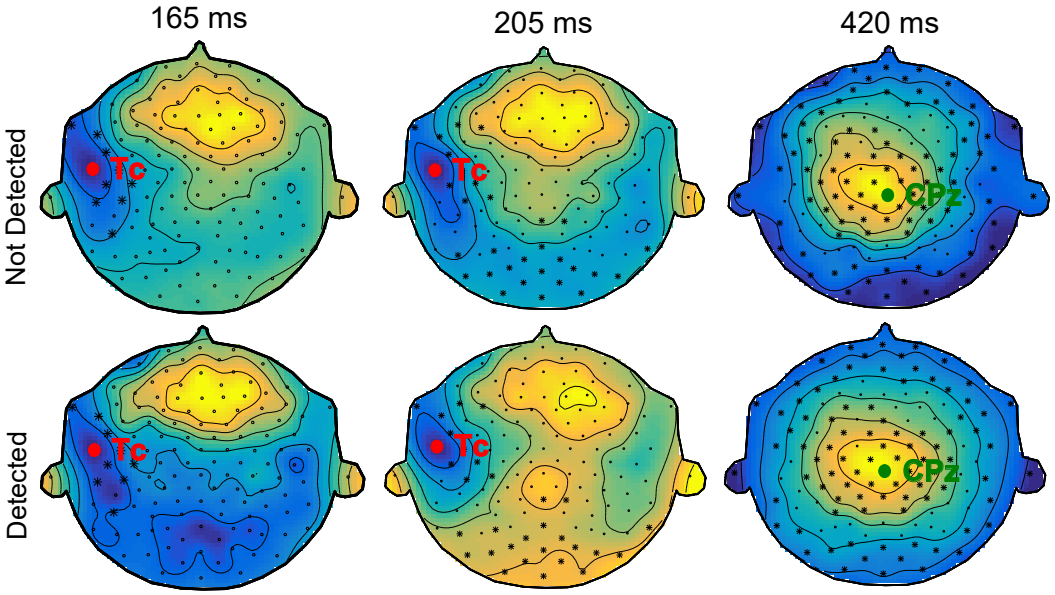

Fig. 6. Normalized grand average scalp topographies with respect to stimulus detection. Channels that vary significantly with respect to stimulus detection, based on cluster-based non-parametric permutation testing [23], are indicated with a star (*).

Fpz a negative component is present with a maximum at 225 ms. There is a significant difference between detected and undetected stimuli during the N165 and N205 at Tc-Fpz and during the P420 at both Tc-Fpz and Ti-Fpz.

C. Modulation of Nociceptive EPs by Stimulus Parameters

The AIC values computed for each model at the maximum P420 (CPz-A1A2 at 420 ms) and the maximum N205 (Tc-FPz at 205 ms) are shown in Table II. Model number 4, the ERP explained by a combination of stimulus parameters and detection has the lowest value of the AIC for both components and is therefore used for further analysis of the EP. Additionally, by checking the AIC for models with additional interactions ($SP_x * TRL$ and $SP_x * D * TRL$), it was determined that the current version of model 4, without interactions, has the lowest AIC possible.

Figure 8 shows the model coefficients of model 4 for the EP at Tc-FPz and CPz-A1A2 re-scaled to their physical quantities. The scale of each physical unit is adapted to correspond to variations of the physical quantity within the experiment. At CPz-A1A2 all coefficients significantly modulate the EP. The first and the second pulse (after both 10ms and 40ms) have a positive value during the P420 and amplify it's amplitude. The amount of received stimuli has a negative coefficient during the P420, which means that the amplitude of the P420 decreases with respect to the amount of received stimuli. However, the modulation by stimulus

Model	AIC at P2	AIC at N2
1	2.5285e4	2.6947e4
2	2.5849e4	2.6948e4
3	2.6127e4	2.6998e4
4	**2.5248e4**	**2.6913e4**
5	2.5845e4	2.6984e4

TABLE II

AIC VALUE OF THE TESTED STATISTICAL MODELS AT THE MAXIMUM VALUE OF THE P420 COMPONENT AT CPZ-A1A2 AND THE MAXIMUM VALUE OF THE N205 COMPONENT AT TC-FPZ

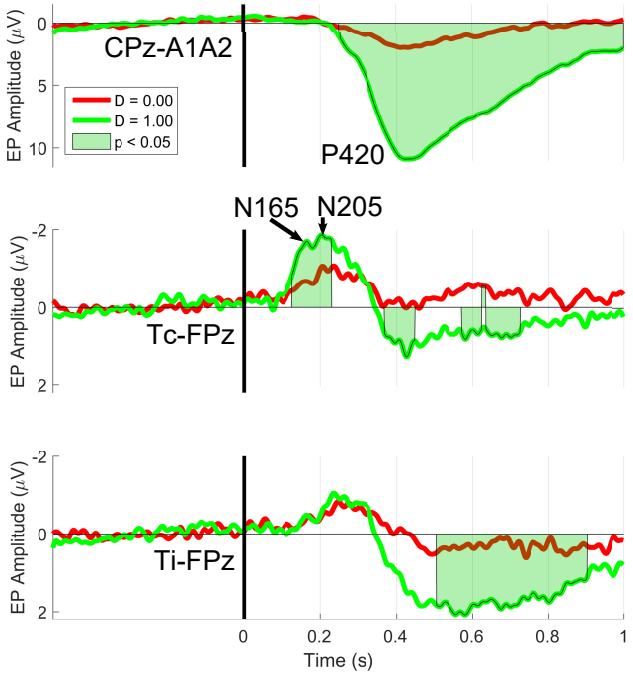

Fig. 7. Channel grand averages at the CPz-A1A2, Tc-FPz and Ti-FPz (for comparison). Times on which the signal varies significantly with respect to stimulus detection, based on cluster-based non-parametric permutation testing [23], are indicated in green.

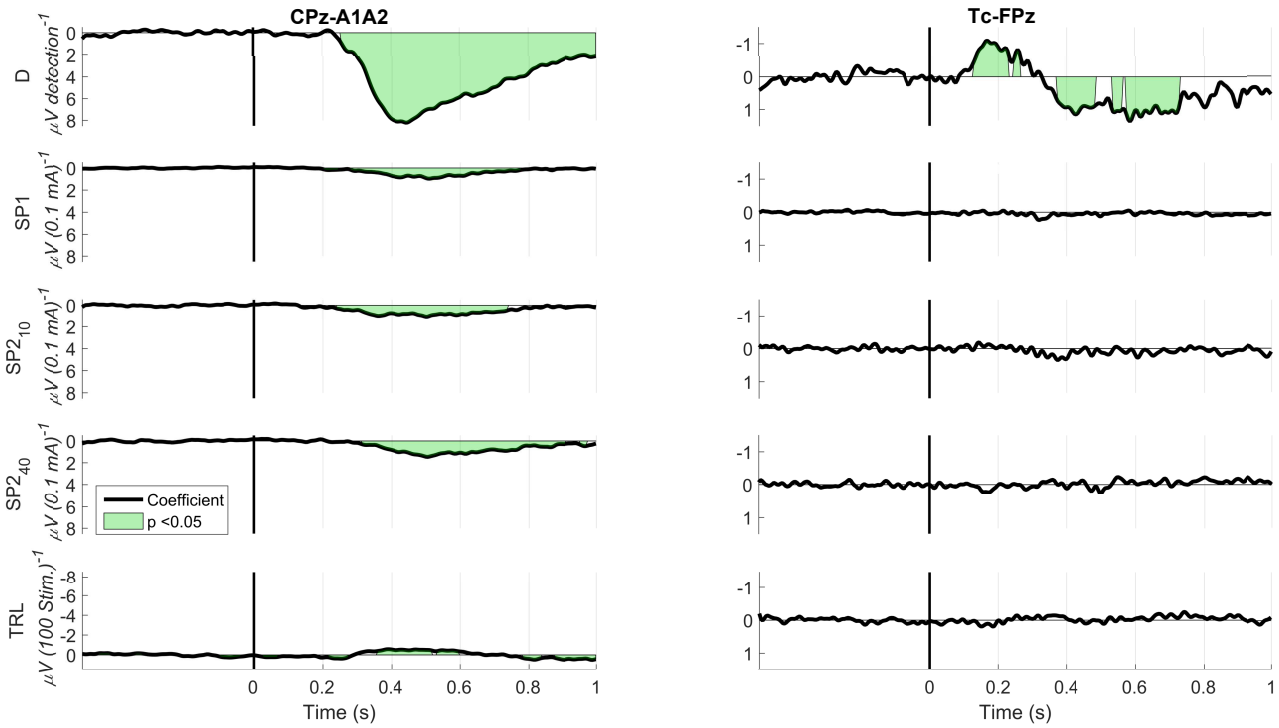

Fig. 8. The model coefficients and their significance based on a Wald t-test at CPz-A1A2 and Tc-FPz. The influence of the first pulse and second pulse is computed by the coefficients β_{SP1} and β_{SP2}. The influence of stimulus detection and the number of received stimuli is computed by the coefficients β_D and β_{TRL}. At CPz-A1A2 all coefficients are significant during the post-stimulus interval. However, at Tc-FPz only stimulus detection significantly modulates the EP amplitude.

detection is much more prominent than other modulations, as the detection of a stimulus severely increases the amplitude of the P420.

Model coefficients at Tc-FPz show no significant modulation of pulse amplitude or the number of received stimuli at all, over the entire EP interval. Like the P420 at CPz-A1A2, stimulus detection is the main reason for variation of the N205 at Tc-FPz according to the LMM coefficients.

IV. DISCUSSION

We have performed a psychophysical experiment to study the effect of temporal stimulus properties on conscious stimulus detection and simultaneously measured cortical brain activity using EEG. During the experiment, we varied the number of pulses and the interval between the pulses. Using the combination of psychometric experimental data and measures of brain activity, we can not only study the effect of stimulus properties on the detection probability, but also study the underlying patterns in brain activity associated with stimulus detection. During the experiment, the brain potentials evoked by detected intra-epidermal electrocutaneous stimuli elicited three main components: the N165, N205 and P420. However, undetected stimuli only comprised two visible components: the N165 and N205. We study the influence of stimulus detection by looking at the grand average of detected and undetected stimuli. Furthermore, the extend to which this modulation is related to stimulus parameters or to the processes related to detection itself can be analyzed using a linear mixed model.

A. Linear Mixed Model

A linear mixed model was used to analyze the modulation of the EP by stimulus parameters and detection. Because this method does not rely on pooled averages of the data with respect to combinations of experimental parameters such as in the classical ANOVA, but uses all trials as repeated measures instead, it results in a statistically more efficient estimate of the coefficients. However, including all trials in a LMM does require the assumption of linearity. This assumption can be particularly checked by studying the residuals. When the evoked potential is modulated by a non-linear function, the residual is expected to deviate from the normal distribution. An analysis of our model residuals along the entire EP interval by graphing a continuous boxplot, skewness and kurtosis of the model residual did not reveal such deviations. Furthermore, the significant coefficients are continuous over the model computations we ran for every time-point. Therefore, we believe our statistical model provides a relevant description of variations in our data.

B. Nociceptive Detection Threshold

The nociceptive detection probability was measured by application of intra-epidermal electrical stimuli using a needle electrode [25]. This device preferentially stimulates nociceptive specific Aδ-fibers if stimuli are lower than twice

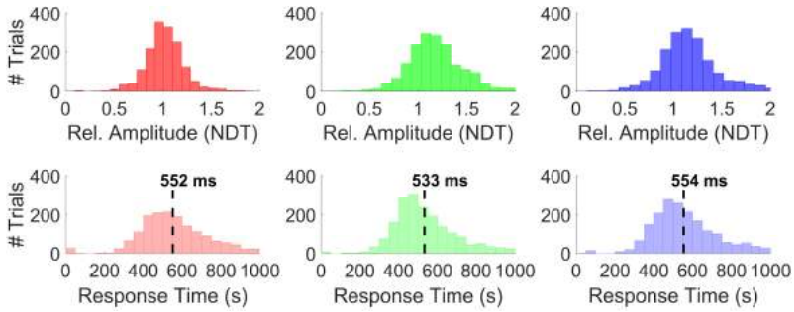

Fig. 9. Relative amplitudes and response times of the applied stimuli. The relative amplitude of stimuli is normally distributed with respect to the detection threshold by the tracking algorithm.

the detection threshold [19]. The adaptive algorithm used for tracking of the NDT applied stimuli with a randomized amplitude. Since the distribution of those stimuli was closely centered around the detection threshold, most stimuli were within this range (Figure 9). Stimuli that were higher than twice the detection threshold were excluded from the experiment to reduce the influence of Aβ-fibers. Therefore, stimulus- and detection-related brain activity and the NDT measured in this experiment are mostly mediated by the activation of nociceptive Aδ-fibers.

The measured detection probabilities and associated thresholds were comparable to those found in previous studies using a similar electrode [1]. Studies using a single-needle electrode [19, 26] found a threshold which was approximately 5 times lower, which effectively results in a similar current density around the needle due to the lower amount of needles. The model coefficients in Table I show that the detection probability is mainly modulated by the addition of a second pulse and by the amount of received stimuli. Figure 5 shows that the detection probability increases much more with respect to the addition of a second pulse than one would expect based on probability summation, which means that the detection of the second pulse is facilitated by the first pulse. However, there is no difference in facillitation with respect to the inter-pulse interval, indicating that the facilitatory effect of the first pulse remains constant for at least 40ms.

C. Modulation of the Central Component: P420

Based on the latency and topography of the observed P420, it seems to correspond to the P2 that was identified in earlier nociceptive EP studies [27, 28]. However, it's amplitude is lower than in most nociceptive EP studies because the stimulus is close to the detection threshold. In previous studies on NEPs the P420 has been related to modulation by attention [29–31] or modulation by stimulus probability [32]. In this study, the stimulus probability remained equal because the inter-stimulus interval was randomized using a uniform distribution and the same amount of every stimulus was applied. The LMM coefficient of habituation (Figure 8) is significantly negative around the observed P420, indicating that the amplitude decreases with respect to the amount of received stimuli, which might be caused by the decrease of the subject's attention over time.

During this experiment we observed another essential property of the P2: The P420 peak amplitude is negligible when a stimulus is not detected, and significantly larger when a stimulus is detected. This means that the P2 is only evoked when a stimulus is consciously detected by the subject. Therefore, the P2 cannot be regarded as a direct correlate of stimulus processing, but rather as a representation of the cognitive processes related to stimulus perception.

D. Modulation of the Lateral Components: the N165 and N205

The significant negative lateral components that were observed at Tc-FPz, the N165 and N205, match the N1 and N2 identified in literature [27, 28, 33] respectively, based on their waveform and topography. Similar to Legrain et al. [32], the N2 shows a contra-lateral topography, instead of a lateralized topography. Since the N2 is thought to be related to attentional modulation and stimulation at the same location will cause an uni-lateral modulation of attention, this might explain the contra-lateral enhancement of the N2 in our data. In the grand average, the N1 and N2 are visible for both detected and undetected stimuli, and vary significantly with stimulus detection. Using a LMM, only stimulus detection appears to modulate the N1 and N2 amplitude. Even though adding the pulse amplitudes to the model leads to an increase in AIC, the coefficients related to the pulse-amplitudes are very small, are not significant and show a seemingly random variation along the entire EP interval. Therefore, we conclude that the N1 and N2 only vary with respect to stimulus detection.

It remains unexplained why there still is a clear N2 present, even when a stimulus is undetected. In earlier studies on nociceptive processing [32], the N2 is related to attentional modulation of nociceptive processing. Therefore, it is possible that the N2 modulates the chance of a stimulus being detected. This would lead to an inverted relationship: instead of the detection of a stimulus leading to an elevated N2, a higher N2 increases the chance of detection leading to a higher detection probability.

V. CONCLUSION

It was shown that nociceptive stimulus detection modulates stimulus processing in the brain. Detection of stimuli

causes significant central and contralateral changes. The central P420, which corresponds to the P2 in literature, is modulated by a combination of stimulus detection, pulse amplitudes, and the number of received stimuli. However, pulse amplitudes and the number of received stimuli only account for a minor part of the variation in P2, while stimulus detection accounts for the major part of the P2 component. The contralateral N165 and N205, which correspond to the N1 and N2 in literature, are significantly modulated by stimulus detection and only indirectly correlated to changes in stimulus parameters. Since stimulus detection is significantly modulated by stimulus parameters, stimulus parameters indirectly modulate the N1, N2 and P2 by modulating the detection probability.

References

[1] R. Doll, A. Maten, S. Spaan, P. Veltink, and J. Buitenweg, "Effect of temporal stimulus properties on the nociceptive detection probability using intra-epidermal electrical stimulation," *Experimental Brain Research*, vol. 234, no. 1, pp. 219–227, 2016.

[2] E. M. van der Heide, J. R. Buitenweg, E. Marani, and W. L. Rutten, "Single pulse and pulse train modulation of cutaneous electrical stimulation: A comparison of methods," *J Clin Neurophysiol*, vol. 26, no. 1, pp. 54–60, 2009.

[3] A. Mouraux, E. Marot, and V. Legrain, "Short trains of intra-epidermal electrical stimulation to elicit reliable behavioral and electrophysiological responses to the selective activation of nociceptors in humans," *Neuroscience Letters*, vol. 561, pp. 69–73, 2014.

[4] C. Vossen, H. Vossen, E. Joosten, J. Van Os, and R. Lousberg, "Does habituation differ in chronic low back pain subjects compared to pain-free controls? A cross-sectional pain rating ERP study reanalyzed with the ERFIA multilevel method," *Medicine (United States)*, vol. 94, no. 19, 2015.

[5] R. Doll, J. Buitenweg, H. Meijer, and P. Veltink, "Tracking of nociceptive thresholds using adaptive psychophysical methods," *Behavior Research Methods*, vol. 46, no. 1, pp. 55–66, 2014.

[6] R. Doll, G. van Amerongen, J. Hay, G. Groeneveld, P. Veltink, and J. Buitenweg, "Responsiveness of electrical nociceptive detection thresholds to capsaicin-induced changes in nociceptive processing.," *Experimental Brain Research*, vol. 234, no. 9, pp. 2505–2514, 2016.

[7] R. J. Doll, "Psychophysical methods for improved observation of nociceptive processing," Thesis, 2016.

[8] E. Salinas, A. Hernández, A. Zainos, and R. Romo, "Periodicity and firing rate as candidate neural codes for the frequency of vibrotactile stimuli," *Journal of Neuroscience*, vol. 20, no. 14, pp. 5503–5515, 2000.

[9] Y. Vázquez, E. Salinas, and R. Romo, "Transformation of the neural code for tactile detection from thalamus to cortex," *Proceedings of the National Academy of Sciences*, vol. 110, no. 28, E2635–E2644, 2013.

[10] M. Ploner, J. Gross, L. Timmermann, and A. Schnitzler, "Pain processing is faster than tactile processing in the human brain," *Journal of Neuroscience*, vol. 26, no. 42, pp. 10 879–10 882, 2006.

[11] M. Bushnell and A. Apkarian, "Representation of pain in the brain," in *Wall and Melzack's Textbook of Pain, 5th edition*, McMahon and Kotzenburg, Eds. Elsevier, 2006, pp. 107–124.

[12] L. Garcia-Larrea, M. Frot, and M. Valeriani, "Brain generators of laser-evoked potentials: From dipoles to functional significance," *Neurophysiologie Clinique*, vol. 33, no. 6, pp. 279–292, 2003.

[13] O. Hauk, M. H. Davis, M. Ford, F. Pulvermüller, and W. D. Marslen-Wilson, "The time course of visual word recognition as revealed by linear regression analysis of ERP data," *NeuroImage*, vol. 30, no. 4, pp. 1383–1400, 2006.

[14] O. Hauk, F. Pulvermüller, M. Ford, W. D. Marslen-Wilson, and M. H. Davis, "Can I have a quick word? Early electrophysiological manifestations of psycholinguistic processes revealed by event-related regression analysis of the EEG," *Biological Psychology*, vol. 80, no. 1, pp. 64–74, 2009.

[15] N. J. Smith and M. Kutas, "Regression-based estimation of ERP waveforms: I. the rERP framework," *Psychophysiology*, vol. 52, no. 2, pp. 157–168, 2015.

[16] ——, "Regression-based estimation of ERP waveforms: II. nonlinear effects, overlap correction, and practical considerations," *Psychophysiology*, vol. 52, no. 2, pp. 169–181, 2015.

[17] H. Vossen, G. van Breukelen, H. Hermens, J. van Os, and R. Lousberg, "More potential in statistical analyses of event-related potentials: A mixed regression approach," *International Journal of Methods in Psychiatric Research*, vol. 20, no. 3, e56–e68, 2011.

[18] P. Steenbergen, J. Buitenweg, J. Trojan, E. van der Heide, T. van den Heuvel, H. Flor, and P. Veltink, "A system for inducing concurrent tactile and nociceptive sensations at the same site using electrocutaneous stimulation," *Behavior Research Methods*, vol. 44, no. 4, pp. 924–933, 2012.

[19] A. Mouraux, G. Iannetti, and L. Plaghki, "Low intensity intra-epidermal electrical stimulation can activate A-delta nociceptors selectively," *Pain*, vol. 150, no. 1, pp. 199–207, 2010.

[20] R. Doll, P. Veltink, and J. Buitenweg, "Observation of time-dependent psychophysical functions and accounting for threshold drifts," *Attention, Perception, and Psychophysics*, vol. 77, no. 4, pp. 1440–1447, 2015.

[21] R. Oostenveld, P. Fries, E. Maris, and J.-M. Schoffelen, "Fieldtrip: Open source software for advanced analysis of MEG, EEG, and invasive electrophysiological data," *Computational Intelligence and Neuroscience*, vol. 2011, 2011.

[22] A. Delorme and S. Makeig, "EEGLAB: An open source toolbox for analysis of single-trial EEG dy-

namics including independent component analysis," *Journal of Neuroscience Methods*, vol. 134, no. 1, pp. 9–21, 2004.

[23] E. Maris and R. Oostenveld, "Nonparametric statistical testing of EEG- and MEG-data," *Journal of Neuroscience Methods*, vol. 164, no. 1, pp. 177–190, 2007.

[24] H. Akaike, "Information theory and an extension of the maximum likelihood principle," in *Selected Papers of Hirotugu Akaike*, E. Parzen, K. Tanabe, and G. Kitagawa, Eds. New York, NY: Springer New York, 1998, pp. 199–213.

[25] P. Steenbergen, J. R. Buitenweg, J. Trojan, E. M. van der Heide, T. van den Heuvel, H. Flor, and P. H. Veltink, "A system for inducing concurrent tactile and nociceptive sensations at the same site using electrocutaneous stimulation," *Behavior Research Methods*, vol. 44, no. 4, pp. 924–933, 2012.

[26] K. Inui, T. Tran, M. Hoshiyama, and R. Kakigi, "Preferential stimulation of A-delta fibers by intraepidermal needle electrode in humans," *Pain*, vol. 96, no. 3, pp. 247–252, 2002.

[27] R.-D. Treede, S. Kief, T. Hölzer, and B. Bromm, "Late somatosensory evoked cerebral potentials in response to cutaneous heat stimuli," *Electroencephalography and Clinical Neurophysiology*, vol. 70, no. 5, pp. 429–441, 1988.

[28] M. Miyazaki, H. Shibasaki, M. Kanda, X. Xu, K. Shindo, M. Honda, A. Ikeda, T. Nagamine, R. Kaji, and J. Kimura, "Generator mechanism of pain-related evoked potentials following CO2 laser stimulation of the hand: Scalp topography and effect of predictive warning signal," *Journal of Clinical Neurophysiology*, vol. 11, no. 2, pp. 242–254, 1994.

[29] A. Beydoun, T. J. Morrow, J. F. Shen, and K. L. Casey, "Variability of laser-evoked potentials: Attention, arousal and lateralized differences," *Electroencephalography and Clinical Neurophysiology/Evoked Potentials Section*, vol. 88, no. 3, pp. 173–181, 1993.

[30] R. Zaslansky, E. Sprecher, C. Tenke, J. Hemli, and D. Yarnitsky, "The P300 in pain evoked potentials," *Pain*, vol. 66, no. 1, pp. 39–49, 1996.

[31] L. García-Larrea, R. Peyron, B. Laurent, and F. Mauguière, "Association and dissociation between laser-evoked potentials and pain perception," *NeuroReport*, vol. 8, no. 17, pp. 3785–3789, 1997.

[32] V. Legrain, J. M. Guérit, R. Bruyer, and L. Plaghki, "Attentional modulation of the nociceptive processing into the human brain: Selective spatial attention, probability of stimulus occurrence, and target detection effects on laser evoked potentials," *Pain*, vol. 99, no. 1-2, pp. 21–39, 2002.

[33] V. Kunde and R.-D. Treede, "Topography of middle-latency somatosensory evoked potentials following painful laser stimuli and non-painful electrical stimuli," *Electroencephalography and Clinical Neurophysiology/Evoked Potentials Section*, vol. 88, no. 4, pp. 280–289, 1993.

6 Discussion & Conclusion

To understand the nociceptive system in terms of models, phenomena related to the behavior of the nociceptive system with respect to nociceptive stimuli have to be observed. The aim of this work was to provide a method to observe such phenomena, by combining the technique of multiple threshold tracking with techniques to record and analyze cortical activity. To do this, a statistical analysis method to process and interpret evoked potentials was developed, which was based on linear mixed regression. We described the quality and content of electrical brain responses of pain free subjects to electrocutaneous stimuli during multiple threshold tracking by analyzing the variance of averaged responses and by exploration of the use of a linear mixed model to explain the variability in these responses, which was the primary objective of this thesis. As a secondary objective we wanted to analyze if and how brain responses are associated with the properties of applied stimuli, the amount of previously received stimuli and the response of the subject concerning the stimulus. The research questions related to both objectives are discussed in this section. Furthermore, recommendations are made for future research directions.

6.1 Discussion

6.1.1 Can a linear mixed model be used to improve analysis of evoked potentials during multiple threshold tracking?

The combination of background EEG activity and noise is generally much larger than the amplitude of stimulus-related brain activity. While an EP mainly contains content from 0 to 30 Hz, EEG background activity generally has a $\frac{1}{f}$ frequency spectrum with its main amplitude in the low frequency ranges [1]. In Chapter 4 it was shown that for the most prominent EP component, the P2, the maximum amount of explained variance using a pooled average over the amplitudes was 3.6%. Although one might improve the amount of explained variance by averaging for every combination of parameters, this does not lead to an interpretable signal as is shown in Figure 2 of Chapter 4. However, by using a LMM, we can include more parameters in the analysis without decreasing the SNR.

To which extend can a LMM be used to describe the data? And to which extend can a LMM improve the quality of the measurements?

With averaging an inverse relation between the amount of explained variance and the SNR exists because averaging over more combinations of parameters leads to smaller subsets of trials, which will lead a higher variance of the estimated EP. More specifically, the standard error of the estimate decreases with $\frac{1}{\sqrt{n}}$ with respect to the amount of averaged trials. A LMM allows for inclusion of all trials that can be expected to have a linear variation with respect to the LMM parameters, without decreasing the amount of variance explained. With respect to averaging, a LMM therefore has the benefit that variation of the EP can be estimated with respect to all parameters with the benefit of having a reduction of background activity based on all trials [1]. In this way, the maximum amount of explained variance in Chapter 4 was increased from 3.6% to 24.4% by using a LMM, while the SNR also improved.

An essential assumption of the LMM is linearity of the model parameters. When one of the parameters in the model has a non-linear effect on the EP, a LMM might no longer lead to an increase in the percentage of explained variance. In Chapter 3 it was shown that with a sufficiently low amount of background activity, such a non-linearity can be readily identified based on the distribution of the residual. For analysis of entire EP intervals, the kurtosis and skewness of the residual could be used instead of a histogram. However, kurtosis and skewness might no longer suffice for identification of a non-linear effect when the standard error of the estimates of skewness and kurtosis becomes too big to visually identify any possible non-linearities. In this case the histogram will not provide any reliable information either. This possibly leads to errors in the statistical model which is a potential weakness of using a LMM. However, one might reduce the chance on such errors by extensive testing of potential statistical models of the signal and selecting the best generalizable model using the AIC.

Are the LMM coefficients significant in exploratory data?

An exploratory dataset provided by M. Schooneman [2] was analyzed in Chapter 4. The LMM in Chapter 4 showed significant modulation of the EP at the Cz channel by all parameters including both pulses, the number of received stimuli and stimulus detection. The coefficient of the first pulse modulates an earlier part of the EP at Cz than the coefficient of the second pulse and the coefficient of stimulus detection. Furthermore, a major part of the EP is significantly negatively modulated by the amount of received stimuli: due to habituation the EP will be lower with respect to stimuli of the same amplitude at the end of the experiment. While conventional averaging would not have enabled analysis of the influence of stimulus amplitude and the amount of received stimuli simultaneously, the LMM successfully accounts for those effects and shows which effects significantly modulate the EP.

6.1.2 How is neurophysiological activity related to stimulus parameters during multiple threshold tracking?

In Section 2.2 of the Background (Chapter 2), it was described how cerebral activity can be both directly and indirectly influenced by a stimulus. An intra-epidermal stimulus generates an action potential in a group of nociceptive nerve fibers, of which the number of activated fibers will depend on the amplitude of the pulse (Figure 6.1: A1). Subsequently, nerve fibers transmit the action potential through one of the several tracts leading to the cerebrum (Figure 6.1: A2), each exhibiting it's own delay, modulation and temporal summation characteristics.

The input to the cerebral systems related to stimulus processing arrives in the thalamus first, after which it will be relayed to several cortical areas (Figure 6.1: B1). While the input from afferent nerve fibers to the thalamus and the subsequent activity in the SI closely follow a stimulus pattern, downstream areas such as the SII (and subsequently the IC and the ACC) have been shown to have very weak phase-locking to a rhytmic stimulus [3]. Therefore, activity in the SI can be expected to be directly modulated by stimulus parameters, while activity from the SII, IC and ACC might be more closely related to stimulus detection, of which the probability is described by the psychometric curve.

[1] When a categorical variable is added, the increase of SNR will depend on the amount of trials within the same category. Additionally, the SNR of subject-specific estimates of EPs in an LMM will depend on the amount of trials within one subject.

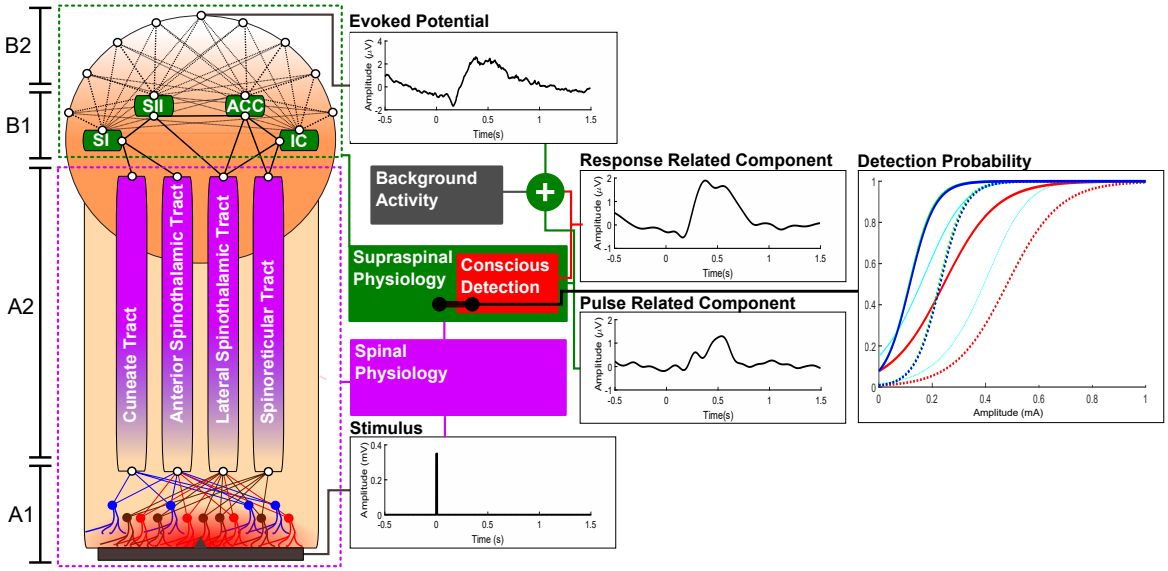

Figure 6.1: *The evoked potential is a summation of neural activity from multiple brain areas. While some areas are associated with low-level processing of the stimulus, other areas only activate when a stimulus is consciously detected. The probability of conscious detection is described by the psychometric curve. Although the detection probability is directly modulated by stimulus parameters, stimulus detection itself is the result of a stochastic process. Therefore, the effects of stimulus amplitude and stimulus detection are not fully collinear, and can be succesfully identified individually using a LMM.*

For nociceptive stimuli, stimulus processing occurs simultaneously in the SI and SII [4], indicating that brain activity related to stimulus processing and activity related to stimulus detection might be present simultaneously. Since a single EEG channel measures the summation of electrophysiological activity in multipe brain areas due to conduction, the EEG represents a combination of multiple types of activity (Figure 6.1: B2).

In Chapter 3 we formulated a LMM that can assist in decomposing electrophysiological activity in the EEG into stimulus-related and detection-related activity, and showed how it can be used to analyse evoked potentials. We used this LMM for analysis of the EEG in Chapters 4 and 5.

Can evoked potentials be used in combination with multiple threshold tracking to observe relations between stimulus properties and the neurophysiological response?

Evoked potentials cannot be used in combination with multiple threshold tracking using conventional analysis methods. It was shown in Chapter 4 that such a conventional analysis, using averaging, leads to signals with a very low signal to noise ratio which cannot be interpreted. However, in Chapter 3 a method was outlined which can be used to identify relations between stimulus parameters and the EP based on linear regression. As described earlier in this discussion, this method can be used successfully to improve the quality of EP estimates and to estimate the influence of stimulus parameters on brain activity.

Which stimulus parameters are significantly related to the neurophysiological response during multiple threshold tracking?

In Chapter 4 it was shown that the central EP, as was measured by EEG at the Cz channel, is significantly related to the amplitude of both pulses of a stimulus ($p<0.05$), the amount of received stimuli ($p<0.05$) and stimulus detection ($p<0.05$). In Chapter 5 this result was reproduced, since it was shown that the EP, this time measured at the CPz-A1A2 derivation, is significantly related to the amplitude of both pulses of a stimulus ($p<0.05$), irrespective of the inter-pulse interval, the amount of received stimuli ($p<0.05$) and stimulus detection ($p<0.05$). At the Tc-FPz derivation, the neurophysiological response is only significantly related to stimulus detection ($p<0.05$). At both derivations stimulus detection had the largest influence on the variation of the EP.

To which extend is neurophysiological activity dependent on stimulus parameters?

Using multiple threshold tracking, we could measure variations in brain activity with respect to stimulus parameters and conscious stimulus detection. In Chapter 4 it was shown that the EP at the Cz channel varies with respect to stimulus parameters and stimulus detection. However, stimulus detection was accountable for a major part of the variation of the central EP within the experiment.

Similarly, it was shown in Chapter 5 that stimulus detection is of major influence on the EP. Using cluster-based non-parametric contrast testing on scalp topographies, it was shown that stimulus detection causes significant central and lateral changes of the EP. Furthermore, those scalp topographies showed that changes of the EP at 165ms and 205ms occur mainly contralateral with respect to the stimulated side. Using the scalp topographies, we could determine that variations of the EP with respect to stimulus detection are the largest at the T7-FPz and the Cz-A1A2 derivations.

Using a linear mixed model, we could test if this significant variation of the average EP with respect to stimulus detection is due to variations in stimulus detection itself, or due to variation of the pulse amplitude which is collinear with stimulus detection. Based on the model coefficients, it was demonstrated that conscious detection of nociceptive stimuli is of major influence on the amplitude of the evoked potential, while stimulus parameters only account for a minor part of the observed variations.

6.2 CONCLUSION

In this thesis a method to account for the effects of multiple correlated stimulus parameters was developed. The method uses linear mixed models to describe the variation in EEG data. Although linear mixed models are established in statistics and already used in fMRI research, they are rarely used for the analysis of EEG signals. In research, the experimental design is generally adapted to generate balanced and normally distributed data which is suitable for averaging and ANOVA. However, this severely restrains the possibilities for experimental paradigms in EEG research, since only a limited amount of parameter combinations is allowed. To analyze data during multiple threshold tracking, we are forced to use an alternative method to effectively deal with variations in stimulus parameter, leading to the development of such a method in this thesis.

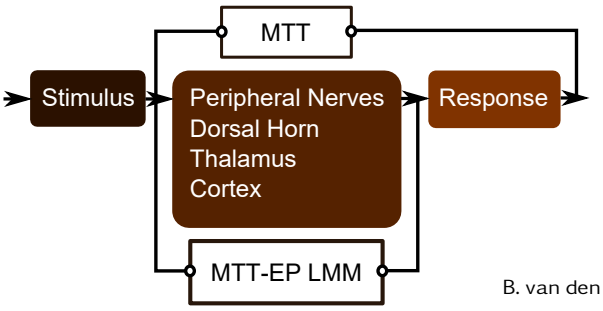

Figure 6.2: While the MTT method relied on subjective response of the participants, MTT-EP measurements can objectively assess changes in nociceptive processing by analyzing brain activity using a LMM.

The combination of EP analysis using LMMs and multiple threshold tracking opens up interesting possibilities for the measurement of peripheral and central sensitization in the nociceptive system. While diagnostics so far depend on subjective measures of pain and sensitization, we can now objectively observe changes in the nociceptive system using brain activity (Figure 6.2).

It was demonstrated that for multi-stimulus EEG data the quality of an evoked potential estimate is improved by using a linear mixed model, which effectively deals with correlation between and within parameters in the data. Furthermore, using a linear mixed model enables us to study stimulus-related brain activity at the subject-level and group-level simultaneously, which brings us one step closer to the development of objective diagnostics based on brain activity.

Using a linear mixed model, it was shown that conscious detection of nociceptive stimuli is of major influence on the amplitude of the evoked potential, while stimulus parameters only account for a minor variations. This means that variation in stimulus parameters mainly influences the observed components of the evoked potential by modulating the detection probability of the stimulus.

6.3 Recommendations

The work presented throughout this thesis only covers a small part of the work that could be done on the analysis of nociceptive stimulus-related brain activity. To start with, the data from the experiment in this thesis includes much more relevant information, which could not yet be analyzed due to constraints of time and resources. Furthermore, the developments made in this thesis provide interesting options for future research.

6.3.1 MTT-EP Experiments

Each MTT-EP session in the experiment in Chapter 5 took 2 hours in total with at least 35 minutes of stimulation and measurement using the MTT algorithm via LabView. Although participants in the experiment were very collaborative and patient, a general complaint was that the measurement period of 35 minutes was too long, which might have caused a loss of attention and sleepiness causing alpha-band background activity. Currently the MTT-EP algorithm has on average a 5 second inter-stimulus interval, which serves to prevent an overlap between measured evoked potentials and for communication with the stimulation device via Bluetooth. This inter-stimulus interval might be

decreased by studying to which extend subsequent EPs might overlap or influence eachother and by optimization of the Bluetooth communication, to decrease the duration of the measurement period.

6.3.2 Spatial Attention

In the MTT-EP experiments in this work, participants knew on which side a stimulus could be expected. However, there is experimental evidence that this spatial attential modulates components of the evoked potential [5]. To remove the 'bias' of spatial attention, two stimulators could be used, each stimulating a different side of the body. By analyzing brain activity with respect to the stimulated side (*ipsilateral* and *contralateral*), an estimate can be obtained of the behavior of the evoked potential without modulation by spatial attention.

6.3.3 MTT-EP LMM Retesting

In this thesis, a method was outlined for analysis of evoked potentials during multiple threshold tracking using linear mixed regression. To prevent false significance due to retesting, the requirement was imposed that a coefficient should be significant for at least 4 time points. A more theoretical treatment on multiple testing of LMM coefficients of EPs is required to provide more information on how we might justify this 'rule-of-thumb' .

6.3.4 Influence of Conscious Stimulus Detection on Nociceptive Processing

In Chapter 5, it was found that a model without interaction between stimulus detection and stimulus parameters has the highest AIC. Therefore, this model was considered to be the most likely model and used for further analysis of the EP. However, there is experimental evidence that conscious stimulus detection might change the way a stimulus is processed by top-down modulation [6]. A further investigation of detected and undetected EPs separately, e.g. by fitting a variety of linear models to each of both categories independently, might provide further evidence to detemine if conscious stimulus detection changes the way a stimulus is processed.

6.4 FUTURE RESEARCH

6.4.1 Extension of the LMM Framework

Although outside the scope of this thesis, the Matlab library that was developed in association with this thesis, which is outlined in Appendix A, has been extended to deal with LMM analysis of variations in space (e.g. topographies) and frequency (e.g. wavelet spectra). It was outside the scope of this thesis to develop a framework for LMM analysis of variations in space and frequency. However, generalization of the LMM framework will help to identify more relations between stimulus parameters and the EEG signal, which can help to establish how neural oscillations are influenced by stimulus parameters (using frequency analysis) and how parameter related signal components are distributed over the scalp (using topography analysis). An example of scalp topographies of LMM coefficients in shown in Figure 6.3.

6.4.2 Relating Neural Oscillations to Stimulus Detection

Research on visual stimuli has shown that visual stimulus detection is dependent on power of the α-band in EEG oscillations [7, 8]. Furthermore, the perception of stimulus timing was shown to be dependent of the phase of the α-band [9]. Using the data from this thesis, the relation between neural oscillations and stimulus detection might also be studied for nociceptive stimuli, which can help to provide more information about the neural mechanism involved in nociceptive stimulus detection.

6.4.3 Real-time Detection Prediction

In this thesis, it was shown the N1, N2 and P2 compenents of the EP are closely related to stimulus detection. Therefore, we can use the relation between EP components and stimulus detection, to predict if a stimulus is detected based on brain activity. One way to do so is by relating stimulus detection to the EP and stimulus parameters using the GLMM in Equation 6.1.

$$D \sim 1 + EP + SP1 + SP2_{10} + SP2_{40} + TRL + (1 + EP + SP1 + SP2_{10} + SP2_{40} + TRL|Subject) \quad 6.1$$

By computing the GLMM over the first 50 stimuli of every stimulus type in each subject, a total of 63.3% of all subject responses to subsequent stimuli can be classified correctly using the trained

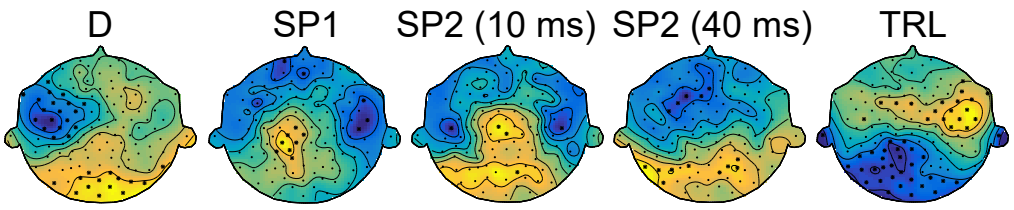

Figure 6.3: Normalized scalp topographies of LMM coefficients at 205 ms after stimulus application (during the N2) with respect to stimulus detection (D), the first pulse (SP1), the second pulse with 10 and 40 ms IPI (SP2) and the number of received stimuli (TRL).

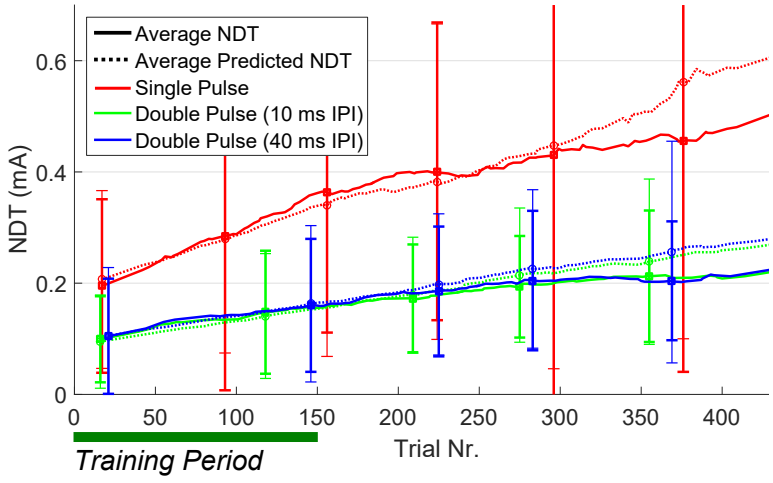

Figure 6.4: Nociceptive detection threshold predicted by a GLMM classifier of stimulus detection, trained on the first 50 stimuli of each type.

GLMM classifier. The predicted subject response allows us to compute the nociceptive detection threshold without relying on the subject's reponses themselves, as is demonstrated in Figure 6.4. However, it still has to be shown if the prediction by the GLMM classifier provides enough information to let the MTT algorithm track the NDT correctly without subjective responses. Furthermore, a GLMM classifier is far from optimal, and application of state-of-the-art machine learning techniques might severely improve the classification performance on stimulus detection.

Bibliography

[1] W. S. Pritchard, "The brain in fractal time: 1/f-like power spectrum scaling of the human electroencephalogram", *International Journal of Neuroscience*, vol. 66, no. 1-2, pp. 119–129, 1992.

[2] M. Schooneman, "Measurement of evoked potentials during multiple threshold tracking of nociceptive electrocutaneous stimuli", Thesis, 2015.

[3] Y. Vázquez, E. Salinas, and R. Romo, "Transformation of the neural code for tactile detection from thalamus to cortex", *Proceedings of the National Academy of Sciences*, vol. 110, no. 28, E2635–E2644, 2013.

[4] M. Ploner, J. Gross, L. Timmermann, and A. Schnitzler, "Pain processing is faster than tactile processing in the human brain", *Journal of Neuroscience*, vol. 26, no. 42, pp. 10 879–10 882, 2006.

[5] V. Legrain, J. M. Guérit, R. Bruyer, and L. Plaghki, "Attentional modulation of the nociceptive processing into the human brain: Selective spatial attention, probability of stimulus occurrence, and target detection effects on laser evoked potentials", *Pain*, vol. 99, no. 1-2, pp. 21–39, 2002.

[6] L. Tiemann, E. May, M. Postorino, E. Schulz, M. Nickel, U. Bingel, and M. Ploner, "Differential neurophysiological correlates of bottom-up and top-down modulations of pain", *Pain*, vol. 156, no. 2, pp. 289–296, 2015.

[7] L. Iemi, M. Chaumon, S. Crouzet, and N. Busch, "Spontaneous neural oscillations bias perception by modulating baseline excitability", *Journal of Neuroscience*, vol. 37, no. 4, pp. 807–819, 2017.

[8] A. Achim, J. Bouchard, and C. M. Braun, "EEG amplitude spectra before near threshold visual presentations differentially predict detection/omission and short–long reaction time outcomes", *International Journal of Psychophysiology*, vol. 89, no. 1, pp. 88–98, 2013.

[9] A. Milton and C. Pleydell-Pearce, "The phase of pre-stimulus alpha oscillations influences the visual perception of stimulus timing", *NeuroImage*, vol. 133, pp. 53–61, 2016.

Appendices

A Neuroassyst EEG Toolbox

In combination with the study performed for this Master's assignment, a Matlab (The MathWorks Inc., version R2015b) library was developed for a generalized implementation of the analytical methods presented in this thesis for EEG data. The goal of this library is to present students with a plug-and-play Matlab interface for EEG data analysis. In this section, the functions and the workflow of this library is documented.

A.1 Input and Pre-processing

A.1.1 General Input

Every main function in the NA_EEG toolbox requires input in the form of a struct with configurations, which is referred to in this documentation as 'cfg'. Some configurations have to be present in the cfg struct throughout the entire workflow, while others are function specific. Since every function specific struc component has a unique name, the same cfg struct can be used for the entire analysis. General configurations, which should be defined before starting the analysis, include:

cfg.configuration_name: Name for saving the configuration struct.

cfg.analysis: Name of the current analysis.

cfg.recording_path: Only required if EEG is recorded. Recording path.

cfg.raw_data_path: Path to the folder containing raw EEG data.

cfg.processed_data_path: Path to the folder containing all processed data.

cfg.pictures_path: Path to the folder where pictures should be stored.

cfg.fieldtrip_path: Path to the folder containing the FieldTrip library [1].

cfg.subjects: Cell array of names of each subject folder.

cfg.eeg_format: Format of the raw EEG data. Can be .cnt or .Poly5.

cfg.n_amplifier_channels: The number of channels used for EEG recording.

cfg.fsample: The sampling frequency of the EEG amplifier.

cfg.layout: Path to the layout file of the EEG cap.

cfg.labelfile: Path to a file including all label names.

cfg.effects: Experimental parameters that you want to analyze.

cfg.effect_labels: Names of experimental parameters when displayed in figures.

cfg.units: Units of experimental parameters when displayed in figures.

A.1.2 initialize_analysis(cfg)

(Re)initializes all configurations and folders within the folder [cfg.preprocessed_data]/[cfg.analysis].

This function only requires the general input parameters.

A.1.3 estimate_thresholds(cfg)

Initializes the data_frame for every subject with data from the multiple threshold tracking experiment and estimates the subject's thresholds per subject individually.

cfg.estimate_thresholds.moving_window: Number of subsequent stimuli from the same type that should be used for estimation of the detection threshold.

A.1.4 clean_data(cfg)

Filters EOG components from the EEG signal by application of an independent component analysis algorithm [2] and provides an interface for trial selection based on trial statistics (using the FieldTrip library [1]).

This function only requires the general input parameters.

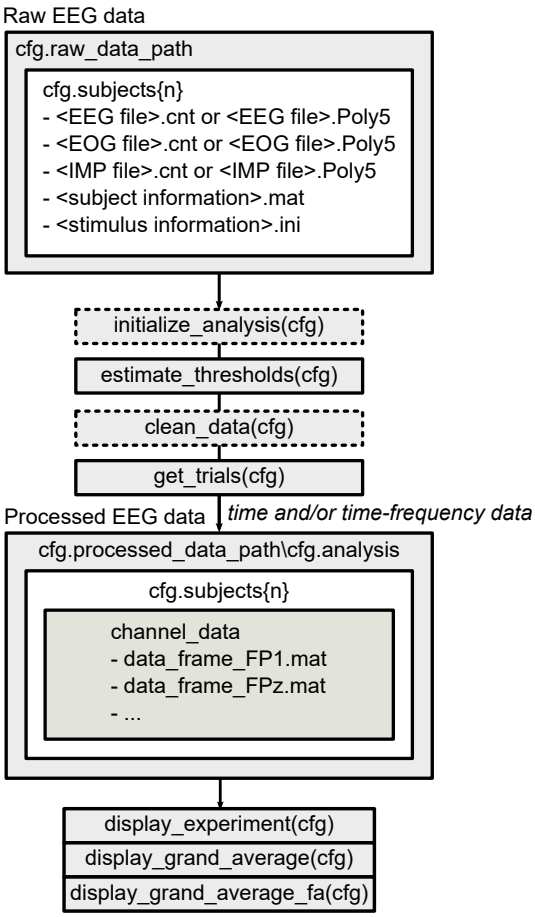

Figure A.1: *Workflow for pre-processing of EEG data.*

A.1.5 get_trials(cfg)

Performs all simple preprocessing on data, such as high-pass and low-pass filtering, and gets the epochs from the data based on the trigger signal using FieldTrip [1]. Additionally, this function can be used to compute time-frequency data of each epoch using the wavelet transform. Subsequently data is stored in one data_frame per trial.

cfg.get_trials.use_clean_data: Use the data returned by the function 'clean_data(cfg)'? Input is 'yes' or 'no'.

cfg.get_trials.type: Get the data from all channels, or only from specific derivations? Input is 'all' or 'derivations'.

cfg.get_trials.extra_derivations: Cell array with the names of derivations you want to analyze.

cfg.get_trials.remove_invalid_trials: Remove trials that have a high/low value of the relative stimulus amplitude and/or remove trials at the start of the experiment. Input is 'yes' or 'no'.

cfg.get_trials.remove_start_length: Amount of trials to remove at the start of the experiment.

cfg.get_trials.min_relative_amplitude: Minimum relative amplitude (in NDT) of the stimulus.

cfg.get_trials.max_relative_amplitude: Maximum relative amplitude (in NDT) of the stimulus.

cfg.get_trials.hpfilter: Filter the signal with a high-pass filter? Input is 'yes' or 'no'.

cfg.get_trials.hpfreq: Filter cut-off frequency (-3 dB point).

cfg.get_trials.hpfiltord: Filter order.

cfg.get_trials.lpfilter: Filter the signal with a low-pass filter? Input is 'yes' or 'no'.

cfg.get_trials.lpfreq: Filter cut-off frequency (-3 dB point).

cfg.get_trials.lpfiltord: Filter order.

cfg.get_trials.demean: Do baseline correction of the trials? Input is 'yes' or 'no'.

cfg.get_trials.trialdef.prestim: Amount of time before the stimulus to include into one epoch.

cfg.get_trials.trialdef.poststim: Amount of time after the stimulus to include into one epoch.

cfg.get_trials.fa.__: Struct containing the same options as cfg.get_trials, and additional options defining pre-processing options for frequency analysis. Additional options are displayed below.

cfg.get_trials.fa.analyze: Do frequency analysis of the epochs using a wavelet transform? Input is 'yes' or 'no'.

cfg.get_trials.fa.width: Wavelet length of the Wavelet transform, as the number of periods.

cfg.get_trials.fa.min_freq: Minimum frequency for time-frequency analysis.

cfg.get_trials.fa.max_freq: Maximum frequency for time-frequency analysis.

cfg.get_trials.fa.freq_step: Frequency step of the wavelet transform.

cfg.get_trials.fa.time_step: Time step of the wavelet transform.

cfg.get_trials.fa.baselinetype: Baseline type of the time-frequency analysis. Input can be 'relative' (amplitude indexed by the average baseline frequency), 'absolute' (absolute amplitude) or 'relchange' (percentage of change with respect to the average baseline frequency).

A.1.6 acquisition(cfg)

Opens a TMSi Polybench interface for recording of EEG data using a TMSi REFA amplifier. Raw data recorded using this interface is stored in the folder defined by cfg.recording_path.

This function only requires the general input parameters.

A.2 LINEAR MIXED MODELS

A.2.1 me_analysis

Analysis of EEG data using a linear mixed model can be done by four functions which all require the same input struct:

- me_analysis_prepare(cfg)
- me_analysis_run_matlab(cfg)
- me_analysis_run_r(cfg)
- me_analysis_load(cfg)

cfg.me_analysis.me: Name of the mixed-effects analysis, which will be used for saving model statistics.
cfg.me_analysis.type: Do mixed-effects analysis all channels, or only on specific derivations? Input is 'all' or 'derivations'.
cfg.me_analysis.ep_analysis: Do mixed-effects analysis of the EP? Input is 'yes' or 'no'.
cfg.me_analysis.frequency_analysis: Do mixed-effects analysis of time-frequency data? Input is 'yes' or 'no'.
cfg.me_analysis.time_range: Time range within the epochs to do mixed-effects analysis.
cfg.me_analysis.frequency_range: Time range within the time-frequency spectra to do mixed-effects analysis.
cfg.me_analysis.derivations: Cell array containing the derivation names to use for mixed-effects analysis (if the analysis type is 'derivations').
cfg.me_analysis.center_data_mean: Center the experimental parameters? Input is 'yes' or 'no'.
cfg.me_analysis.center_ep_mean: Center the EP and/or the time-frequency spectrum? Input is 'yes' or 'no'.
cfg.me_analysis.scale_data_var: Scale the experimental parameters based on their standard deviation? Input is 'yes' or 'no'.

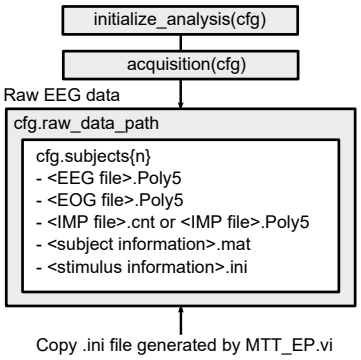

Figure A.2: Workflow for recording of EEG data.

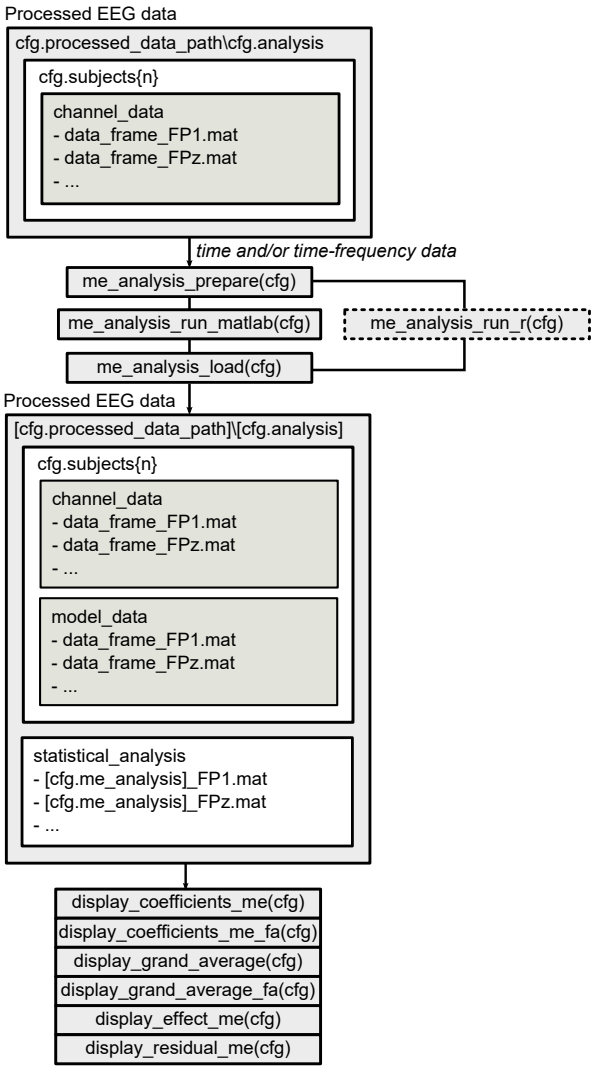

Figure A.3: Workflow for analysis of EEG data using linear mixed models.

cfg.me_analysis.scale_ep_var: Scale the EP and/or the time-frequency spectrum based on the standard deviation? Input is 'yes' or 'no'.

cfg.me_analysis.downsampling_factor: With which factor should data be downsampled to speed up analysis?

cfg.me_analysis.r_dir: Directory including R scripts for mixed-effects analysis.

cfg.me_analysis.r_app_path: Path to the R application (.exe).

cfg.me_analysis.formula: Formula for the linear mixed effects model in Wilkinson notation [3].

cfg.me_analysis.nr_fixed: Number of fixed effects.

cfg.me_analysis.nr_random: Number of random effects.

A.2.2 me_analysis_prepare(cfg)

Prepares data for mixed-effects analysis by centering and scaling of data and saving it in a convenient format.

A.2.3 me_analysis_run_matlab(cfg)

Computes the mixed-effects model using Matlab. P values are computed based on a Wald t-test.

A.2.4 me_analysis_run_r(cfg)

Computes the mixed-effects model using R. P values are computed based on a Wald χ-square test.

A.2.5 me_analysis_load(cfg)

Loads model output of the mixed-effects models. This function saves model statistics to the 'statistical_analysis' folder. Furthermore, it saves the fit and residual of every EEG epoch in a new data frame for every subject.

A.3 Display

A.3.1 display_experiment(cfg)

Summarizes the MTT stimulus-response pairs of one subject in a figure (e.g. Figure A.4).

cfg.display_experiment.subject: Subject number of the subject that should be displayed.

cfg.display_experiment.start: Trial number of the first trial that should be displayed.

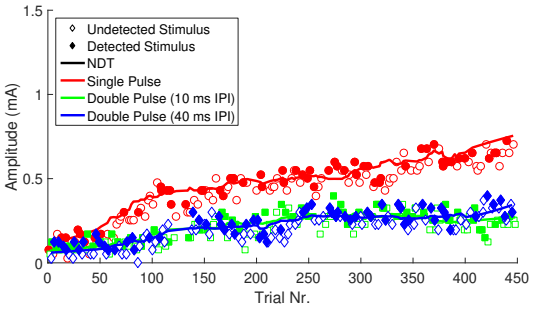

Figure A.4: Summary of the SRPs of one of the subjects, which is displayed by ***display_experiment(cfg)****.*

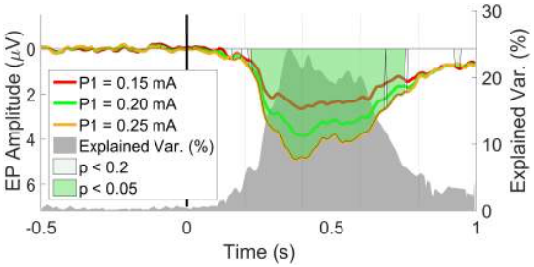

Figure A.5: Grand average of the model fit at the Cz electrode of detected stimuli versus undetected stimuli, which is displayed by ***display_grand_average(cfg)****. Time-points with significant model coefficients are marked in green.*

cfg.display_experiment.end: Trial number of the last trial that should be displayed.

cfg.display_experiment.fontsize: Fontsize.

A.3.2 display_grand_average(cfg)

Display grand averages over the data in the time domain, computed over levels of a specific factor (e.g. Figure A.5). Optionally: Show the amount of variance explained by the grand average. Optional: Do cluster-based non-parametric permutation testing of the contrasts between grand averages [4].

cfg.display_grand_average.derivation: EEG derivation of which the grand average should be plotted.

cfg.display_grand_average.effect: The factor over whose levels a grand average is computed.

cfg.display_grand_average.font_size: Trial number of the last trial that should be displayed.

cfg.display_grand_average.ylim: Lower and upper limit of the y-axis e.g. [1 2].

cfg.display_grand_average.min_sample_size: Minimum amount of trials for a grand average to be computed.

cfg.display_grand_average.show_var: Show amount of variance explained.

A.3.3 display_grand_average_fa(cfg)

Display grand averages over the data in the time-frequency domain, computed over levels of a specific factor (e.g. Figure A.6). This function uses all settings defined by cfg.display_grand_average and additional settings, which are outlined below. Optional: Show the amount of variance explained by the grand average. Optionally: Do cluster-based non-parametric permutation testing of the contrasts between grand averages [4].

cfg.display_grand_average.fa.zlim: Lower and upper limit of the color axis.

display_grand_average.fa.ylim: Lower and upper limit of the frequency axis.

cfg.display_grand_average.fa.xlim: Lower and upper limit of the time axis.

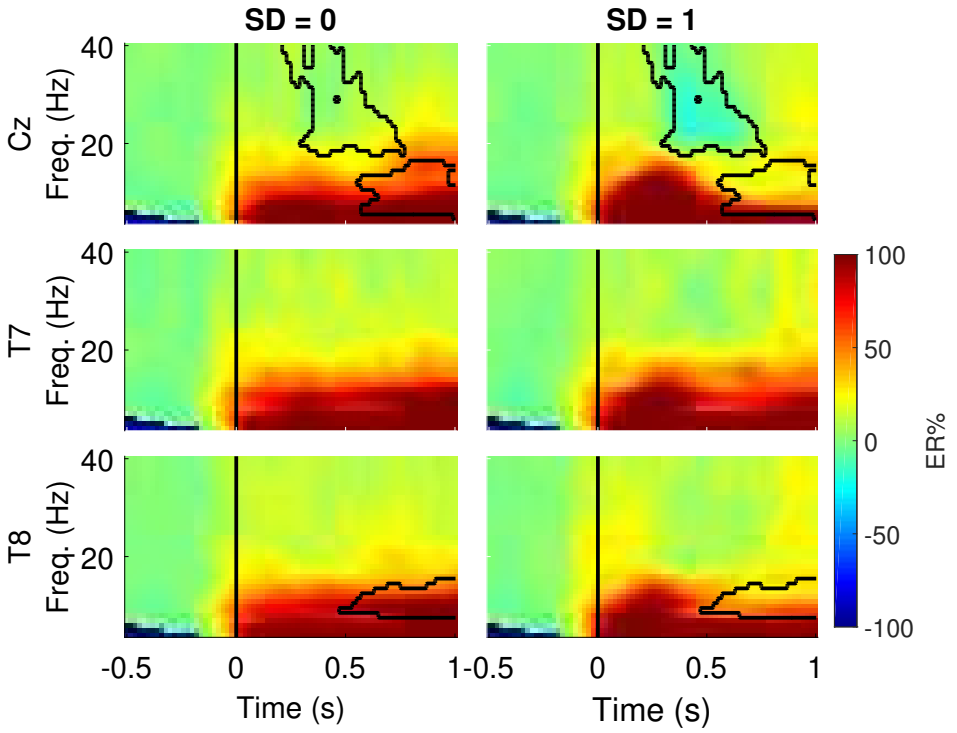

*Figure A.6: Grand average non-phase-locked time-frequency spectra, which are displayed by **display_grand_average_fa(cfg)**. Areas where the difference between detected and undetected stimuli was found significant by cluster-based non-parametric permutation testing (p<0.05) are marked by a line.*

A.3.4 display_coefficients_me(cfg)

Display the coefficients of the fixed effects over time (e.g. Figure A.7). Optionally: show if the effect coefficient is significant.

cfg.display_coefficients_me.derivation: EEG derivation of which the coefficients should be plotted.

cfg.display_coefficients_me.font_size: Fontsize within the figure.

cfg.display_coefficients_me.p_significance: Significance level of the P value.

cfg.display_coefficients_me.p_exploratory: Exploratory significance level of the P value.

cfg.display_coefficients_me.min_length: Minimum amount of samples (after downsampling) that a coefficient should be lower than the significance level to be considered significant.

A.3.5 display_effect_me(cfg)

Display variations of the EP due to variations of parameters with respect to the intercept (e.g. Figure A.9).

cfg.display_effect_me.derivation: EEG derivation of which the effects should be shown.

cfg.display_effect_me.effect: Cell array of parameters that should be varied.

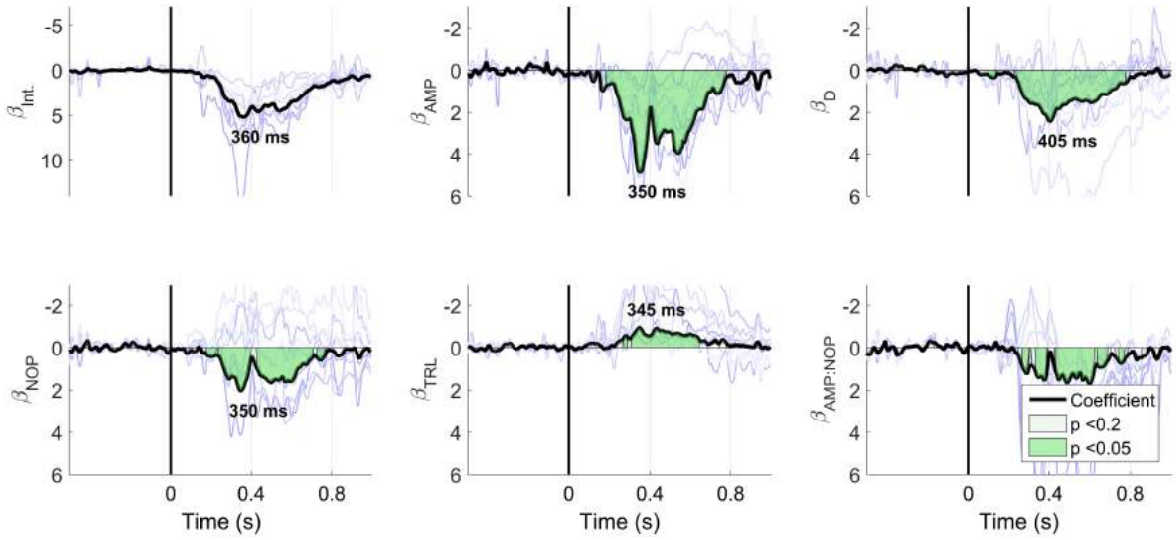

*Figure A.7: Fixed coefficients of a linear mixed model, which are displayed by **display_coefficients_me(cfg)**. Subject-specific coefficients are displayed as blue lines on the background.*

cfg.display_effect_me.range: Cell array of vectors. Each vector indicates which values of the respective parameters should be shown.

cfg.display_effect_me.font_size: Font size.

cfg.display_effect_me.ylim: Lower and upper limit of the y-axis e.g. [1 2].

A.3.6 display_residual_me(cfg)

Display residual plots of the model, including a continuous boxplot, residual/fit-plot, histogram, qq-plot, skewness and kurtosis (e.g. a continuous boxplot produced by this function is shown in Figure A.8).

cfg.display_residual_me.font_size: Font size.

A.4 DEVELOPMENT

Currently, the NA_EEG toolbox is still under development. Besides the presented set of functions, a wide variety of 'sandbox' functions in under development, including:

- Display of grand average topographies
- Display of model coefficient topographies
- Display of space-time-frequency grand averages
- Display of space-time-frequency coefficients

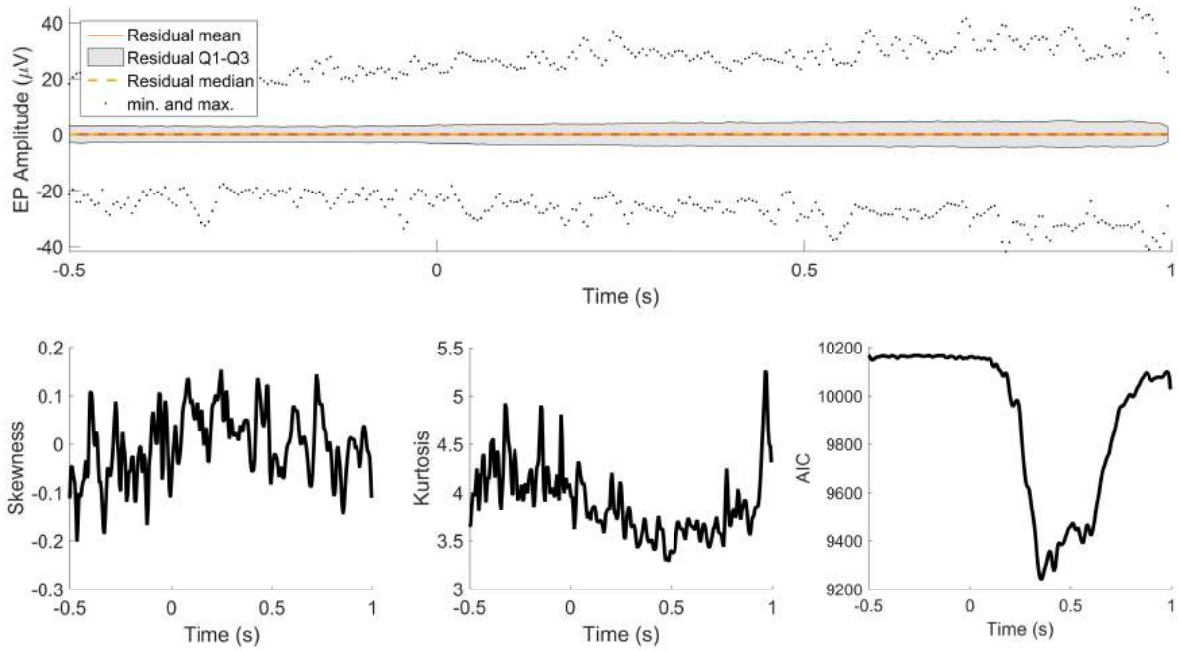

Figure A.8: Continuous boxplot, skewness, kurtosis and AIC of a linear mixed model, which are displayed by ***display_residual_me(cfg)****.*

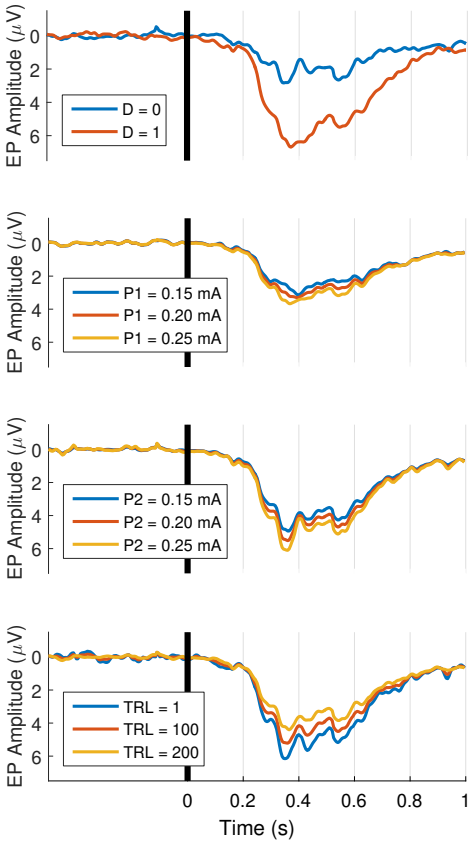

Figure A.9: The effect of variation of model parameters with respect to the model intercept at Cz, which is displayed by ***display_effect_me(cfg)****.*

Bibliography

[1] R. Oostenveld, P. Fries, E. Maris, and J.-M. Schoffelen, "Fieldtrip: Open source software for advanced analysis of MEG, EEG, and invasive electrophysiological data", *Computational Intelligence and Neuroscience*, vol. 2011, 2011.

[2] A. Delorme and S. Makeig, "EEGLAB: An open source toolbox for analysis of single-trial EEG dynamics including independent component analysis", *Journal of Neuroscience Methods*, vol. 134, no. 1, pp. 9–21, 2004.

[3] G. N. Wilkinson and C. E. Rogers, "Symbolic description of factorial models for analysis of variance.", *Appl Stat*, vol. 22, pp. 392–399, Jan. 1973.

[4] E. Maris and R. Oostenveld, "Nonparametric statistical testing of EEG- and MEG-data", *Journal of Neuroscience Methods*, vol. 164, no. 1, pp. 177–190, 2007.

B Experimental Protocol

University of Twente

Biomedical Signals and Systems

Research theme Nociceptive and Somatosensory Processing

Standard Operating Procedure

BSS-NSP-M002
MTT-EP Experiments

Initial version:	02-11-2017
Replacing version:	02-11-2017
Last revision:	06-11-2017
Valid from:	10-11-2017

	Name	Function	Date	Signature
Written by	B. van den Berg	PhD NSP	06-11-2017	
Reviewed by	J.R. Buitenweg	PI-NSP	07-11-2017	
Approved by	J.R. Buitenweg	PI-NSP	07-11-2017	

Contents

Scope

This standard operating procedure applies to all researchers and research assistants working on internal or external projects in which the MTT-EP experimental procedure is used for assessment of human nociceptive properties.

Background

Sensitivity of ascending pathways in the nociceptive system is reflected in nociceptive thresholds in human subjects. Thresholds can be estimated using electrical stimulation of nociception specific nerve fibers. Electrocutaneous stimulation using a needle electrode has been shown to selectively stimulate nociception related Aδ-fibers with currents lower than twice the detection threshold [1-3]. Varying stimulus parameters (e.g. number of pulses, pulse duration and inter pulse interval) result in different thresholds [4]. A needle electrode [3, 5] is placed on the right hand. Electrical stimuli are generated with a custom-built stimulator (University of Twente). Stimuli are applied with a frequency of approximately 0.3 Hz to the subject, which should release a button-switch to indicate perception of the stimuli.

Nociceptive activity can be quantified by recording and analyzing the EEG signal time-locked to the stimuli. The average time-locked signal, referred to as the evoked potential (EP) describes transient synchronized activity of large neural networks within the cortex. Additionally, non-phaselocked activity can be quantified using the wavelet-transformed signals, and refers to synchronization and desynchronization of local neural networks. Therefore, it is important to accurately measure the EEG signal to exclude noise and artifacts from external and internal disturbances.

To measure the EEG signal during nociceptive threshold measurement, a setup for EEG measurement can be combined with a setup for threshold measurement, as is depicted in Figure 1.

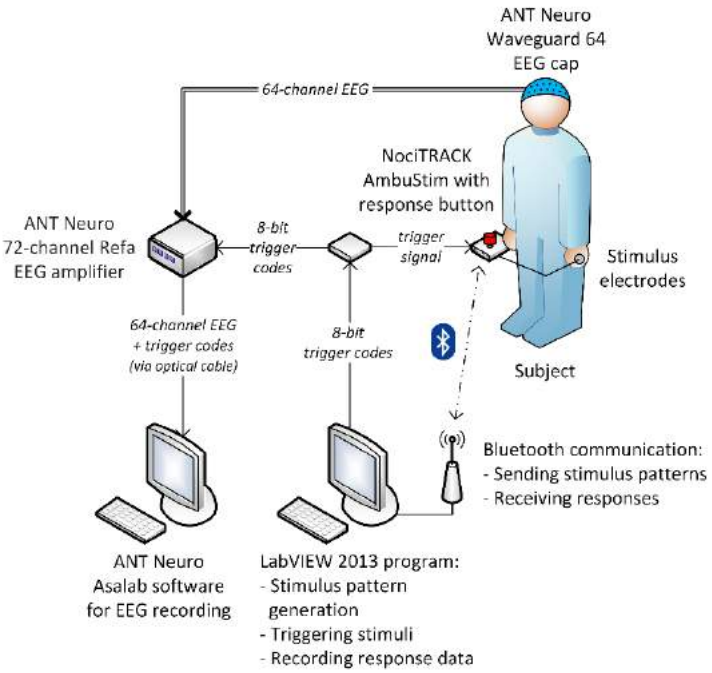

Figure 1: Example setup combining EEG measurement with nociceptive stimulation and nociceptive threshold measurement.

Required Materials

Description	#	Specification
General		
Computers	2	One computer with LabView 2013 SP or higher, MTT-EP stimulation software (build in LabView). The computer should have at least the following specifications: - Windows 7 64-bit, or higher - Intel Core i5 1.6 GHz, or higher - 4 GB RAM, or more - Bluetooth adapter One computer with Matlab 2015b or higher, TMSi Polybench Designer, and a custom-made TMSi Polybench recording application. The computer should have at least the following specifications: - Windows 7 64-bit, or higher - 64-bit operating system - Intel Core i5 1.6 GHz, or higher - 8 GB RAM, or more
Tape	0.5 m	Non-allergenic skin-friendly medical tape. E.g. Leukofix.
Medical abrasive gel	2 cl	Medical abrasive gel to remove dead skin cells.
Cleansing liquid	2 cl	Alcohol, 70 % Ethanol
Cleansing tissues	2	Tissues
Cleansing sticks	2	Cotton-top cleansing sticks
Multiple Threshold Tracking		
Stimulator	1	NociTRACK AmbuStim single-channel stimulator, capable of generating a minimum current of 8 µA and a maximum current of 16 mA. Shown in Figure 4.
Charger	1	NociTRACK charger for AmbuStim stimulators
Trigger generator	1	Arduino-based trigger generation system, which can be connected to the computer (input) via USB A to B cable, connected to the NociTRACK AmbuStim stimulator (output 1) via a BNC cable and connected to the EEG amplifier via a DB25 parallel cable. Shown in Figure 3 D-E-F.
USB A to B cable	1	Cable for connection of the trigger generator to the computer.
BNC cable	1	Cable for connection of the trigger generator to the NociTRACK AmbuStim stimulator. Should have a length of at least 2 meters.
Parallel cable	1	Cable for connection of the trigger generator to the EEG amplifier. Should have a length of at least 2 meters.
Stimulation electrode	1	Sterile IES-5 electrode for intra-epidermal electrocutaneous stimulation. Shown in Figure 9.
Grounding electrode	1	TENS electrode, which will serve as a ground during the stimulation. Shown in Figure 10.
Stimulator-to-electrode cable	1	A custom-made double cable that connects the stimulation and grounding electrode to the stimulator.
EEG Measurement		
Amplifier	1	TMSI Refa 136-channel amplifier, with 128 unipolar, 4 bipolar and 4 auxiliary input channels.

Medical power supply	1	TMSi power supply with on-off switch, to supply electricity to the EEG amplifier.
Fiber-to-USB converter	1	TMSi optical fiber-to-USB converter.
Optical fiber	1	TMSi optical fiber, used to communicate between the EEG amplifier and the computer via the TMSi fiber-to-USB converter.
USB A to B cable	1	USB A to B cable used to connect the TMSi fiber-to-USB converter to the computer.
EEG caps	2	TMSi 128-channel low-noise actively shielded caps with an EBA multi-connector. A small-medium or medium-large size cap have to be available for different head sizes of the subjects.
EBA multi-connectors	4	EBA multiconnectors from 1-32 Hirose to microcoax cables, to connect the headcap to the amplifier.
Color-coded measurement tape	1	Tape for measuring the required EEG cap size.
Syringes	2	10 ml Luer-Lok tip syringe (B-D Plastipak) for injection of EEG gel into cap electrodes.
Blunt needles	2	Blunt needle (16G) for injection of EEG gel into cap electrodes and scratching the skin.
EEG electrode gel		Electro-gel (ECI), for injection in EEG cap electrodes.
EEG electrode paste		Ten20 Conductive EEG paste (Ten20).
Towel	2	Large size towel for covering the shoulders during application of electrode gel, and another medium size towel for subjects to dry the hair after measurement.
ECG electrodes	5	Ag/AgCl pre-gelled disposable electrodes (Kendall H1245 G) with a diameter of 24 mm for recording at the earlobes).
Bipolar snap electrode pain with shielded carbon cable	1	TMSi ExG shielded bipolar cable with 2 snap connectors, to attach the EOG electrodes.
Shielded unipolar cable	3	TMSi ExG shielded unipolar cable with 1 snap connector, to attach the ground and to earlobe electrodes.
Power cable	1	Power cable for medical power supply.
Comfortable chair	1	Comfortable chair for participants to relax during the experiment. The chair should especially provide rest to the muscles around the head and neck, since those might disturb the measurement.
Focus image	1	Small image or sign for subjects to look at during the experiment. Shown in Figure 14.

Procedure

A. General Preparation

Time: > 1 hour before session

1. Send potential participants an information e-mail containing the official patient information letter. After they confirm their participation, send them another e-mail with specific information about the experiment. These e-mails can contain a text like the one shown in Figure 2 The second mail should tell potential participants to:
   - The date, time and location of the experiment.
   - Where to meet the researcher and contact information.
   - Bring a towel to the experiment, and possibly some shampoo/conditioner and hair gel.
   - Preferably wear lenses to the experiment if they have the option to choose between lenses and glasses.
   - No alcohol is allowed within 24h before the experiment.
   - Drink the same amount of coffee as they normally do.
2. If you expect participants with another language, make sure translations are available.
3. Plan an experimental date with potential participants via e-mail or telephone.
4. After a date has been planned, inform the BHV responsible (Marcel Weusthoff) about the date and time of the experiment.
5. Regularly charge the electric chair. However, do not leave the charger connected for more than a few hours, since this might damage the battery.
6. **Always make sure that sufficient sterilized electrodes are available**. If this is not the case, sterilize a batch of electrodes according to "*SOP - Sterilization of IES-5 and BiModEl Electrodes*".
7. Make sure that you know in which lab the experiment takes place and which numbers to call in case of an emergency.

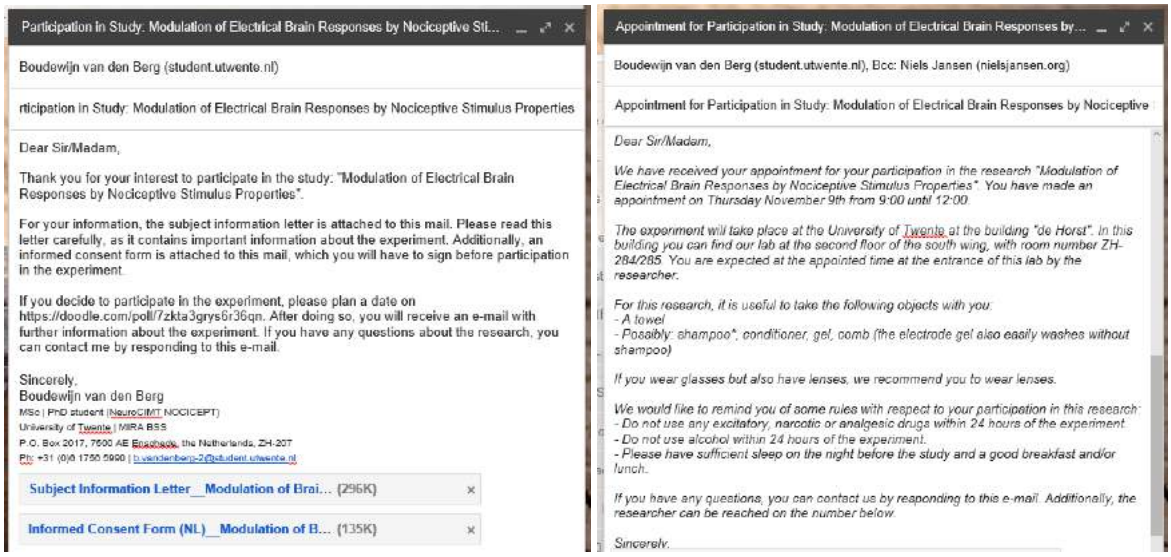

Figure 2: Example e-mails.

B. EEG System Preparation

Time: > 1 hour before session

1. Attach the EEG amplifier to the power adapter.
2. Attach the fiber-to-EEG converter via the optic cable to the EEG amplifier and via a USB A to B cable to the EEG computer.
3. Connect the trigger generator to the computer using the USB A to B cable.
4. Connect the trigger generator to the EEG amplifier using the parallel cable.
5. Attach the EBA multi-connectors to the individual EEG inputs.
6. Connect the unipolar snap cable of the grounding electrode to GND.
7. Connect the bipolar snap cable of the EOG electrodes to channel 129.
8. Connect the unipolar snap cable for the left earlobe electrode to channel 13 (M1/A1) and the unipolar snap cable for the right earlobe electrode to channel 19 (M2/A2).
9. Attach a small sign or image in front of the chair, for subjects to focus on a single point during the experiment.

For more information about the connections, please refer to Figure 3.

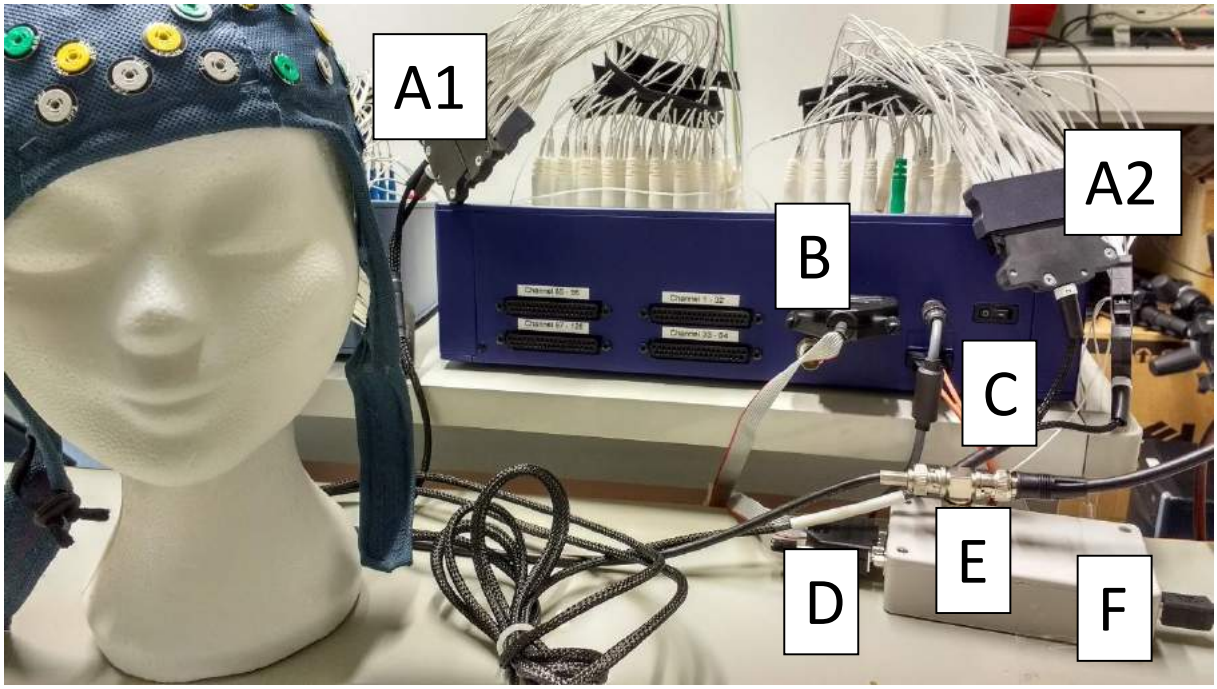

Figure 3: Connections between EEG system, trigger generator and EEG cap. A1 and A2 are EBA multi-connectors connecting the cap to individual inputs of the EEG amplifier. B is the parallel input of the EEG amplifier, which should be attached to D, the parallel output of the trigger generator. The orange double cable at C is the optical output of the EEG amplifier, which should be connected to the EEG computer via the TMSi fiber-to-USB adapter. The gray cable above the optical fiber is the power cable, which should be connected to the power via the TMSi medical power supply. E is the BNC output of the trigger generator, which should be connected to the BNC input of the stimulator, and optionally to the oscilloscope, using a splitter. F is the USB input to the trigger generator, which should be connected to the LabView computer.

C. Stimulator System Preparation

Time: > 1 hour before session

1. Connect the trigger generator to the stimulator via the BNC cable.
2. Connect the response-time cable of the stimulator to channel 133 on the EEG.
3. Connect the stimulator-to-electrode cable to the stimulator.
4. Charge the stimulator **with the stimulator turned off**, using the NociTRACK charger.

For more information about the connections, please refer to Figure 4.

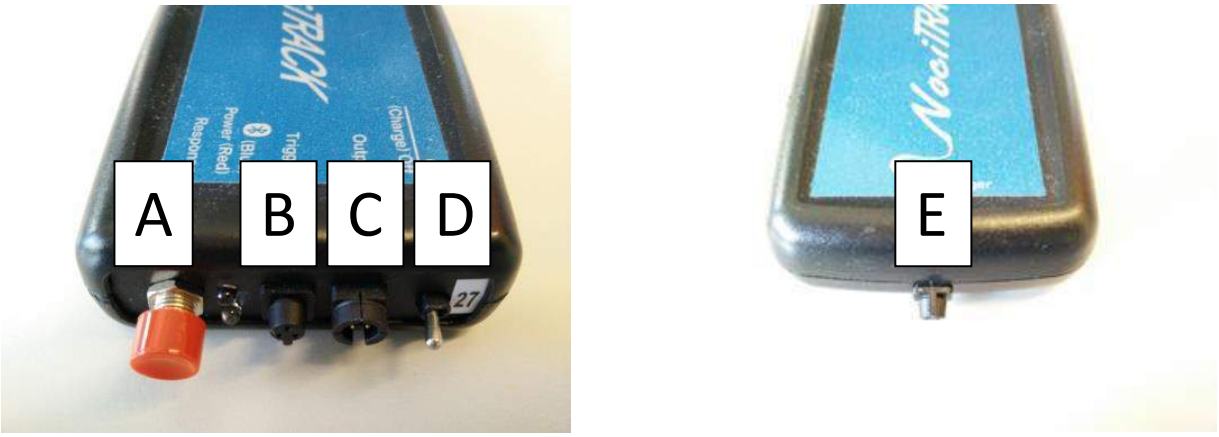

Figure 4: Inputs and outputs of the NociTRACK AmbuStim stimulator. A is a response button, which is actuated by the subject to indicate if the stimulus is perceived. B is a connection to the stimulator cable. C is an input for the trigger signal. D is the power switch. E is the input for the charger. The stimulator should be switched off while charging.

E. Materials Preparation

Time: > 1 hour before session

1. Make sure that the following materials are ready for use and easy to reach:
   a) Electrode caps
   b) Colored measurement tape
   c) EEG electrode gel and paste
   d) Two syringes
   e) Blunt needles (in the package) for gel injection into the electrodes
   f) Medical abrasive gel
   g) Tissues and cotton sticks
   h) Alcohol
   i) Electrodes for on the earlobes
   j) Circular tape for earlobe electrodes
   k) Gel for earlobe electrodes
   l) ECG electrodes for the ground and for EOG measurement
   m) One TENS electrode.
   n) One IES-5 electrode in the package.

D. System Start-up

Time: > 20 minutes before session

1. Turn on both computers.
2. Turn on the power supply of the EEG amplifier.
3. Turn on the EEG amplifier.
4. Turn on the NociTrack.
5. Calibrate the NociTrack according to the "*Manual - Stimulator_Calibration*".
6. Print and store the calibration report.

E. Labview Initialization

Time: > 10 minutes before session

On the LabView computer:

1. Open the LabVIEW program "MTT-EP 2017".
2. Wait until FrontPanel.vi started. Press the arrow button.
3. A new screen will open (Figure 1). Fill in the Patient ID (do not add personal information) and press "Continue".
4. A new screen will open (StimCom Bluetooth Control).
   - Click on "Search" to start searching for a AmbuStim stimulator (Figure 2A)
   - The number of the AmbuStim is indicated on the stimulator
   - If the AmbuStim does not appear on the screen, check if the stimulator is turned on and press "Search" again.
   - Click on the AmbuStim which is to be connected, but do not press "Connect" yet (Figure 2B).

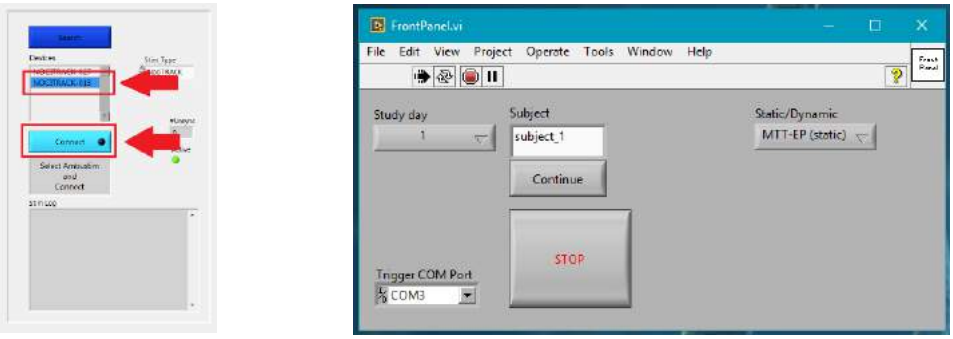

Figure 5: Left, the Bluetooth connection interface for the NociTRACK AmbuStim stimulator. First, press 'Search'. If the correct stimulator device has been found (doublecheck with the number on the stimulator), press 'Connect'. Right, the initial interface of the experimental application. Fill in the subject ID, confirm the COM port of the trigger generator in 'Device Manager', and press 'Continue'.

E. EEG initialization

Time: > 10 minutes before session

1. Start up the Matlab by pressing the shortcut of 'EEG MTT-EP 2017'.
2. Run the first part of the Matlab script by pressing CNTRL + ENTER.
3. Matlab will ask for information about the experiment (Figure . Fill in the subject ID (same as in LabView) and information about the experiment and the subject.
4. The recording application in TMSi Polybench will start. Press the 'IMPEDANCE' button to go to the impedance measurement interface (Figure 6).
5. Turn your phone to airplane mode.

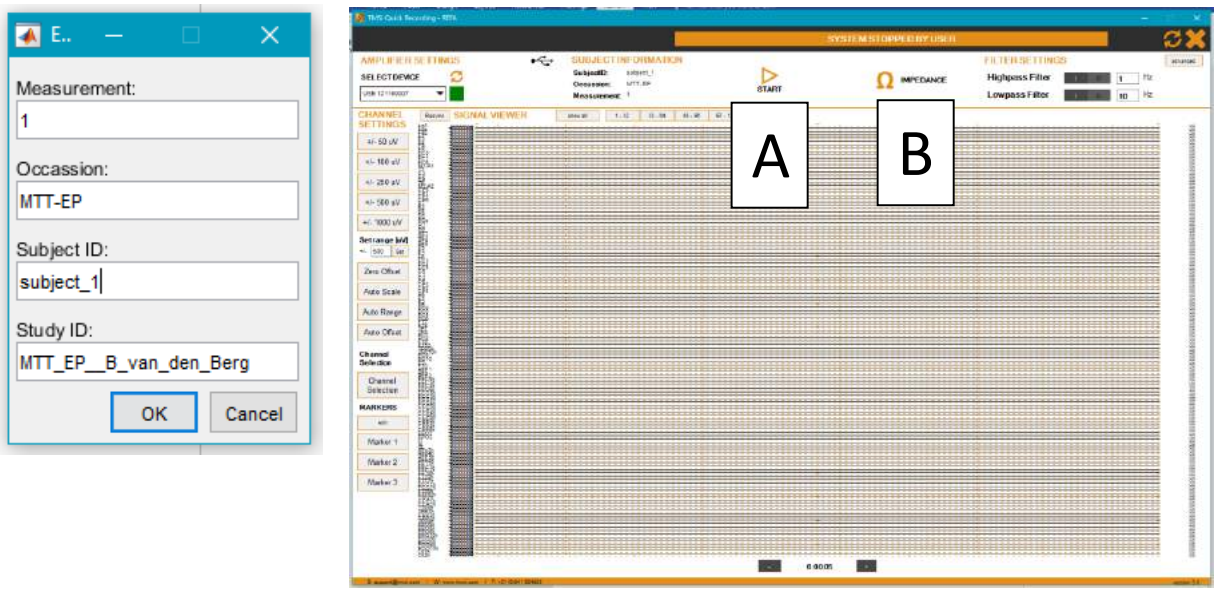

Figure 6: Left, the Matlab prompt which is opened after running the 'acquisition' function. Right, the initial screen of the TMSi Polybench interface for impedance measurement and recording which contains a button to start signal acquisition (A) and a button to start impedance measurement (B) .

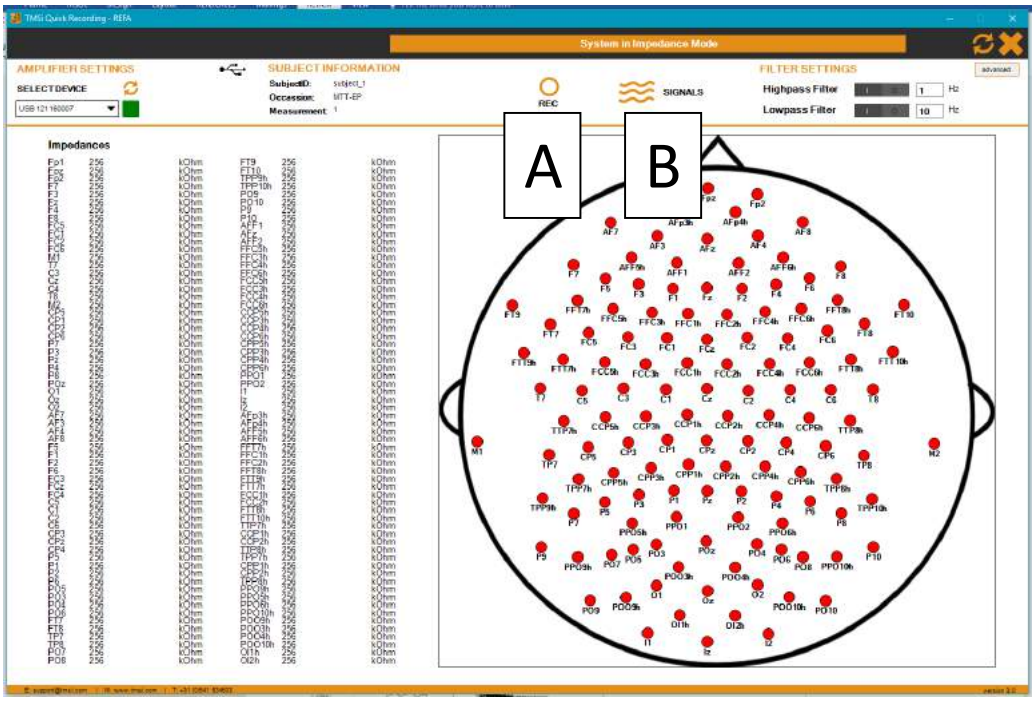

Figure 7: Interface for impedance measurement. Colors indicate impedance. Red shows that an electrode is not connected or contains no gel (> 250 kOhm) and black, yellow and green indicate a bad (250 – 20 kOhm), moderate (20 – 5 kOhm) and good (5 – 0 kOhm) impedance respectively. The interface contains a button to record the impedances (A) and a button to go back to the signal interface (B).

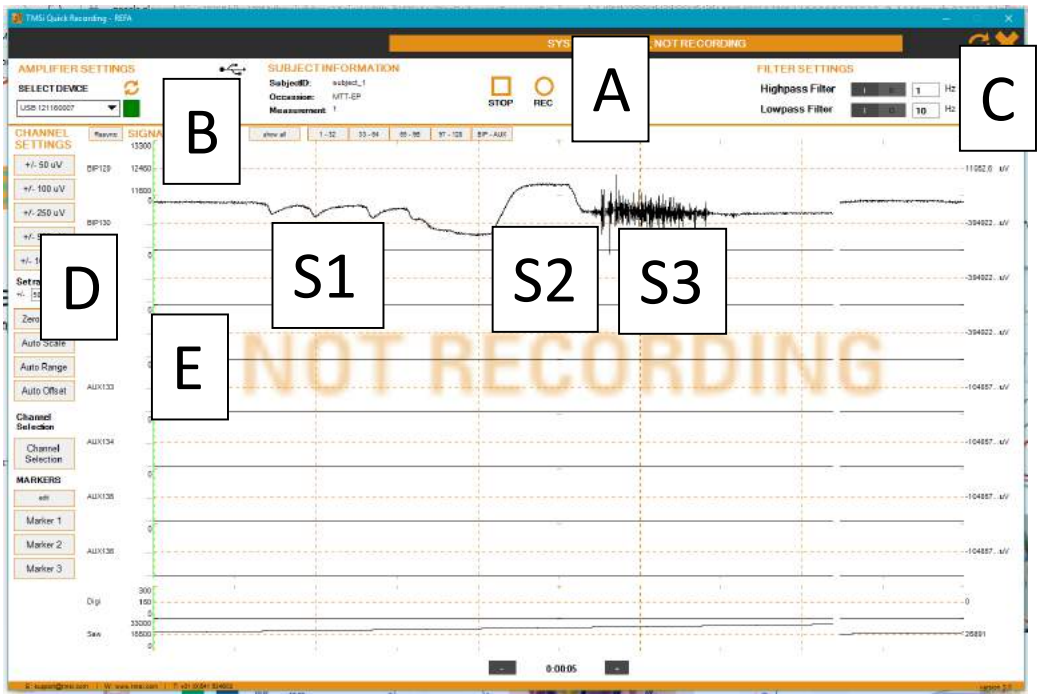

Figure 8: Interface for EEG recording. The interface contains a button to start recording (A), buttons to control which channels are visible (B), an interface for implementing high-pass and low-pass filters on the visualization (C), buttons to automatically center and scale the data (D) and an indicator whether the application is recording or not (E). The signal on the image shows the EOG channel with an blinking (S1), eye movement (S2) and EMG activity due to cheek contraction.

F. Subject reception and preparation

Time: start of the session

1. Meet with the subject at the entrance of the lab. To do so, be present at the entrance 10 minutes before the start of the session and leave the lab door open.
2. Give the subject a hard-copy of the information letter and the informed consent (preferably, the subject has already received and read the information letter in advance, via e-mail). Ask the subject:
   - **"Do you have any questions?"**
   - **"Would you like to participate in the study?"**
   - **"Do you want to sign the informed consent?"**
3. Explain to the subject what is going to happen. Ask the subject:
   - **"Please, set the mobile phone to airplane mode."**
   - **"Do you need to go to the toilet? The session will take approximately 2 hours."**
4. Instruct the subject:
   - **"Sit-down on the chair and set the chair to a comfortable position."**
   - **"Make sure there is sufficient space for the legs."**
   - **"The chair should be inclined slightly backwards to relieve the muscles around the neck."**
5. Use the colored measurement tape to measure which size of the cap is required.
6. Measure the distance between the nasion and the inion.
7. Measure the distance between the pre-auricular points.
8. Place the electrode cap on the head of the subject, by pulling over the forehead towards the back.
9. Ask the subject:
   - **"Please adjust the cap to fit as tightly as possible on the head."**
   - **"Please, attach the strap around the chin as tightly as possible, and pull the rope at the side of the cap for a better fit."**
10. Using the measured distances, make sure that the Ccap electrode is exactly in the middle of those measured positions. If necessary, slightly adjust the position of the cap, and ask the subject for feedback on the fit.
11. Use medical abrasive gel and a cotton stick to clean the positions of:
    - The ground electrode
    - The earlobe electrodes
    - The EOG electrodes
12. Use a tissue with alcohol to clean the same locations.
13. Explain the subject:
    - **"You will not feel anything from EEG measurement."**
    - **"Gel will be injected into the electrodes. To improve conduction, the skin will be scratched a bit with a blunt needle. This should not hurt, if it does, pleas say so."**
    - **"If you discomfort, you can indicate this at any time."**
14. Make sure that the location of the ground electrode is dry and attach the ground electrode.
15. Take the needle and the syringe. Show to the subject you take a new needle from the package and fill the needle and syringe with gel.
16. Fill the electrodes in the cap with gel by injecting gel while scratching the skin by turning the blunt needle with a circular motion. Use the back end of a cotton stick for extra scratching if necessary.

17. Use the impedance display on the screen to make sure impedances are below 5 kOhm.
18. Attach the earlobe and the EOG electrodes.
19. In the impedance interface of the EEG recording application, press 'RECORD' (Figure 7 A) to save information about the impedances.
20. Go to the signal interface by pressing the "SIGNAL" (Figure 7 B) button.
21. Select the channels BIP-AUX (Figure 8 B) and test electrode signals by letting the subject turn the eyes (EOG), bite on the cheeks and swallow water (EMG).
22. Explain to the subject that you will attach the electrodes for stimulation:
    - **"The first electrode is an electrode with small pins that will not penetrate the skin, but solely serve to stimulate the upper layer of skin."**
    - **"The second electrode is a sticky electrode which serves as a ground."**
23. Attach the electrodes as depicted in Figure 11. Ask the subject:
    - **"Please, hold the IES-5 electrode at the back of the right hand."**

    Attach the electrode with medical tape and ask the subject:
    - **"Is the pressure on the electrode needles painless?"**

    Glue the TENS electrode right behind the IES-5 electrode on the wrist, as is depicted in Figure 11. Ask the subject:
    - **"Can you press the electrode firmly onto the skin?"**
24. Attach the stimulator-to-electrode cable to the electrodes.

Figure 9: The IES-5 electrode.

Figure 10: The TENS electrode, which serves as a ground for stimulation.

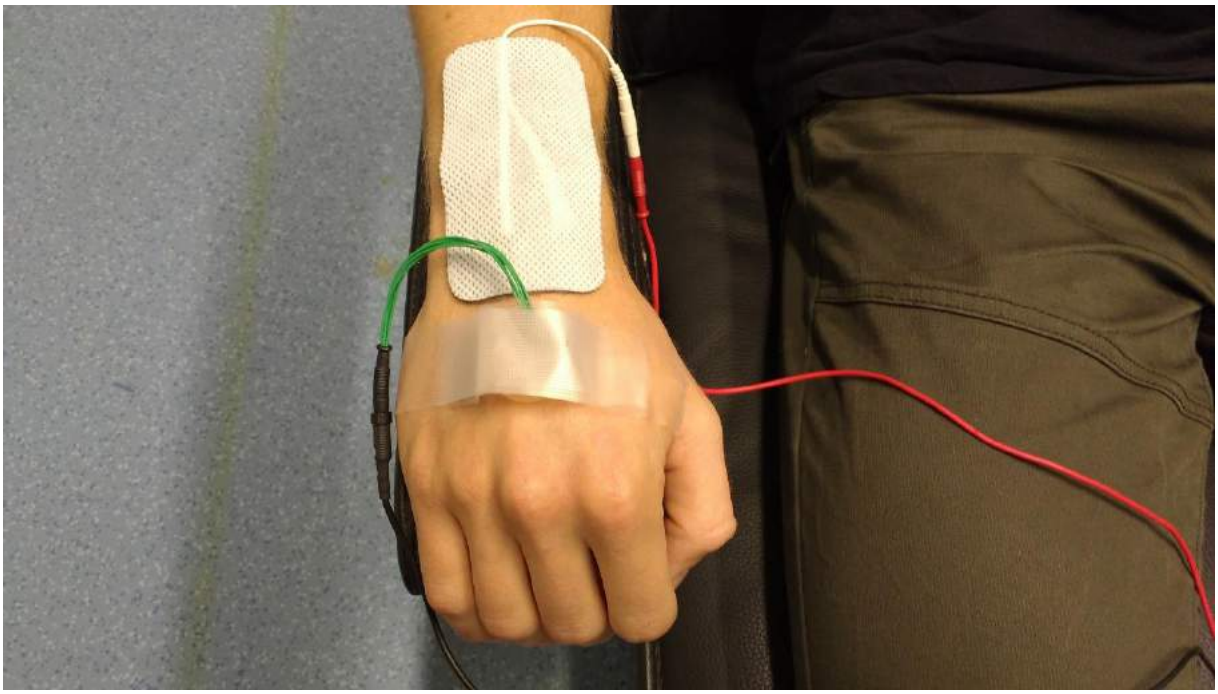

Figure 11: Example placement of the IES-5 and the TENS electrode.

G. Familiarization

Time: 40 minutes after start of the session

1. Explain to the subject:
   - **"First, a measurement will be made for familiarization and initialization of the experiment."**
   - **"I will press on start in the application. However, the measurement will not start until you press the response button. You can pause or stop the experiment by releasing the response button."**
2. Ask the subject:
   - **"Please, hold the stimulator in the hand opposite to the side of stimulation."**
3. Explain to the subject:
   - **"The first measurement will just serve to get acquainted with the stimuli. Therefore, you should hold the response button as long as possible and release the response button if the stimuli start to hurt. If the sequence reaches 1 mA, the measurement will stop automatically."**
4. Press 'Connect' in the LabView interface to connect to the stimulator.
5. A screen will open for measurement of the initial detection threshold (Figure 12). When the subject is ready, start the first measurement via the LabView interface by pressing 'Stimulate' and tell the subject that he/she can start by pressing the response button.
6. Explain that:
   - **"The second measurement will serve to determine the initial detection threshold. Therefore, you should release the response button as soon as you feel a sensation that you ascribe to the stimulus."**

7. When the subject is ready, start the second measurement via the LabView interface and tell the subject that he/she can start by pressing the response button.
8. If necessary, the second measurement can be repeated by starting the measurement a third time via the interface. If the second measurement was successful, press 'Continue' in the LabView interface.
9. A new screen will appear (Figure 13), which is the control interface for multiple threshold tracking.

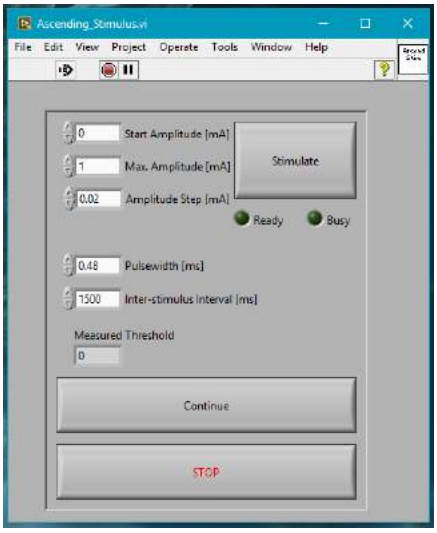

Figure 12: Interface for familiarization and measurement of the initial detection threshold.

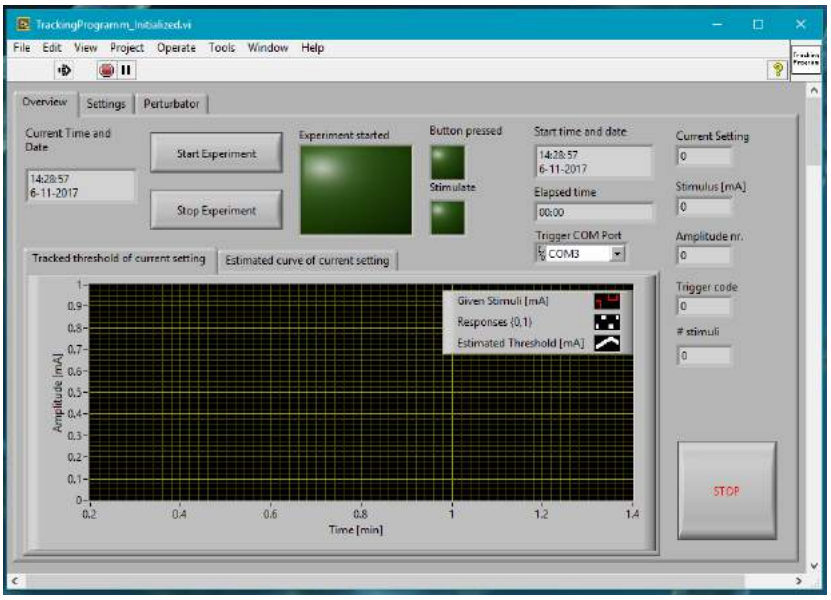

Figure 13: Interface for multiple threshold tracking.

H. Experiment

Time: 50 minutes after start of the experiment

1. Press 'record' in the EEG recording application.
2. Explain the experimental procedure to the subject:
   - **"To receive stimuli, you have to press the button."**
   - **"You have to release the button immediately when you feel a sensation that you prescribe to the stimulus."**
   - **"After releasing the button, you can re-press the button after approximately one second."**
   - **"If you need a short break, you can wait longer before re-pressing the button."**
3. Ask the subject:
   - **"Please, blink as few times possible while holding the response button."**
   - **"Keep looking towards the focus image on the wall while holding the response button."**
   - **"Try to relax and not move while holding the response button."**
   - **"Do not talk while holding the response button."**
   - **"Keep your attention focused on the detection of stimuli."**
   - **"Doing this will greatly enhance the signal quality."**
4. Press "Start Experiment".
5. Indicate the subject may now press the button and start the procedure
6. A message will pop-up after 50 minutes indicating the end of the session.
7. Press the "Stop" button in LabView to stop the program.
8. Press the "Stop Recording" button in the EEG recording application.

I. Round-up

1. Inform the subject:
   - **"The experiment was completed successfully."**
2. Turn-off the stimulator and disconnect the subject from all cables.
3. Instruct the subject:
   - **"You can take off the EEG cap."**
   - **"You can wash your hair in the sink in the lab, or downstairs in the shower, (ZH-109, go down the stairs close to the red couches, in front of the stairs.)."**
4. When the subject is ready to leave, tell the subject:
   - **"Thank you for your participation in the experiment."**

   - Give the student the financial compensation for participation in the experiment.
   - Ask the subject if he/she would like to be informed about the result of the experiment.
   - Provide the subject with contact information in case he/she has any questions.

J. Clean-up

1. Turn-off the software, and the EEG amplifier.
2. Clean the cap electrodes directly after the experiment.
3. Dry the cap on the ventilator.
4. Put all equipment back where it belongs.

Figure 14: Focus image, to keep the eyes of the subject oriented in one direction, reducing EOG artefacts.